INFORMATION TO USERS

This manuscript has been reproduced from the microfilm master. UMI films the text directly from the original or copy submitted. Thus, some thesis and dissertation copies are in typewriter face, while others may be from any type of computer printer.

The quality of this reproduction is dependent upon the quality of the copy submitted. Broken or indistinct print, colored or poor quality illustrations and photographs, print bleedthrough, substandard margins, and improper alignment can adversely affect reproduction.

In the unlikely event that the author did not send UMI a complete manuscript and there are missing pages, these will be noted. Also, if unauthorized copyright material had to be removed, a note will indicate the deletion.

Oversize materials (e.g., maps, drawings, charts) are reproduced by sectioning the original, beginning at the upper left-hand corner and continuing from left to right in equal sections with small overlaps. Each original is also photographed in one exposure and is included in reduced form at the back of the book.

Photographs included in the original manuscript have been reproduced xerographically in this copy. Higher quality 6" x 9" black and white photographic prints are available for any photographs or illustrations appearing in this copy for an additional charge. Contact UMI directly to order.

University Microfilms International
A Bell & Howell Information Company
300 North Zeeb Road, Ann Arbor, MI 48106-1346 USA
313/761-4700 800/521-0600

Order Number 9416075

Geochemistry of organic particulates in shallow water continental shelf environments

Snidvongs, Anond, Ph.D.

University of Hawaii, 1993

U·M·I

300 N. Zeeb Rd.
Ann Arbor, MI 48106

GEOCHEMISTRY OF ORGANIC PARTICULATES IN SHALLOW WATER CONTINENTAL SHELF ENVIRONMENTS

A DISSERTATION SUBMITTED TO THE GRADUATE DIVISION OF THE UNIVERSITY OF HAWAII IN PARTIAL FULFILLMENT OF THE REQUIREMENTS FOR THE DEGREE OF

DOCTOR OF PHILOSOPHY

IN

OCEANOGRAPHY

DECEMBER 1993

By

Anond Snidvongs

Dissertation Committee:

Stephen V. Smith, Chairman
Marlin J. Atkinson
Yuan-Hui Li
Fred T. Mackenzie
Robert A. Kinzie III

ACKNOWLEDGEMENTS

I would like to thank the masters and crews of the R.V. Pramong No. 2 and R.V. Chulavijai No. 1 for their help on board their vessels. Underwater sediment sampling and benthic flux experiments were assisted by Supakorn Chinvanno and Nudol Molee. Laboratory analyses of samples were performed by Ted W. Walsh, Chaiyong Yuangtong and Penjai Sompongchaiyakul. Lastly, I thank my dissertation committee members, Drs. Marlin J. Atkinson, Robert A. Kinzie, Yuan-Hui Li, Fred. T. Mackenzie and Stephen V. Smith, for their advice and repeated reviewing of the manuscript.

This research was supported in part by the Unesco Regional Office for Science and Technology for Southeast Asia and the U.S. National Science Foundation LMER/BRIE Project (awarded to Dr. S. V. Smith). Salary during my stay in Hawaii and travel to Thailand was partially provided by the East-West Center, Chulalongkorn University and University of Hawaii.

ABSTRACT

Net ecosystem production of organic and inorganic phosphorus, nitrogen and carbon in the upper Gulf of Thailand was estimated by mass transport models. Human activities within 50 km from the coast supply about 50% of the P and 40% of the N requirements of the bay. Up to 40% of the total N input may be derived from N_2 fixation by dense population of planktonic cyanobacteria *Trichodesmium* observed near the bay head. The upper Gulf of Thailand is a net consumer of DIP but a net producer of CO_2. This opposite trend occurs because the bay consumes high C:P ($\approx$400:1) terrestrial organic material while producing low C:P ($\approx$100:1) planktonic organic matter.

Organic diagenesis in the upper Gulf of Thailand sediments was studied using an electron balance approach. Generally, O_2 reduction alone can explain benthic respiration in most parts of the Gulf of Thailand except at stations located less than 15 km from river mouths where organic matter input is high. At these locations, SO_4^{2-} reduction is required to balance the budgets. Sediment denitrification is a minor reaction in terms of organic carbon respiration but can be an important N sink. Net denitrification in sediments near river mouths may be limited by the nitrification step which is subsequently limited by O_2 uptake across the sediment-water interface. In other parts of the bay, denitrification is limited by low sediment organic content.

The same model is also applied to Tomales Bay (California) sediments where oxidant limitation is more severe. On average, Tomales Bay sediments require about 18 meq m^{-2} d^{-1} of oxidants, in addition to O_2, NO_3^- and SO_4^{2-}, in order to balance the

electrons generated by organic carbon oxidation. This electron imbalance is explained by minor reduction reactions and groundwater nutrient input to the bay.

Respiratory CO_2 regenerated in the Gulf of Thailand sediments reacts with $CaCO_3$. In oxic sediments, the coupling between organic carbon respiration and $CaCO_3$ dissolution is near 1:1. In the SO_4^{2-} reducing zone, the coupling is about 0.4:1 (assuming FeS formation). $CaCO_3$ dissolution rate in oxic sediments is about 100 times faster than the rate in the SO_4^{2-} reducing zone with the same degree of undersaturation.

TABLE OF CONTENTS

Acknowledgements iii

Abstract iv

List of Tables x

List of Figures xi

Chapter 1: Introduction 1

Environmental Setting 3

Scope of the Dissertation 10

Biogeochemical Modeling Concepts 10

References 11

Chapter 2: Nutrient Mass Balance in the Upper Gulf of Thailand 14

Introduction 14

Methods 14

Field Sampling Procedures 14

Laboratory Analysis of Water and Particulate Samples 16

Sediment Removal of Elements 19

The Solute Transport Model 19

The Particle Transport Model 22

The Null Hypothesis 24

Propagation of Errors 24

Results 25

Discussion 40

Additional Nutrient Sources and Sinks 40

Net Ecosystem Production in the Upper Gulf of Thailand and Some of Its Consequences 45

Phosphorus Metabolism 45

Organic Carbon Metabolism 49

Nutrient Limitation of Net Ecosystem Production 52

Possible Causes and Consequences of N:P Ratio Variation in the Upper Gulf of Thailand 56

Conclusion 60

References 61

Chapter 3: Comparison of Benthic Nutrient Regeneration in the Upper Gulf of Thailand and in Tomales Bay, with Emphasis on Nitrogen Cycling 67

Introduction 67

Benthic Phosphorus Regeneration 68

Benthic Nitrogen Regeneration 69

Benthic Carbon and Nitrogen Redox Models 71

O_2 Reduction 73

$O_2 + SO_4^{2-}$ Reduction 77

$O_2 + SO_4^{2-} + CO_2$ Reduction 79

Methods 81

Benthic Flux Measurements in the Upper Gulf of Thailand 81

Analyses of Gulf of Thailand Sediments 86

Tomales Bay Benthic Flux Dataset 88

Results 90

Gulf of Thailand 90

Tomales Bay 108

Discussion 125

Nitrogen Cycling in Coastal Marine Sediments: Some Conceptual Models 125

Nitrogen Reactions in the Upper Gulf of Thailand Sediments 132

Nitrogen Reactions in Tomales Bay Sediments 135

Conclusion 139

References 140

Chapter 4: Interaction Between Benthic Respiration and Calcium Carbonate Dissolution in Sediments: An *In Situ* Kinetic Model 148

Introduction 148

Methods 150

Core Sampling and Chemical Analyses 150

$CaCO_3$ Saturation State 154

Results 155

Sediments Without SO_4^{2-} Reduction: Stations 1, 2, 3, and 4 160

Sediments With SO_4^{2-} Reduction: Stations 5, 6, and 7 162

$CaCO_3$ Dissolution Models 167

Interaction Between Oxic/Suboxic Respiration and $CaCO_3$ Reaction 167

Model Synthesis 167

Application of the Model to Observed Data 169

Kinetic Analysis of *In Situ* $CaCO_3$ Dissolution 172

Model Synthesis 172

Application of the Model to Observed Data 173

Discussion 174

Conclusion 184

References 185

Chapter 5: General Conclusion 190

Appendix A: Water Sampling Stations in the Upper Gulf of Thailand 192

Appendix B: Water Chemistry Data of the Upper Gulf of Thailand 193

Appendix C: Geometric Mean Linear Regression and Statistical Testing for Outliers 199

LIST OF TABLES

Table — Page

2.1. Nominal Precision of Analytical Methods 17

2.2. Averaged Chemical Composition at Segment Boundaries 28

2.3. Some Hydrodynamic Variables Related to Particle Transport 32

2.4. Statistical Analysis for the Mass Balance Models 34

3.1. Averaged Benthic Fluxes in the Upper Gulf of Thailand 91

3.2. Organic Carbon Input at the Sediment-Water Interface 92

3.3. Nitrogen Balance of the Upper Gulf of Thailand Sediments 102

3.4. Calculated Nitrification and Denitrification Rates in the Gulf of Thailand Sediments 105

3.5. Minor Electron Transfer Mechanisms in Tomales Bay Sediments 124

4.1. Concentration Gradients at the Core Bases 155

4.2. Relative Changes in TA and DIC Concentration Gradients in Sediments . . 170

4.3. Specific $CaCO_3$ Dissolution Rates in Oxic Sediments 174

4.4. The Best-Fit $g_x CD\%_x^o$ for n Between 3 and 5 and x Between 0 and 25 180

LIST OF FIGURES

Figure — Page

1.1. Bottom Topography of the Gulf of Thailand 4

1.2. Averaged Monthly Water Discharge by the Five Major Rivers 5

1.3. Averaged Monthly Temperature, Evaporation and Rainfall in the Study Area 7

2.1. The Map of the Upper Gulf of Thailand Divided into Segments 18

2.2. Relative Dispersion Coefficient For Suspended Particulates as a Function of v_s/ku_* 23

2.3. Vertical Sections of Salinity Along the East and West Transects in the Upper Gulf of Thailand 26

2.4. The Depth Integrated Brunt-Väisälä Stability Frequency 27

2.5. Numerical Estimation of K_x and K_y for the Upper Gulf of Thailand 31

2.6. The Phosphorus Mass Balance for $K_i^!/K_i$ ratio of 1 35

2.7. Phosphorus Transfer Among Segments in the Upper Gulf of Thailand 36

2.8. Nitrogen Transfer Among Segments in the Upper Gulf of Thailand 38

2.9. Comparison of Denitrification Rates Estimated from Water Column N and from Benthic N Flux 39

2.10. Organic Carbon Transfer Among Segments in the Upper Gulf of Thailand 41

2.11. Relative N:P Ratio Between Organic and Inorganic Pools as a Function of Distance from the Bay Head 57

2.12. The N:P Ratio of Various Pools as a Function of Distance from the Bay Head 59

3.1. A Map of the Upper Gulf of Thailand Showing Benthic Flux Stations 82

3.2. A Map of Tomales Bay Showing Benthic Flux Stations 89

3.3. DIC Flux Versus O_2 Reduction in the Gulf of Thailand Sediments 94

3.4. DIC Flux Versus O_2+NO_3^- Reduction in the Gulf of Thailand Sediments . . . 95

3.5 DIC Flux Versus O_2+SO_4^{2-} Reduction in the Gulf of Thailand Sediments . . . 96

3.6. DIC Flux Versus O_2+SO_4^{2-}+NO_3^- Reduction in the Gulf of Thailand Sediments 97

3.7. DIC Flux Versus Sorption Corrected DIP Flux in the Gulf of Thailand Sediments 99

3.8. Vertical Profiles of Organic P:C Ratio of the Gulf of Thailand Sediments 100

3.9. Vertical Profiles of Organic N:C Ratio of the Gulf of Thailand Sediments 103

3.10. Comparison of Sediment Denitrification Rates in the Gulf of Thailand Estimated by Three Methods 106

3.11. Time Series of Benthic O_2 Flux in Tomales Bay 109

3.12. Time Series of Benthic DIC Flux in Tomales Bay 110

3.13. Time Series of Benthic TA Flux in Tomales Bay 111

3.14. Time Series of Benthic DIP Flux in Tomales Bay 112

3.15. Time Series of Benthic NH_4^+ Flux in Tomales Bay 113

3.16. Time Series of Benthic NO_3^- Flux in Tomales Bay 114

3.17. DIC Flux Versus O_2 Reduction in Tomales Bay Sediments 115

3.18. DIC Flux Versus O_2+NO_3^- Reduction in Tomales Bay Sediments 116

3.19 DIC Flux Versus O_2+SO_4^{2-} Reduction in Tomales Bay Sediments 118

3.20. DIC Flux Versus O_2+SO_4^{2-}+NO_3^- Reduction in Tomales Bay Sediments . . 119

3.21. Sorption Corrected DIP Flux Versus O_2+SO_4^{2-}+CO_2 Reduction in Tomales Bay Sediments 120

3.22. Sorption Corrected DIP Flux Versus $O_2+SO_4^{2-}+CO_2+NO_3^-$ Reduction in Tomales Bay Sediments 121

3.23. Time Series of Model Denitrification Rate in Tomales Bay Sediments . . . 126

3.24. A Diagram for Nitrogen Cycling in Coastal Sediments 128

3.25. A Diagram for Electron Cycling in Coastal Sediments 129

3.26. Benthic NO_3^- Flux Versus Model Sediment Denitrification Rate in the Gulf of Thailand 133

3.27. Benthic NO_3^- Flux Versus Model Sediment Denitrification Rate in Tomales Bay 136

3.28. Monthly Denitrification and Nitrification Rates in Tomales Bay Sediments 137

4.1. A Map of the Upper Gulf of Thailand Showing Core Sampling Stations . . 151

4.2. $CaCO_3$ Contents of the Upper Gulf of Thailand Sediments 156

4.3. Organic Carbon Contents of the Upper Gulf of Thailand Sediments 157

4.4. Vertical Profiles of Porewater TA in the Upper Gulf of Thailand 158

4.5. Vertical Profiles of Porewater DIC in the Upper Gulf of Thailand 159

4.6. Vertical Profiles of $CaCO_3$ Saturation States of Porewater in the Upper Gulf of Thailand 161

4.7. Monthly Data of Organic Content of the Gulf of Thailand Surface Sediments 164

4.8. Vertical Profiles of Porewater DIP:DIC in the Upper Gulf of Thailand . . . 165

4.9. An Example of the IAP Versus Specific $CaCO_3$ Dissolution Rate 175

4.10. The Best-Fit $CaCO_3$ Solubilities for This Study 176

4.11. A Comparison of This Study Best-Fit Solubility with Other Studies 177

4.12. Specific $CaCO_3$ Dissolution Rate Versus Saturation State 182

CHAPTER 1

INTRODUCTION

The continental shelf, which includes bays and estuaries, is the transition zone between the land and the ocean. In this shallow-water environment, biogeochemical transformations of elements among organic and inorganic phases are important and rapid. These transformations play key roles in elemental cycles, especially those of C, N and P, at local and global scales (Peterson and Melillo, 1985; Smith and Mackenzie, 1987; Lerman et al., 1991). An example of a local contribution to the organic matter cycle in coastal systems may be fishery production (Nixon et al., 1986). A global scale contribution of coastal systems may be as a source of several trace atmospheric gases, such as CO_2 (Smith and Mackenzie, 1987), CH_4 (Hovland and Judd, 1992), and N_2O (Seitzinger, 1988). These gases are potentially "greenhouse" gases. Organic production can play one or more roles in the biogeochemical cycling of these gases.

One characteristic that makes some coastal systems different from oceanic shoals and open continental shelves is the terrestrial contribution of organic materials. This input can make the net metabolism of those coastal systems net heterotrophic instead of autotrophic (Hopkinson, 1985; Smith and Mackenzie, 1987). By heterotrophic, it is meant that gross primary production minus total system respiration is less than zero (e.g., Smith and Mackenzie, 1987). Elemental cycling of several elements, particularly carbon, is strongly dependent upon the net trophic status of the

system. In a heterotrophic system, there will net production of CO_2 gas, while in an autotrophic system, there will be net consumption of gaseous CO_2.

At least 60% of the world river input of organic C occurs in the tropics (Meybeck, 1982). Most tropical studies of nutrient and carbon cycling have emphasized very large river systems that empty directly onto open continental shelves, e.g. Amazon, Zaire and Orinoco Rivers (Edmond et al., 1981; Van Benekom et al., 1978; Bonilla et al., 1993). Even though those studies have yielded valuable mass balance and flux estimations, they have provided little information on the internal mechanisms that regulate elemental cycling. One disadvantage is that those coastal systems are often too large to be studied in a detailed manner without a massive effort field program. Another disadvantage is the physical oceanography of the open shelf systems can be quite complicated (Muller-Karger et al., 1988), leading to difficulties with the estimation of net reaction rates of elements.

In this dissertation, I chose the upper Gulf of Thailand as my study site because:

1) Terrestrial loading of C, N and P via rivers is largely as organic matter: more than 50% of the C and more than 70% of the N and P are delivered to the gulf as organic materials. These percentages are typical of world rivers (Meybeck, 1982).

2) The Gulf of Thailand is a tropical embayment, with only riverine and one marine water-mass components. Thus, the mixing between these two water masses may be quantified by a relatively simple kinematic model.

3) The upper Gulf of Thailand is strongly affected by the human population along the coastline, through fishery harvesting as well as waste dumping.

4) The net system metabolism of the area has never been analyzed from a biogeochemical perspective.

Environmental Setting

The Gulf of Thailand is a part of the Sunda Shelf, located in the westernmost portion of the Pacific Ocean (Fig. 1.1). The Gulf extends southeast from the Chao Phraya deltaic plain near Bangkok, about 800 km to its mouth. The average width is about 400 km. The gulf is a relatively flat basin with a maximum depth of about 85 m and an average depth of about 50 m (Robinson, 1974; Wyrtki, 1961).

Material exchange between the Gulf of Thailand and the south China Sea is strongly seasonal. Nutrient sources in the South China Sea near the mouth of the Gulf of Thailand include deep-water upwelling and materials discharged from the Mekong River (LaFond, 1963). The magnitudes and variations of these sources are not known.

The upper portion of the Gulf of Thailand (also called the "inner" part by some investigators) emphasized in this study is a nearly square bay about 100 km wide (east-west) and 90 km long (north-south). The western side of the bay (with an average depth of about 15 m) is shallower than the eastern side (with an average depth of about 25 m).

Terrestrial inputs into the upper Gulf of Thailand are mainly through five major rivers along the northern boundary of the bay. The average monthly discharges

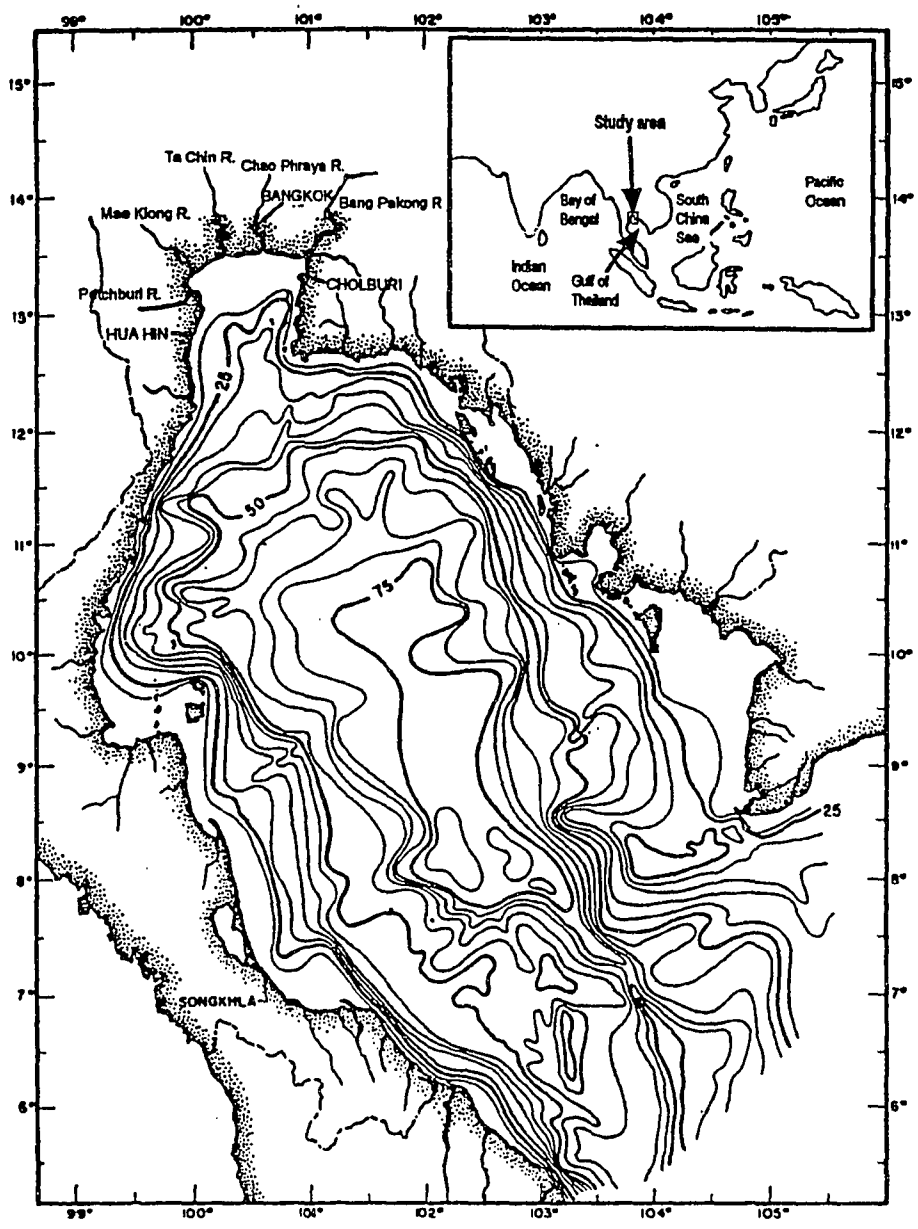

Figure 1.1. Bottom topography of the Gulf of Thailand (contour interval 5 m). Redrawn from Robinson (1974).

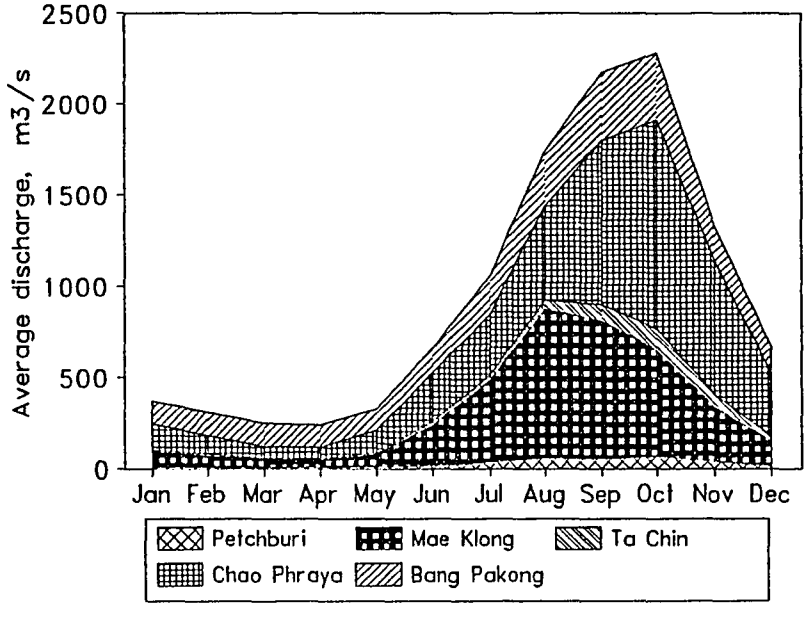

Figure 1.2. The long-term average of monthly water discharge by the five major rivers that empty into the upper Gulf of Thailand. Data from Siripong (1988).

of these rivers are shown in Fig. 1.2. The Chao Phraya River is the largest river, with an average discharge rate of about 430 $m^3 s^{-1}$. Mae Klong and Bang Pakong are the second and third largest rivers, with average flow rates of 320 and 220 $m^3 s^{-1}$, respectively. The last two rivers, Ta Chin and Petchburi, are small rivers that discharge only 50 and 30 $m^3 s^{-1}$ of freshwater, respectively, into the bay.

A comparative study of the Mae Klong and Bang Pakong Rivers (Hungspreugs et al., 1990) reveals that the water chemistry of these two rivers clearly reflects the watershed geology. The Bang Pakong River drains mainly acidic agricultural soils, and thus the water is low in both pH and alkalinity. The water also has a high SO_4^{2-}:Cl ratio. In contrast, the watershed of the Mae Klong River consists mainly of quartzite, sandstone and limestone. Thus, the water is high in pH and alkalinity. The Mae Klong water is also enriched in dissolved $SiO_2(aq)$, Ca^{2+} and Mg^{2+} relative to the Bang Pakong water. The major element chemistry of the Chao Phraya and Ta Chin Rivers is not known but probably resembles the chemistry of the Bang Pakong River because of similarity in watershed geology.

The long-term average of monthly air temperature, rainfall and evaporation at three meteorological stations along the coastline--Hua Hin (to the west), Bangkok (to the north), and Cholburi (to the east) reported by the Meteorological Department (1987)--is shown in Fig. 1.3.

Prevailing wind over the upper Gulf of Thailand is strongly influenced by the monsoon system. The southwest monsoon is usually dominant in May through

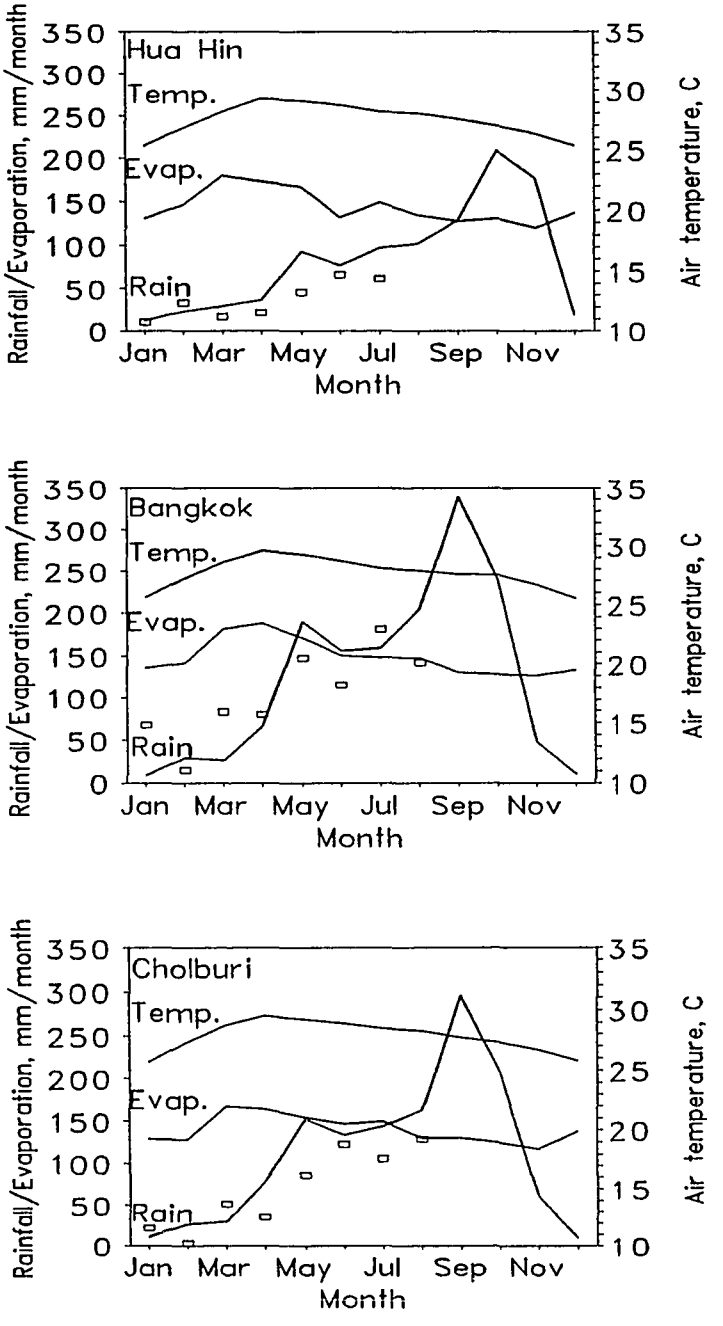

Figure 1.3. The long-term average of monthly air temperature, evaporation and rainfall at three meteorological stations near the upper Gulf of Thailand (data from Meteorological Department, 1985 and 1987). Observed monthly rainfall at these stations between January and July 1989 is shown by open squares (unpublished data, Meteorological Department).

September, and the northeast monsoon is usually dominant in December and January. Wind patterns during the monsoon transition months are highly variable and difficult to predict (Meteorological Department, 1985).

The tides in the upper Gulf of Thailand are mixed, dominated by semidiurnal tides (Siripong, 1988). The mean tidal range is highest at the head of the bay (about 1.5 m) and lowest near the mouth (about 1 m).

Water circulation in the upper Gulf of Thailand is driven by the combined effects of river runoff, slope current, tides, winds and atmospheric pressure differences (Siripong and Tamiyavanich, 1984; Menasveta et al., 1986). There are disagreements among investigators on the circulation patterns in the bay. On the one hand, Vongvisessomjai et al. (1978) derived a hypothetical circulation model based on wind stress and geostrophic theory and concluded that net flow is anticlockwise during the southwest monsoon months and clockwise during the northeast monsoon months. This model has been widely accepted by coastal engineers and environmental planners. On the other hand, direct measurements of residual currents appear to indicate an opposite pattern, i.e. clockwise during the southwest monsoon and anticlockwise during the northeast monsoon (Robinson, 1974; Neelasri, 1981; Silpipat, 1987). Unfortunately each dataset of direct measurements covers only one tidal cycle as well as representing only a few stations in the upper gulf.

In terms of transport, the residual current (possibly wind driven) is much smaller than the tidal current. By examining two direct measurement datasets (Siripong and Tamiyavanich, 1984; Silpipat, 1987), I found that the residual north-

south current velocities over a tidal cycle after correction for riverine water discharge are very small, on the order of 10^{-2} cm s^{-1} or less. The residual current velocities are two orders of magnitude smaller than that of the tidal current.

Surface salinity in the upper Gulf of Thailand is strongly affected by river runoff, but freshwater effects on mid-depth and bottom salinity are much smaller (Bunpapong and Piyakarnchana, 1987). During the low runoff months (January to May), surface salinities are the same as bottom salinities (about 30-32 ‰), even at stations less than 10 km from the river mouths. During high runoff months (June to December), surface salinity at some of the stations near river mouths can be less than 1 ‰. In some years, the effect of high river runoff on surface salinity can be seen as far as 50 km from the river mouths (Bunpapong and Piyakarnchana, 1987).

Seawater temperature of the upper Gulf of Thailand is 30 $\pm$ 1°C between February and October and 26 $\pm$ 1°C between November and January (Tamiyavanich and Rojanavipart, 1984).

The upper Gulf of Thailand is a productive marine region. Net primary production rates by phytoplankton in the bay are in the range of 100-500 mmol C m^{-2} d^{-1} (Steemann-Nielsen and Jensen, 1957; Rao, 1965; Lursinsap and Charoenruay, 1972). If a C:N:P uptake ratio of 106:16:1 (Redfield et al., 1963) is assumed, this phytoplankton primary production rate would require 15-75 mmol m^{-2} d^{-1} of DIN and 1-5 mmol m^{-2} d^{-1} of DIP. The supplies of organic and inorganic nutrients by rivers are two orders of magnitude less than this estimated primary production requirement, indicating the importance of nutrient recycling. The lower Gulf of Thailand to the

south is probably not a significant nutrient source, because the nutrient concentration in the lower Gulf is lower than that in the upper Gulf. Evidently, internal nutrient recycling is very rapid, suggesting the possibility of a near balance between primary production and ecosystem respiration.

Benthic macrophytes are rare in the upper Gulf of Thailand. The abundance of benthic microalgae is not known. Because the water is turbid, benthic primary production is probably less important than plankton production.

Scope of the Dissertation

In this dissertation I will explore three biogeochemical aspects of a shallow-water tropical embayment, the upper Gulf of Thailand:

1) The mass balance of C, N and P in the study area, and the nutrients that may limit net ecosystem production (Chapter 2);

2) The function of benthic nutrient regeneration and possible controlling factors (Chapter 3);

3) The interaction between benthic respiration and $CaCO_3$ dissolution in sediments (Chapter 4).

Biogeochemical Modeling Concepts

In this dissertation, the biogeochemical behavior of elements will be modeled based on observational data from natural environment, without any manipulations. This modeling approach requires both assumptions and procedures of cross checking the results. Transfer pathways of elements among reservoirs are constructed based on previous knowledge or on reasonable theoretical arguments. In each model, some

variables that can be independently estimated by direct observations will be compared with the model predicted values as criteria to test the model validity.

References

Bennekom, A. J. Van, Berger, G. W., Helder, W. and De Vries, R. T. P. 1978. Nutrient distribution in the Zaire estuary and river plume. Neth. J. Sea Res. 12: 296-323.

Bonilla, J., Senior, W., Bugden, J., Zafiriou, O. and Jones, R. 1993. Seasonal distribution of nutrients and primary productivity on the eastern continental shelf of Venezuela as influenced by the Orinoco River. J. Geophys. Res. 98(C2): 2245-2257.

Bunpapong, M. and Piyakarnchana, T. 1987. Some trend in the upper gulf water quality. In: Sontirat, S. (ed.) Proceeding of the Fourth Seminar on the Water Quality and the Quality of Living Resources in Thai Waters. Bangkok: National Research Council of Thailand, pp. 270-273.

Edmond, J. M., Boyle, E. A., Grant, B. and Stallard, R. F. 1981. The chemical mass balance in the Amazon plume I: The nutrients. Deep-Sea Res. 28A: 1339-1374.

Hopkinson, C. S. Jr. 1985. Shallow-water benthic and pelagic metabolism: evidence of heterotrophy in the nearshore Georgia Bight. Mar. Biol. 87: 19-32.

Hovland, M. and Judd, A. G. 1992. The global production of methane from shallow submarine sources. Continental Shelf Res. 12: 1231-1238.

Hungspreugs, M., Dharmvanij, S., Utoomprukporn, W. and Windom, H. L. 1990. A comparative study of the trace metal fluxes of the Bang Pakong and the Mae Klong Rivers, Thailand. Sci. Total Environ. 97/98: 89-102.

LaFond, E. C. 1963. Physical oceanography and its relation to the marine organic production in the South China Sea. In: Ecology of the Gulf of Thailand and the South China Sea. La Jolla: Scripps Ins. Oceanogr. Ref. 63-6, pp. 5-33.

Lerman, A., Mackenzie, F. T. and Geiger, R. J. 1989. Environmental chemical stress effects associated with carbon and phosphorus biogeochemical cycles. In: Levin, S. A., Harwell, M. A., Kelly, J. R. and Kimball, K. D. (eds.) Ecotoxicology: Problems and Approaches. New York: Springer-Verlag, pp. 315-350.

Lursinsap, A. and Charoenruay, M. 1972. The estimation of phytoplankton production in the Gulf of Thailand from chlorophyll, oxygen determination and light data. In: Proc. Third CSK Symp. Bangkok: CSK Committee, pp. 339-356.

Menasveta, P., Navanarasest, M. and Rungsupa, S. 1986. Environmental setting of the Gulf of Thailand with special reference to the Sichang Islands. Galaxea 5: 7-13.

Meteorological Department 1985. Wind Rose of Thailand: 30-Year Period (1951-1980). Bangkok: Meteorological Department, Ministry of Communications, 52 pp.

Meteorological Department 1987. Climatological Data of Thailand: 30-Year Period (1956-1985). Bangkok: Meteorological Department, Ministry of Communications, 52 pp.

Meybeck, M. 1982. Carbon, nitrogen, and phosphorus transport by world rivers. Am. J. Sci. 282: 401-450.

Muller-Karger, F. E., McClain, C. R. and Richardson, P. L. 1988. The dispersal of the Amazon's water. Nature 333: 56-59.

Neelasri, C. 1981. The mean flow in the upper part of the Gulf of Thailand during a transition period of the monsoon. In: Proceeding of the Second Seminar on the Water Quality and the Quality of Living Resources in Thai Waters. Bangkok: National Research Council of Thailand, pp. 57-63.

Nixon, S. W., Oviatt, C. A., Frithsen, J. and Sullivan, B. 1986. Nutrients and the productivity of estuarine and coastal marine ecosystems. J. Limnol. Soc. Sth. Afr. 12: 43-71.

Peterson, B. J. and Melillo, J. M. 1985. The potential storage of carbon caused by eutrophication of the biosphere. Tellus 37: 117-127.

Rao, D. V. S. 1965. The measurement of total carbon dioxide in dilute tropical waters. Aust. J. Mar. Freshw. Res. 16: 273-280.

Redfield, A. C., Ketchum, B. H. and Richards, F. A. 1963. The influence of organisms on the composition of sea-water. In: Hill, M. N. (ed.) The Sea, Volume 2. New York: Wiley-Interscience, pp. 26-77.

Robinson, M. K. 1974. The physical oceanography of the Gulf of Thailand, Naga Expedition. Naga Report 3(1): 5-110.

Seitzinger, S. P. 1988. Denitrification in freshwater and coastal marine ecosystems: Ecological and geochemical significance. Limnol. Oceanogr. 33: 702-724.

Silpipat, S. 1987. Circulation pattern in the upper Gulf of Thailand. In: Sontirat, S. (ed.) Proceeding of the Fourth Seminar on the Water Quality and the Quality of

Living Resources in Thai Waters. Bangkok: National Research Council of Thailand, pp. 82-93.

Siripong, A. and Tamiyavanich, S. 1984. The variation of some physical properties of the sea water offshore of Ban Laem, Petchburi Province per tidal cycle. In: Tamiyavanich, S. (ed.) Proceeding of the Third Seminar on the Water Quality and the Quality of Living Resources in Thai Waters. Bangkok: National Research Council of Thailand, pp. 403-413.

Siripong, A. 1988. Seasonal variations of some hydrological, meteorological and oceanographical factors in southeast Asian seas and their effects on marine environment. Unpublished Manuscript, 86 pp.

Smith, S. V. and Mackenzie, F. T. 1987. The ocean as a net heterotrophic system: implication from the carbon biogeochemical cycle. Global Biogeochem. Cycles 1: 187-198.

Steemann-Nielsen, E. and Jensen, A. 1957. Primary oceanic production, the autotrophic production of organic matter in the ocean. Galathea Report 1: 47-135.

Tamiyavanich, S. and Rojanavipart, R. 1984. Physical, chemical and nutrients change in the water column along the eastern coastlines of the inner Gulf of Thailand. In: Tamiyavanich, S. (ed.) Proceeding of the Third Seminar on the Water Quality and the Quality of Living Resources in Thai Waters. Bangkok: National Research Council of Thailand, pp. 183-198.

Vongvisessomjai, S., Arbhabhirom, A. and Fuh, Y. 1978. A mathematical model of oil spill movement, upper Gulf of Thailand. Asian Inst. Tech. Res. Rep. 73: 1-125.

Wyrtki, K. 1961. Physical oceanography of the southeast asian waters. Naga Report 2: 1-195.

CHAPTER 2

NUTRIENT MASS BALANCE IN THE UPPER GULF OF THAILAND

Introduction

Conservation of mass models are useful to estimate the net rates of a series of chemical reactions in natural ecosystems when manipulating the environment is not feasible. In this chapter, the mass balance of dissolved and particulate C, N and P in the vertically homogeneous portion of the upper Gulf of Thailand will be studied using hydrologic models. The study area will be divided into segments. Material transfer among segments will be estimated by a finite segment kinematic model. Salinity will be taken as the conservative tracer to estimate the two horizontal transport terms, advection and mixing, among segments.

Methods

Field Sampling Procedures

Seawater samples were collected in July 1989 at 19 stations in the upper Gulf of Thailand (Appendix A). These stations were part of the fixed station network routinely visited by research vessels from the Marine Fishery Division, Department of Fishery, Ministry of Agriculture and Co-operatives. River water endmembers were also collected in July 1989 from four rivers: Mae Klong River at Ratchburi, Ta Chin River at Nakornchaisri, Chao Phraya River at Nonthaburi and Bang Pakong River at Chachoengsao. All river sampling stations are about 50 km inland of the river mouths, so the seawater effect is assumed to be zero.

Seawater was collected by using Niskin samplers at three levels: surface (about 0.5 m below the actual surface), mid-depth and bottom (about 1 m above the bottom). River water was collected at 1 m below the surface. Sample pH was measured immediately by a plastic body electrode (Cole-Palmer) connected to a custom-made high impedance digital electrometer. The pH meter was calibrated against NBS pH 4 and 7 primary standard buffers (Fisher Scientific) at least 30 minutes before each measurement batch, and the electrode was stored in Tris+seawater secondary standard buffer (Smith and Kinsey, 1978) until use. Instrumental drift was checked between samples against the Tris+seawater secondary standard. Temperature was measured with a digital thermometer.

After these measurements were made, the water samples were quantitatively in-line filtered through Whatman GF/C or Gelman A/E glass-fiber filters (1 μm nominal poresize). The filter membranes used for nutrient and DOC analysis had been precombusted at 400°C. The membranes were subsequently soaked overnight in 10% HCl, rinsed with distilled deionized water and dried at 110°C. The filtered water samples for nutrient and DOC analysis were kept frozen until analysis. Water samples for salinity and total alkalinity analyses were filtered through non-acid treated filter membranes, and the samples were kept at room temperature. Filter membranes to be analyzed for suspended C, N, and P were stored in a freezer. At least six suspended particulate samples were collected from each depth.

Laboratory Analysis of Water and Particulate Samples

Sample salinities were measured at the University of Hawaii with an AGE Minisal salinometer. Total alkalinity (TA) was determined by the Gran Plot titration technique (Edmond, 1970). Borate alkalinity (BA) was estimated from salinity by equations and constants given in Smith and Kinsey (1978). Carbonate alkalinity (CA) was obtained by subtraction of BA from TA. All other alkalinities were assumed to be zero. Dissolved inorganic carbon (DIC = $H_2CO_3+HCO_3^-+CO_3^{2-}$) was calculated from pH and CA using dissociation constants given by Mehrbach et al. (1973).

Dissolved inorganic phosphorus (DIP), $NO_3^-+NO_2^-$, NH_4^+, and $SiO_2(aq)$ were analyzed by Technicon II Autoanalyzer (Smith et al., 1981). Dissolved inorganic nitrogen (DIN) is defined as $NO_3^-+NO_2^-+NH_4^+$. Samples for total dissolved phosphorus (TDP) and total dissolved nitrogen (TDN) were oxidized by UV light followed by the analyses for DIP and DIN (Walsh, 1989). Dissolved organic phosphorus and nitrogen (DOP and DON) were obtained by difference between TDP and DIP, and TDN and DIN, respectively.

Dissolved organic carbon (DOC) was analyzed by persulphate oxidation and IR spectrometry analysis for liberated CO_2 using an Oceanography International total organic carbon analyzer. All dissolved nutrient and DOC analyses were performed by the Hawaii Institute of Marine Biology Analytical Services Facility.

POC and PON collected on filter membranes were quantified using a Carlo Erba NA1500 nitrogen analyzer with CO_2 trap removed. Samples were combusted at 1020°C. POP samples were combusted at 550°C in a muffler furnace and hydrolyzed

with hot 10% HCl solution. The supernatants were analyzed spectrophotometrically for molybdate reactive phosphate by the method of Parsons et al. (1984).

The precision of analytical techniques used in this study is summarized in Table 2.1.

Table 2.1. Nominal precision of analytical methods used in this study

Property	Nominal precision
Salinity	±0.001
Temperature	±0.1°C
pH	±0.002
T.A.	±0.001 meq l^{-1}
DIC	±0.002 mM
DIP/NO_3^-+NO_2^-/NH_4^+	±0.01 μM
DOC/DON/DOP	±0.01 μM
POC	±0.1 μM
PON/POP	±0.01 μM

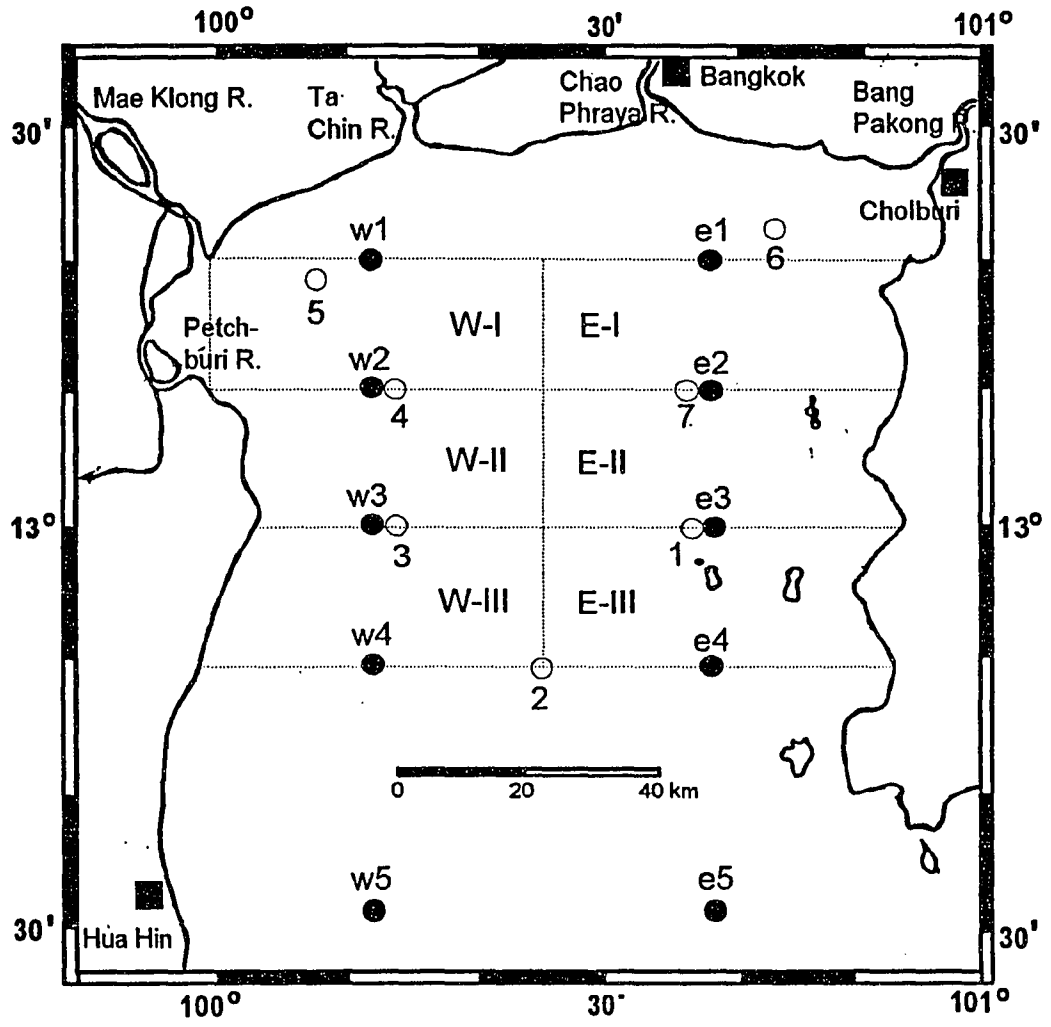

Figure 2.1. The upper Gulf of Thailand divided into segments according to the hydrological model (equation 2.1). Closed circles represent the segment boundary stations. Open circles are core sampling and benthic flux measurement stations.

Sediment Removal of Elements

In September 1991, during the benthic flux measurement cruise (Chapter 3), sediment cores were retrieved from Stations 1 through 7 (Fig. 2.1). These sediment cores were analyzed for sedimentation rates and solid phase chemistry according to procedures given in Chapter 3. The sedimentation rate at each station was multiplied by the average organic C, N, P and $CaCO_3$ contents of deep sediments (sections near the core bases) to derive net elemental removal rates. The sediment removal rate for each segment of the bay was represented by the nearest core or the average of the two nearest cores, as appropriate.

The Solute Transport Model

Observed water motion and salinity along the eastern and western boundaries of the upper Gulf of Thailand (Neelasri, 1981; Siripong and Tamiyavanich, 1984) suggest a possibly limited lateral exchange between the two watermasses (except, perhaps, near the bay head). As a consequence of this, hydrological transport in the bay may not be described by a single longitudinal one dimensional model. In this study, the bay is sub-divided into two halves along a north-south median line. Lateral mixing across the median line is ignored because tidal surge, the principal horizontal mixing force, moves exclusively along the north-south direction. With this assumption, for the portion of the bay where the watermass can be assumed to be vertically homogeneous, the net north-south transfer of salt across a vertical plane *i* can be described by:

$$A_{x,i} \cdot F_{S,i} = Q_i \cdot S_i - K_i \cdot A_{x,i} \cdot \frac{dS}{dx}|_i \qquad (2.1)$$

where: $A_{x,i}$ = the cross-sectional area perpendicular to the north-south axis, $F_{S,i}$ = the net north-south salt flux per unit area, Q_i = advective flow, S_i = salinity, K_i = longitudinal mixing coefficient, and x = distance along the north-south axis (positive southward).

At steady state, equation (2.1) equals zero. Numerical solutions for K_i may be obtained by substitution of the salinity gradient term by the forward salinity difference term, i.e. $(S_{i+1} - S_i)/(x_{i+1} - x_i)$. The $A_{x,i}$'s are chosen such that they correspond to the latitude where water was sampled (Appendix A and Fig. 2.1). At some segment boundaries, where there is more than one sampling station, the water chemistry data is laterally averaged.

Each Q_i is assumed to equal the total freshwater runoff by rivers into each half of the bay. These rivers are the Chao Phraya and Bang Pakong for the East half, and the Petchburi, Mae Klong and Ta Chin Rivers for the West half of the bay. Because at the time of writing this dissertation, river discharge data are not yet available, the long-term average discharge by these rivers for the month of July (Fig. 1.2) are assumed. This assumption is quite appropriate, because the monthly rainfall data observed from January 1989 to July 1989 (Fig. 1.3) indicate that the rainfall pattern for this year is not unusual. The effects of evaporation and rainfall on the water balance are ignored, because for the month of July these two terms nearly balance one another (Fig. 1.3).

Verification that the lateral mixing terms are negligible is done for the study area in the upper Gulf of Thailand based on a two dimensional salt balance model:

$$Q_i \cdot S_i - \langle K_x \rangle \cdot A_{x,i} \cdot \frac{dS}{dx}\Big|_i \pm \langle K_y \rangle \cdot A_{y,i} \cdot \frac{dS}{dy}\Big|_i = 0 \qquad (2.2)$$

where: $\langle K_x \rangle$ and $\langle K_y \rangle$ = average longitudinal and lateral mixing coefficients, respectively, $A_{y,i}$ = the cross-sectional area across the east-west axis, and y = distance along the east-west axis (positive westward). In order to comply with the lateral conservation of salt, the last term in equation (2.2) will be positive for the east and negative for the west halves of the bay.

Equation (2.2) may be rearranged into a linear equation of the form:

$$Factor\ B = \langle K_x \rangle \cdot Factor\ A + \langle K_y \rangle \qquad (2.3)$$

where:

$$Factor\ A = \frac{A_{x,i} \cdot \frac{dS}{dx}\Big|_i}{\pm A_{y,i} \cdot \frac{dS}{dy}\Big|_i}$$

and

$$Factor\ B = \frac{Q_i \cdot S_i}{\pm A_{y,i} \cdot \frac{dS}{dy}\Big|_i}$$

By performing a linear regression analysis between *Factor A* and *Factor B*, the bay-wide average $\langle K_x \rangle$ and $\langle K_y \rangle$ can be estimated for the slope and constant terms.

For a nonconservative soluble element M (e.g., dissolved nutrients and total alkalinity), its mass balance in a segment I bounded to the north and south by vertical planes i and $i+1$ can be described by:

$$V_I \frac{dM_I}{dt} = Q_i (M_i - M_{i+1}) - K_i A_{x,i} \cdot \frac{dM}{dx}\Big|_i + K_{i+1} A_{x,i+1} \cdot \frac{dM}{dx}\Big|_{i+1} + \Delta M_I \quad (2.4)$$

Steady state is also assumed for equation (2.4); thus ΔM_I can be estimated by solving these equations after substituting hydrological and concentration variables with appropriate values.

<u>The Particle Transport Model</u>

The mass balance of non-conservative suspended particulate elements in each segment can be modeled by advection-mixing equations analogous to equation (2.4) if a particulate dispersion coefficient (K_i') is available. From several experiments on particulate transports, K_i' is known to be related to the fluid dispersion coefficient (K_i) by a function involving suspended solid settling velocity (v_{ss}), the Von Karman Constant (k) and shear velocity (u_*) (Graf, 1971). Empirical relationships between K_i'/K_i and v_{ss}/ku_* from various published sources are shown in Fig. 2.2.

The settling velocities (v_{ss}) of organic detritus (10-64 μm) of about 2×10^{-5} m s^{-1} (Burns and Rosa, 1980), and of quartz grains (100 μm) of about 0.01 m s^{-1} (Graf, 1971), are taken to be minimum and maximum v_{ss}, respectively. Shear velocity (u_*) is related to average velocity ($\bar{u}$) by:

$$\frac{\bar{u}}{u_*} = \sqrt{\frac{f}{8}} \quad (2.5)$$

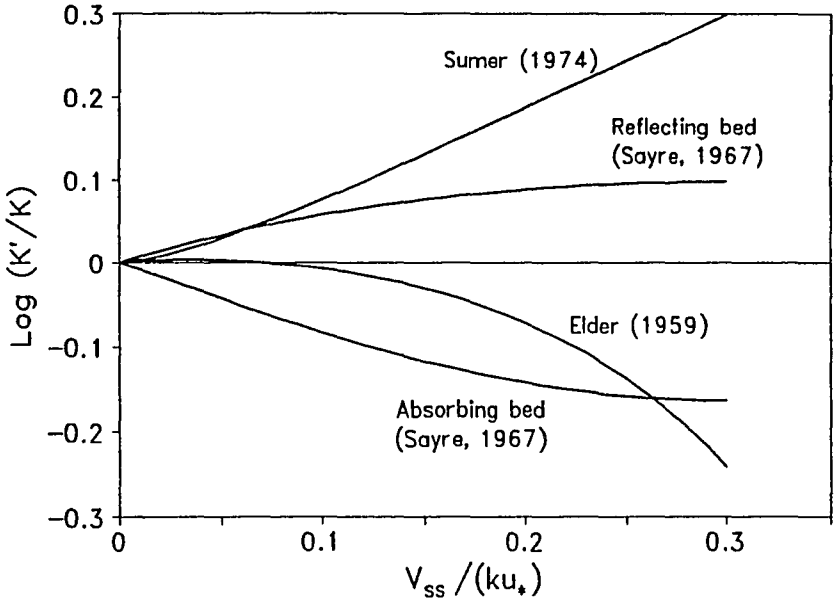

Figure 2.2. Relative dispersion coefficient for suspended particulates (K_i'/K_i) as a function of v_{ss}/ku_*. Sayre's (1967) estimation of K_i' for a reflecting bed may be too low, because he used erroneously wide increment steps in his numerical integration (Sumer, 1974). Elder's (1959) results may represent the case where some particles are reflected and others are absorbed (Graf, 1971).

(Fischer et al., 1979). The friction factor (f) is estimated using the Moody diagram (Fox and McDonald, 1985) based on the Reynolds number of the moving water mass, and the assumed bottom roughnesses of 1 and 10 cm.

The Null Hypothesis

The operational null hypothesis for this study is that the net uptake of dissolved inorganic nutrients (i.e., DIC, DIN or DIP) in a segment is balanced by the net organic nutrient production plus sediment removal. For P, which has no significant internal source/sink, net DIP uptake from the water column must be equal to the sum of net production of dissolved organic P (DOP), particulate organic P (POP) and sediment P (SP). Therefore, we can use these criteria for P as a way to verify the mass transport model used in this study (equation 2.4). For N and C, both of which have significant gas phases, if the mass-balance hypothesis is rejected, gas flux is assumed to balance the mass.

Propagation of Errors

The sensitivity of the result of a mathematical model (ΔM = the net reaction rate for an element M) to a variable α_j is defined by:

$$\frac{\partial \Delta M}{\partial \alpha_j} \tag{2.6}$$

(Cullen, 1985). Conventionally, error propagation due to all variables is taken as the root sum square of all individual errors (e.g., Snedecor and Cochran, 1980). Consequently, the net error of the mass balance model is:

$$\sqrt{\sum_j \left(\frac{\partial \Delta M}{\partial \alpha_j} \epsilon_{\alpha j}\right)^2} \qquad (2.7)$$

where $\epsilon_{\alpha j}$ = error of each individual α_j. When available, standard error is used for α_j, otherwise a nominal error is used.

Results

The results of all chemical analyses of water samples are tabulated in Appendix B. Longitudinal salinity profiles (Fig. 2.3) demonstrate that the effect of river runoff on salinity was intense within the first 14 km from the bay head. The water column near river mouths was vertically stratified and, as a consequence, water chemistry in this part of bay could not be interpreted using equations (2.1) through (2.4). Salinity differences between surface and bottom water at Stations MF1, MF2 and MF3, all located at 7 km from the bay head, were about 2 ‰ or more (Appendix B).

The bay water beyond 14 km boundary was reasonably well mixed vertically (Fig. 2.3). The depth-integrated Brunt-Väisälä stability frequency (Fig. 2.4), which is inversely related to the vertical mixing coefficient (e.g., Bowden, 1983), clearly shows a substantial decrease between 7 and 14 km from the bay head. Thus, the 14 km distance is a reasonable northern boundary for the vertically homogeneous water mass that can be modelled by equation (2.1). The average chemical data at each segment boundary to be used in the mass balance modeling are summarized in Table 2.2.

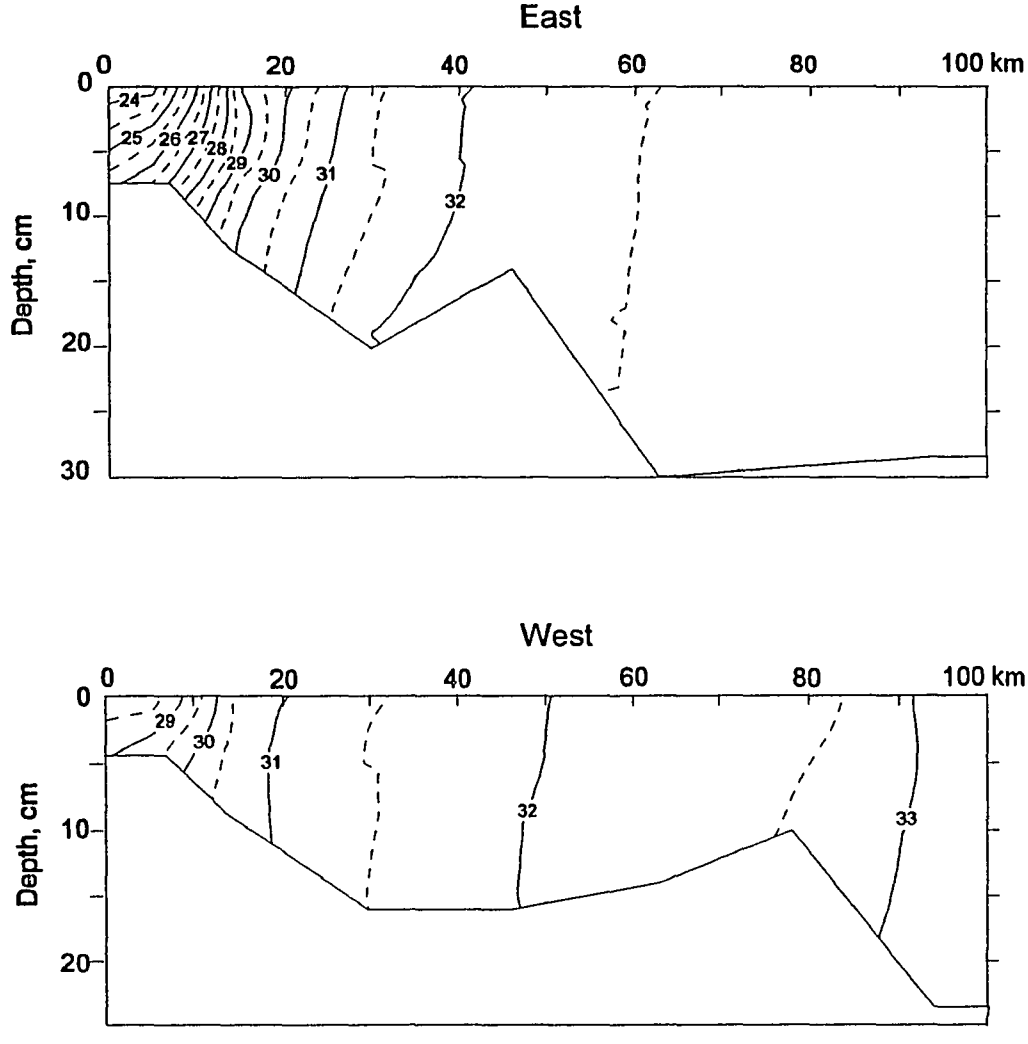

Figure 2.3. Vertical sections of salinity along the East and West transects in the upper Gulf of Thailand.

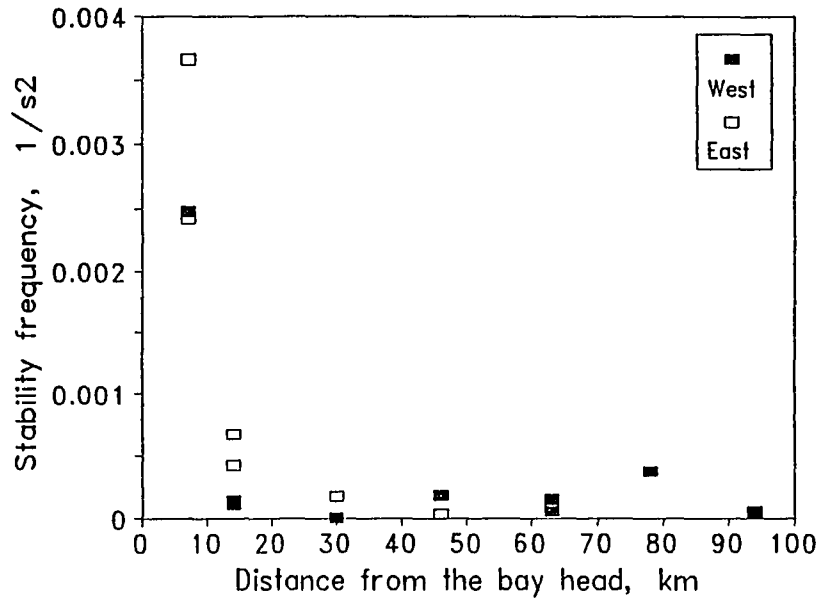

Figure 2.4. The Brunt-Väisälä stability frequency integrated over depth of water mass as a function of distance from the head of the Gulf of Thailand.

Table 2.2. Averaged chemical composition at segment boundaries with standard error of the mean given in parentheses. All units are in mmol m^{-3}, unless specified otherwise.

Boundary	km	S ‰	DIP	DIN	TA meq m^{-3}	DIC	DOP	DON	DOC	POP	PON	POC
West Transect												
w1	14	30.64 (0.07)	0.150 (0.005)	0.198 (0.016)	2331 (14)	2052 (17)	0.340 (0.003)	8.81 (0.42)	64.30 (0.87)	0.947 (0.021)	21.81 (1.52)	183.36 (15.28)
w2	30	31.47 (0.02)	0.125 (0.004)	0.353 (0.014)	2231 (25)	1992 (24)	0.470 (0.038)	7.75 (0.88)	69.51 (3.25)	0.410 (0.009)	8.50 (0.20)	61.75 (4.27)
w3	46	31.97 (0.02)	0.120 (0.008)	0.187 (0.012)	2182 (7)	1980 (6)	0.293 (0.014)	6.61 (0.66)	67.62 (2.65)	0.330 (0.033)	5.77 (0.18)	34.37 (1.24)
w4	63	32.28 (0.02)	0.100 (0.005)	0.170 (0.021)	2175 (6)	1985 (6)	0.227 (0.014)	5.73 (0.41)	64.66 (1.38)	0.300 (0.014)	5.10 (0.32)	35.01 (1.90)
w5	94	33.17 (0.03)	0.096 (0.009)	0.202 (0.020)	2162 (15)	1986 (16)	0.157 (0.007)	5.40 (0.28)	61.32 (2.22)	0.193 (0.008)	3.08 (0.21)	27.50 (0.91)

Table 2.2. (Continued).

Boundary	km	S ‰	DIP	DIN	TA meq m^{-3}	DIC	DOP	DON	DOC	POP	PON	POC
East Transect												
e1	14	29.42 (0.20)	0.180 (0.012)	0.852 (0.193)	2290 (11)	1994 (54)	0.197 (0.030)	9.86 (1.13)	93.18 (8.82)	1.258 (0.135)	38.24 (3.79)	276.27 (29.28)
e2	30	31.65 (0.15)	0.267 (0.015)	0.767 (0.200)	2241 (5)	2014 (4)	0.223 (0.007)	6.83 (0.18)	69.47 (2.01)	0.427 (0.005)	10.22 (0.74)	76.47 (4.09)
e3	46	32.23 (0.02)	0.210 (0.000)	0.515 (0.118)	2225 (10)	1998 (10)	0.200 (0.000)	5.39 (0.00)	69.96 (4.97)	0.310 (0.016)	6.10 (0.58)	50.91 (5.25)
e4	63	32.54 (0.02)	0.133 (0.005)	0.253 (0.068)	2210 (6)	2003 (5)	0.140 (0.006)	5.14 (0.96)	62.27 (3.75)	0.353 (0.024)	4.99 (0.36)	58.38 (3.69)
e5	94	32.88 (0.07)	0.120 (0.007)	0.213 (0.030)	2209 (12)	2018 (12)	0.120 (0.006)	4.69 (0.61)	57.72 (2.36)	0.210 (0.009)	2.99 (0.15)	30.32 (2.23)

When the data are plotted according to equation (2.3), a linear relationship is observed (Fig. 2.5). From the slope, the average K_x of 649 m^2 s^{-1} has an order of magnitude that is comparable to that found for many bays and estuaries (Officer, 1977). This estimated average K_x is also significantly different from zero. The y-intercept indicates the average K_y of only 97 m^2 s^{-1}, which is not significantly different from zero. This result supports the assumption that lateral mixing between water masses in the east and west halves of the bay is negligible. Because lateral mixing is insignificant, it is unnecessary to consider the advective term which is usually 2-3 times smaller than the mixing term.

Shear velocities calculated for the moving water-masses inside the six segments in the upper Gulf of Thailand (Table 2.3) vary between 0.25 and 1.92 m s^{-1}. These shear velocities give calculated $v_{ss}/(ku_*)$ values that are less than 0.1 (Table 2.3). From Fig. 2.2 the extreme K_i'/K_i range that corresponds to the maximum $v_{ss}/(ku_*)$ of 0.1 is between 0.8 and 1.3 (note that the y-axis in Fig. 2.1 is a $\log_{10}$ scale). Because the sea bed is neither a perfect reflecting nor a perfect absorbing bed but is intermediate between these two extreme states, the actual K_i'/K_i ratio could be closer to 1, e.g. Elder's (1959) results (Fig. 2.1). Thus, the K_i'/K_i ratio of 1 is accepted for particle transport models in the upper Gulf of Thailand.

Masses of the different forms of P, N, and C in the water column in each of the six segments are modeled according to equation (2.4). Statistical comparisons between the net uptake of dissolved inorganic nutrients and the net production of organic nutrients plus sediment removal are summarized in Table 2.4. The TA

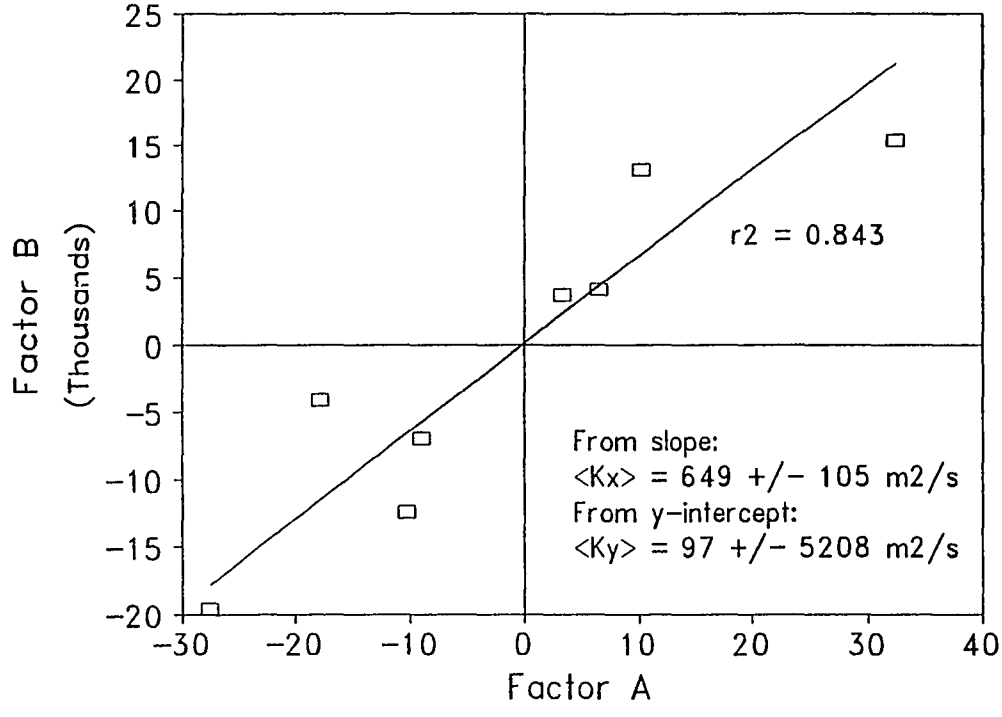

Figure 2.5. Numerical estimation of the average K_x and K_y for the upper Gulf of Thailand system. See equation (2.3) in text.

Table 2.3. Some hydrodynamic variables related to particle transport.

Segments	$\bar{z}$	$\bar{u}$	relative roughness		Reynolds	friction factor		u_*		$v_{ss}/(ku_*)$	
	m	m s^{-1}	min.	max.	Number	min.	max.	min.	max.	min.	max.
W-I	13	0.04	0.00077	0.00769	2.2×10^{6}	0.019	0.036	0.63	0.86	5.8×10^{-5}	4.0×10^{-2}
W-II	15	0.05	0.00067	0.00667	2.9×10^{6}	0.018	0.034	0.74	1.01	4.9×10^{-5}	3.4×10^{-2}
W-III	14	0.08	0.00071	0.00714	4.6×10^{6}	0.018	0.034	1.25	1.72	2.9×10^{-5}	2.0×10^{-2}
E-I	16	0.02	0.00063	0.00625	1.0×10^{6}	0.018	0.032	0.25	0.34	1.5×10^{-4}	9.9×10^{-2}
E-II	18	0.03	0.00056	0.00556	2.3×10^{6}	0.019	0.031	0.52	0.70	7.2×10^{-5}	4.8×10^{-2}
E-III	23	0.09	0.00043	0.00435	7.9×10^{6}	0.016	0.029	1.43	1.92	2.6×10^{-5}	1.8×10^{-2}

balance between net production in the water column and the flux from sediments is also included in Table 2.4.

Evidently the model developed in this study fails to balance C and TA masses in the upper Gulf of Thailand. Correlation coefficients obtained for these two chemical components are low, and the regression slopes are not significantly different from zero ($p > 0.05$; Table 2.4). This insignificance is due to small net uptake/release of TA and DIC compared with their levels in seawater. All DIC and TA varied by less than ± 100 mmol/meq m^{-2} d^{-1}, while the precision of the model (calculated by equation 2.7) was about ± 100 mmol/meq m^{-2} d^{-1} or greater.

The resolution of the mass balance model in this study is sufficient to establish non-zero slopes for P and N mass balances ($p < 0.05$; Table 2.4). As a result, the net reaction rates of these two elements can be further analyzed. When P data are analyzed with DOP excluded, even though the best-fit slope of -2.59 is not significantly different from -1 ($p > 0.1$; Table 2.4), data points are widely scattered and the regression line shows a poor fit to the data (Fig. 2.6a). When DOP is included in the analysis, the best-fit slope of -1.72 is also not significantly different from -1 ($p > 0.2$; Table 2.4), but the linearity is significantly improved (Fig. 2.6b). It seems that DOP does not behave conservatively in some segments in the upper Gulf of Thailand. Apparently, there is net DOP production in Segments W-I and E-II, and net DOP consumption in Segment E-III.

The P mass balance among segments in shown in Fig. 2.7. In this diagram, in order that the steady state P cycle be maintained, there must be a net P input into the

Table 2.4. Statistical analysis for the mass balance models. For P, N, and C, the net uptake of dissolved inorganic forms (as the X variable) is compared with the net production of organic forms plus sediment removal (as the Y variable). The transport of suspended particulates is calculated assuming a K_i'/K_i ratio of 1. Geometric mean regression analysis is performed to test the best-fit slopes from the expected slope of -1 by pooling data from all 6 segments together. For TA, the net TA production in the water column is compared with the benthic TA efflux from sediments. The expected slope for TA is +1.

	P balance w/o DOP	P balance w/ DOP	N balance w/ DON	C balance w/ DOC	TA balance
slope	-2.59	-1.72	-7.28	+1.81	+0.10
S.E.	0.84	0.47	1.55	0.90	0.04
r^2	0.578	0.706	0.818	0.004	0.314
Levels of significance for:					
slope = 0	$p<0.05$	$p<0.05$	$p<0.01$	$p>0.1$	$p>0.05$
slope = -1	$p>0.1$	$p>0.2$	$p<0.02$	$p<0.05$	$p<0.0001$ (from +1)

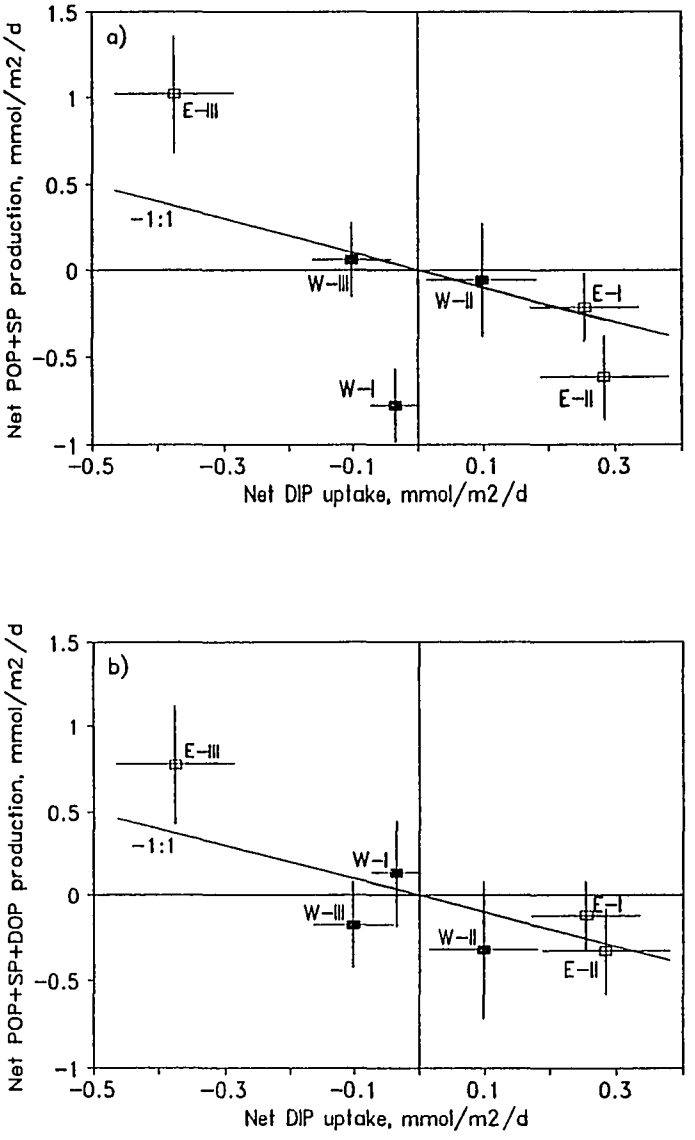

Figure 2.6. The phosphorus mass balance in the upper Gulf of Thailand with and without DOP included (upper and lower panels). The K_i'/K_i ratio of 1 is used for both models. Open and closed squares are for East and West transects, respectively. Error bars indicate the propagated standard error of estimations. Statistical analysis results of these data are summarized in Table 2.4.

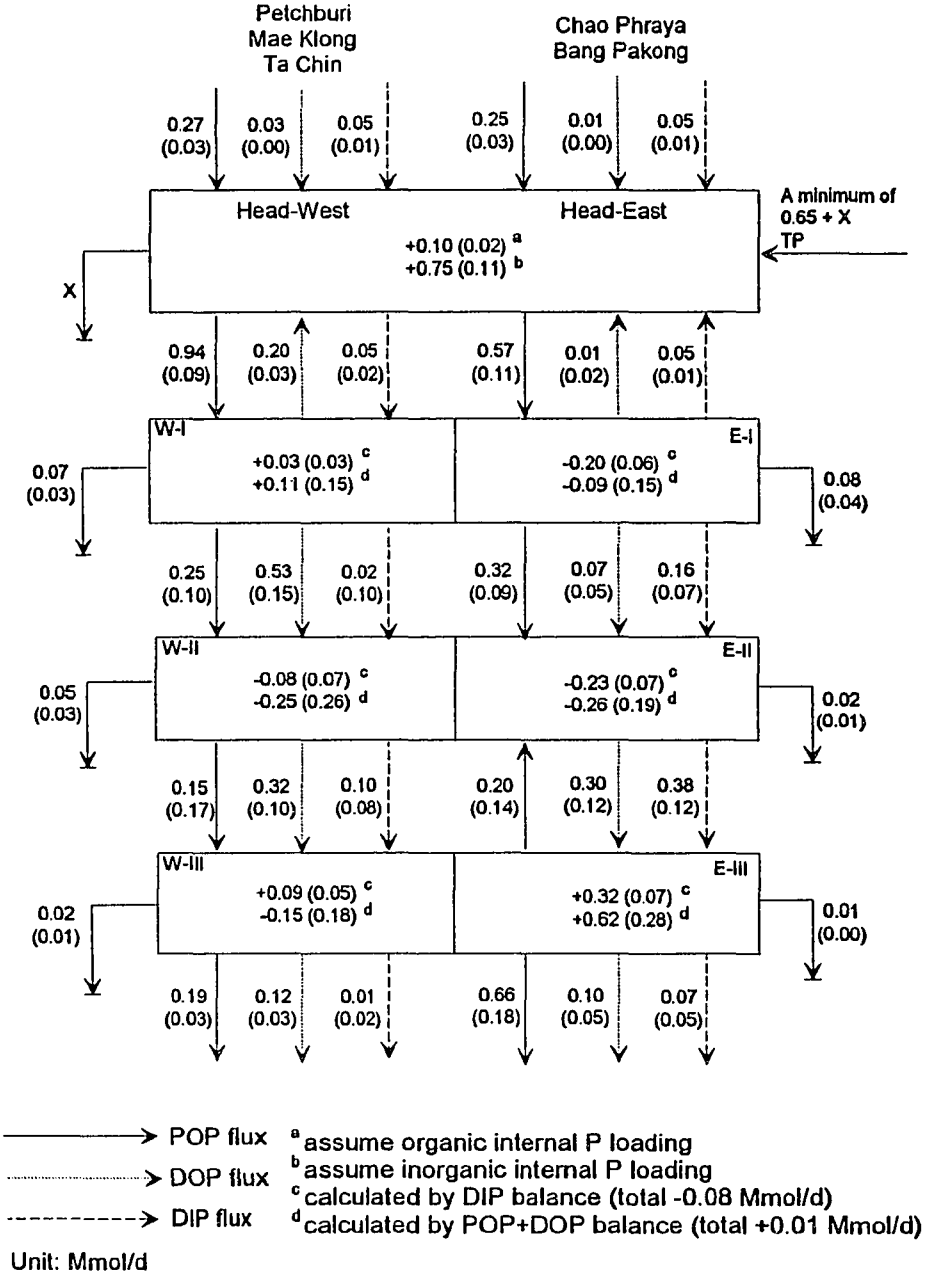

Figure 2.7. Phosphorus transfers among segments in the upper Gulf of Thailand. Numbers in parentheses are the propagated standard errors of the estimated rate. All units are in megamole per day.

head box of at least 0.65 megamole per day (Mmol d^{-1}), plus an unknown amount removed by estuarine and head-box sediments (X; Fig. 2.7). Some possible P sources will be discussed later. Also, in each lower segment in Fig. 2.7, the net organic P production rates calculated from DIP and from POP+DOP+SP mass balances are both shown. These two rates are usually not equal to each other, because they are independently estimated. Yet, the general agreement between the two rates can be seen in Fig. 2.6b.

Nitrogen cycling in the upper Gulf of Thailand, DON included, is summarized in Fig. 2.8. The net denitrification rates are generally higher in segments near the bay head and decrease toward the mouth. This trend is similar to that of sediment denitrification rates modeled in Chapter 3 (Fig. 2.9). However, most rates estimated from water column N in this chapter (except Segments E-I and E-III) are slightly higher than the rates estimated from sediments in the same general area. There are at least two possible explanations. First, the two data sets are from different years and different months of the year. Important factors that control the denitrification rate, such as organic matter delivery and O_2 supply to sediments (see Chapter 3), can vary greatly with time. Second, each estimated rate in this chapter is an integrated rate over an area of about 750 km^2, covering a wide range of habitats from the intertidal shoreline to the center of the bay. In contrast, the estimates in Chapter 3 are based on offshore sediments only. Denitrification rates may well be higher in the shallow-water coastal perimeter, where biological activity is generally higher than in the central portion of the bay.

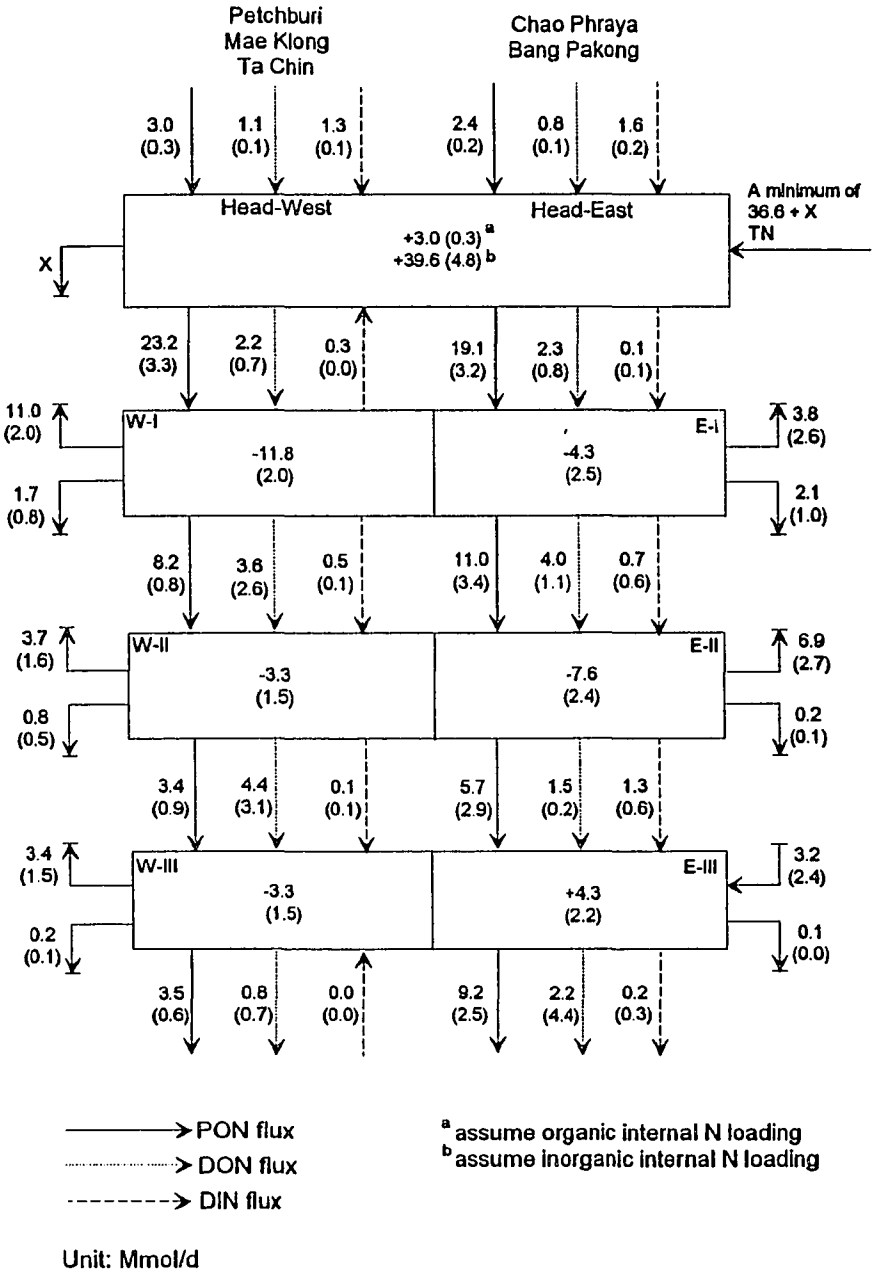

Figure 2.8. Nitrogen transfers among segments in the upper Gulf of Thailand. Numbers in parentheses are the propagated standard errors of the estimated rate.

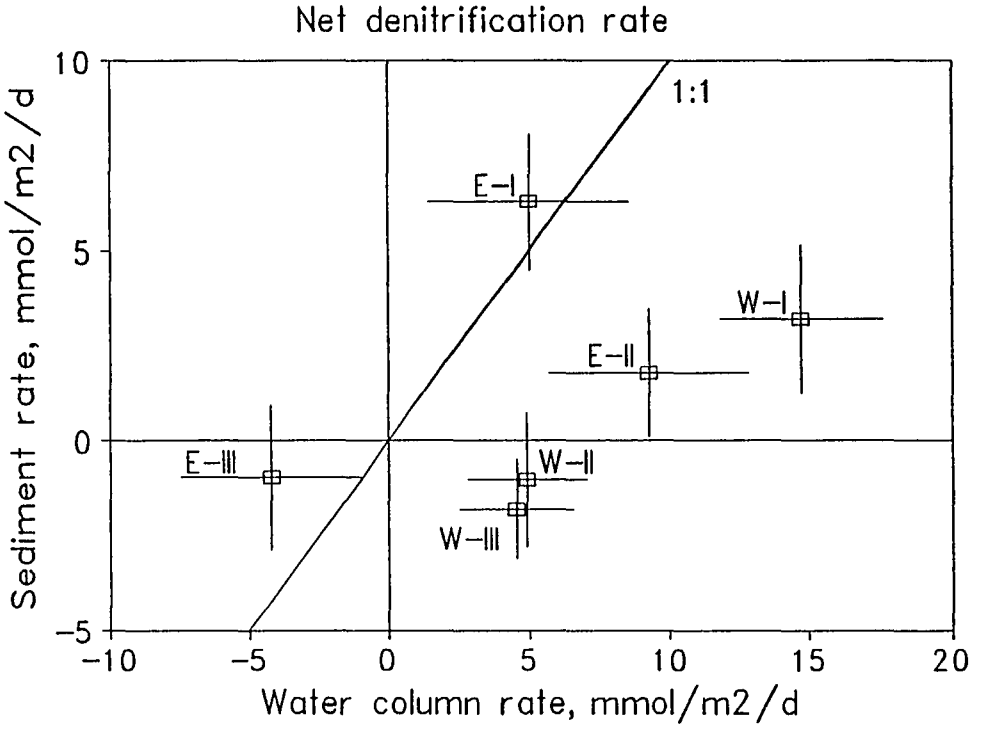

Figure 2.9. Comparison of net system denitrification rates estimated in this chapter (as x variable) with sediment denitrification rates estimated in Chapter 3 (as y variable) for the same general areas. Error bars indicate the propagated standard error of estimations.

Lastly, POC and DOC transfers among segments in the upper Gulf of Thailand are shown in Fig. 2.10. Unlike DIC and TA transfers, where the net changes are small relative to concentrations, the net POC and DOC production in most segments can be estimated with confidence using the hydrologic model. Organic carbon metabolism in the upper Gulf of Thailand will be fully discussed in subsequent sections of this chapter.

Discussion

Additional Nutrient Sources and Sinks

There must be some significant P, N and organic C sources supplying material to the head box and estuaries of the upper Gulf of Thailand (Figs. 2.7, 2.8 and 2.10). A plausible nutrient source may be that involving human activities in estuaries along the northern shoreline of the bay. According to the National Statistical Office (1991), in 1989 there were about 10.2 million registered residents in 9 provinces along the northern boundary of the upper gulf (Bangkok, Nakorn Pathom, Nonthaburi, Pathum Thani, Samut Prakan, Samut Sakorn, Samut Songkhram, Ratchburi and Chachoengsao). This dense urban nutrient source cannot be ignored.

Wollast (1983) estimated that, on a global average, P and N loading into rivers due to human activities is about 20 and 500 mol person^{-1} y^{-1}, respectively. By applying these rates to the 10.2 million population, the total P and N loadings would be 0.6 and 14 Mmol d^{-1}. More recently, Peierls et al. (1991) established another equation for DIN loading per capita. Using this equation, I found that DIN loading

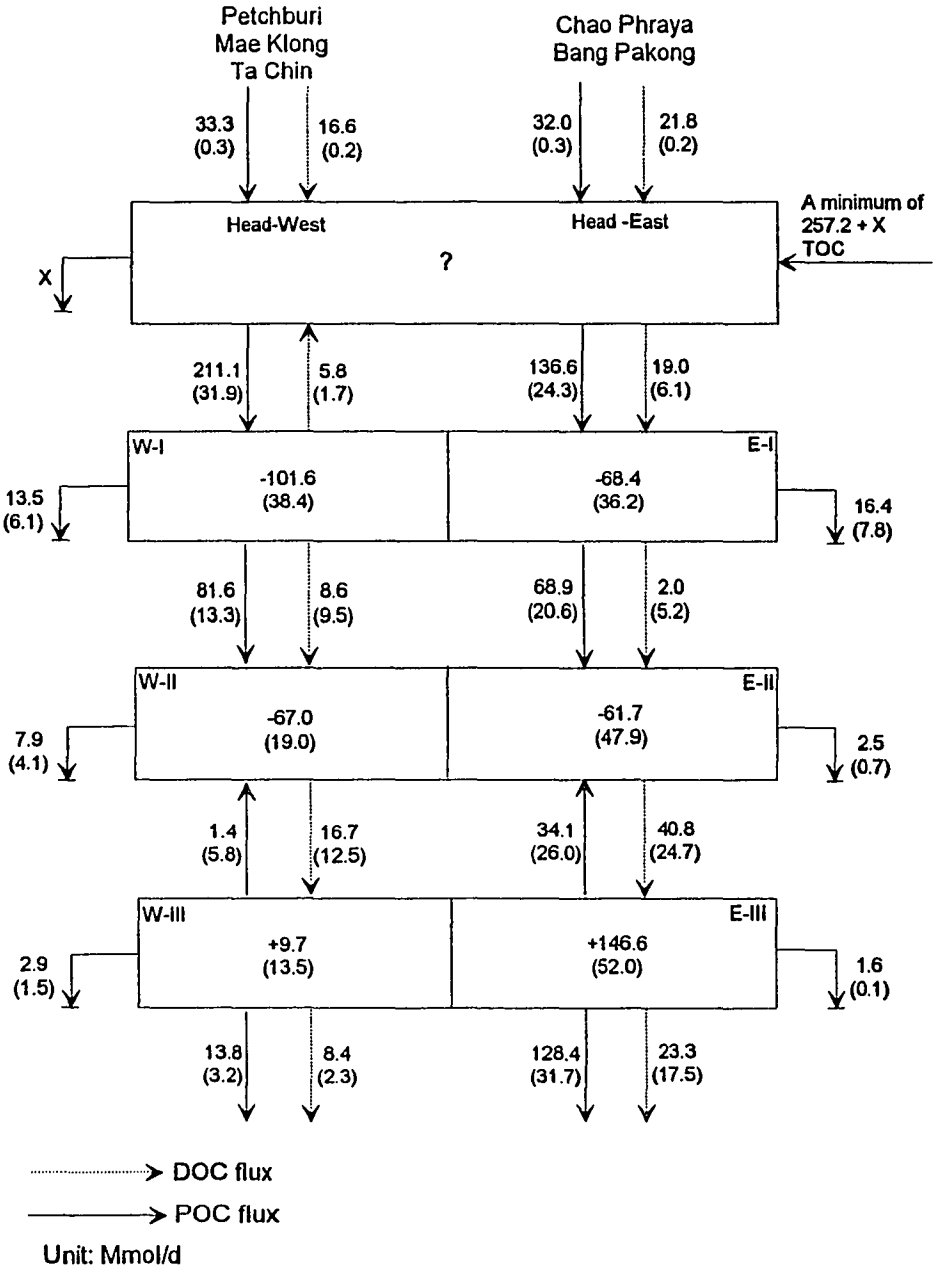

Figure 2.10. Organic carbon transfers among segments in the upper Gulf of Thailand. Numbers in parentheses are the propagated standard errors of the estimated rate.

based on an average human population density of about 2000 km^{-2} near the head of the upper Gulf of Thailand is only about 2 Mmol d^{-1}.

Another way to estimate the municipal P and N loadings may be from the point source BOD loading. It is estimated that the Bangkok Metropolis discharges approximately 250,000 kg BOD d^{-1} into Chao Phraya River via canals and sewer lines (Environmental Health Division, 1984; Menasveta, 1987). This is about one half of the total point source BOD loading by all towns near the five major river systems (Environmental Health Division, 1984). Therefore a total of about 500,000 kg BOD may be discharged into these rivers per day. The total P and total N in these wastes are not known but the average contents of the typical U.S. sewage of 50 g P and 200 g N per kg BOD (N:P molar ratio of 9:1; Laws, 1981; Thomann and Mueller, 1987) will be assumed. With these assumptions, the total point source P and N loadings into estuaries are 0.8 and 7 Mmol d^{-1}, respectively.

Non-point source nutrient loading is very difficult to quantify and the crude calculation made here may not be reliable. According to the review by Thomann and Mueller (1987), the average P and N loadings in the U.S. are 1 and 5 kg ha^{-1} y^{-1}, respectively, for urban areas, and 0.5 and 5 kg ha^{-1} y^{-1}, respectively, for agricultural areas. If 20% of the land area of 5000 km^2 bordering the bay head is urban area and 80% is agricultural area (there is no forested land), non-point source P and N loadings are approximately 0.03 and 0.5 Mmol d^{-1}, respectively. Both of these calculated inputs are small relative to point source nutrient loading.

From the above estimations, it can be seen that the minimum of 0.65 Mmol P d^{-1} required to balance the steady-state P cycle in the head-box (Fig. 2.7) could possibly be met by anthropogenic loading. However, for the N cycle, only 5 to 40% of the total needed (Fig. 2.8) can be provided from human sources. To some extent, the calculated anthropogenic N loading of 2 to 14 Mmol d^{-1} may be underestimated because I did not included the high N:P runoff from agricultural areas (Billen et al., 1991). There are several agricultural and husbandry (poultry) farming practices in the estuaries downstream to the river sampling stations in this study; however, there is no reliable way to quantify nutrient loading by these sources. In the following discussion, the upper limit of about 23 to 35 Mmol d^{-1} N will be assumed to be derived from some other unknown sources.

Planktonic N_2 fixation may partially offset the missing N input. The concentrations of planktonic blue-green algae (probably *Trichodesmium* spp.) in the upper Gulf of Thailand are in the range of 1-20 million trichomes m^{-3} (Boonyapiwat, 1984; Bhovichitra and Manowejbhan, 1984; Patarajinda, 1987), or a total of 3×10^{16} to 6×10^{17} trichomes for the head box volume of 3×10^{10} m^3. The N_2 fixation rate of *Trichodesmium* is approximately 30 pmol $trichome^{-1}$ d^{-1} (Carpenter, 1983). This gives a N_2 fixation range of 0.9 to 18 Mmol d^{-1}. This calculation indicates that planktonic N_2 fixation may contribute a significant amount of N into the upper Gulf of Thailand.

The contribution of N_2 fixation as a source of new N in marine ecosystems is controversial. On the one hand, many scientists believe that N_2 fixation in the plankton-based coastal environment may be insignificant (e.g., Capone and Carpenter,

1982; Howarth et al., 1988a). On the other hand, some scientists argue that N_2 fixation in the tropical ocean has been seriously underestimated (e.g., Carpenter and Romans, 1991). Temperature and the availability of some trace metals (particularly molybdenum) and organic molecules are thought to limit N_2 fixation rate (Paerl et al., 1987; Howarth et al. 1988b). At present, our understanding of the roles of limiting factors in N_2 fixation in tropical estuaries are too incomplete to allow further discussion of this topic. Further studies of this aspect of the N cycle in the upper Gulf of Thailand are strongly recommended.

Benthic N_2 fixation appears to be a minor N source in the head-box. Assuming a total intertidal area of 100 km^2 and an N_2 fixation rate in salt marshes of about 5 mmol m^{-2} d^{-1}, the total benthic fixation rate could be only 0.5 Mmol d^{-1}.

There is apparently net denitrification in the four segments between 14 and 46 km from the bay head (Segments W-I, W-II, E-I, and E-II; Fig. 2.8). The net denitrification rates in these segments are much larger than the horizontal DIN input rates (Fig. 2.8). Clearly, net denitrification in these segments is supported by organic N net produced in the head-box. From Fig. 2.9, it appears that most denitrification probably occurs in the sediments by converting DIN respiratory products into gaseous N. This process can be a significant DIN shunt out of the system and creates a DIN depleted water column (Nixon et al., 1976; Billen and Lancelot, 1985; Seitzinger, 1988; Smith and Hollibaugh, 1989).

Net Ecosystem Production in the Upper Gulf of Thailand and Some of Its Consequences

Phosphorus Metabolism

Regardless of the relative magnitude of organic and inorganic nutrient loading, the head-box always produces more organic P than it consumes via respiration (Fig. 2.7). Therefore, according to a conventional definition (e.g., Smith and Hollibaugh, 1993), the head-box is considered to be a net autotrophic ecosystem with respect to organic P production. The degree of autotrophy will be highest (+0.75 Mmol P d^{-1} which is equivalent to about +0.50 mmol P m^{-2} d^{-1} for the head-box area of 1500 km^2), if the head-box P loading is as DIP and lowest (+0.10 Mmol d^{-1} or about +0.07 mmol P m^{-2} d^{-1}), if the P loading is as organic P.

The head-box TOC:P loading ratio of 397:1 indicates that large amounts of C and P might be brought into the ecosystem as organic substances from outside rather than produced internally. This C:P loading ratio is too high to be generated by phytoplankton which have cellular C:P ratios near the Redfield ratio of 106:1. Although some organic matter might be produced by high C:P benthic macrophytes (Atkinson and Smith, 1983), these plants are not common in the upper Gulf of Thailand and would not able to satisfy the requirement. The only remaining sources are therefore land plant materials, which can have a C:P ratio as high as 900:1 (Lerman et al., 1989), and perhaps some C enriched domestic and industrial organic wastes (Polprasert, 1989). Because of the large organic loading, net autotrophy in the

head-box/estuaries compartment is probably nearer to the lower end, i.e. +0.101 Mmol P d^{-1}, than to the other extreme (+0.75 Mmol P d^{-1}).

When the organic P production in the head-box is combined with the sum of the other six segments of the bay, the overall net organic P production is between +0.03 and +0.76 Mmol P d^{-1} (data from Fig. 2.7). Hence, with respect to P, the upper Gulf of Thailand as a single unit is a net autotrophic coastal ecosystem. This may have something to do with the DIP uptake efficiency by primary producer populations. In the upstream freshwater environment, where P is likely to be the limiting nutrient (see later discussion), primary producers may be less efficient at taking up DIP, leaving high DIP concentrations in river water (>1 μM; Appendix B). In contrast, the marine phytoplankton population in the bay appears to be adapted to lower DIP concentrations than their freshwater counterparts. This efficiency difference initiates net DIP uptake as the water mass flows from rivers through the estuaries and the head-box. Even though there is net respiration of organic P (net heterotrophy) between 14 and 46 km from the bay head, DIP is reused efficiently and the ambient DIP concentration is maintained at about 0.1 to 0.2 μM (Table 2.2; Appendix B). Excess DIP regenerated over consumption in the mid-bay is either returned to the head-box or exported to the more seaward segments (Segments W-III and E-III) where DIP is consumed (Fig. 2.7). The upper Gulf of Thailand apparently supplies 1.07 Mmol d^{-1} POP+DOP but only 0.08 Mmol d^{-1} DIP to the lower gulf.

Besides the river system near the head of the upper gulf, there are at least six other significant rivers that drain into the lower Gulf of Thailand. These rivers are

the Pra Sae, Chantaburi, Pranburi, Chumporn, Tapi, and Pattani Rivers (Environmental Health Division, 1984; Siripong, 1988). The freshwater discharge by these rivers combined is about one half of that at the head of the gulf. There are no reliable data on the DIP, DOP and POP concentrations in most of these lower gulf rivers but according to the Environmental Health Division (1984), reactive PO_4^{3-} concentrations (unfiltered samples) in these rivers were all in the same range as those in five rivers at the head of the upper gulf. There is no reason to believe that the total P concentrations in these rivers may be unusually high. Therefore, a reasonable guess is that the total land-base P delivery to the lower gulf may be about 1.5 times that from the upper gulf alone, i.e. about 1.6 Mmol POP+DOP d^{-1} and 0.1 Mmol DIP d^{-1}. Up to 60% of the total P input could possibly be anthropogenic.

For a steady state total P mass in the water column, P input into the lower Gulf of Thailand must be balanced by sediment output and net exchange between the gulf and the South China Sea (Fig. 1.1). By taking the Pliocene to present sediment thickness of the lower Gulf of Thailand of about 0.5 km (ASEAN Council on Petroleum, 1981) and dividing that by 5 million years, the minimum long-term sedimentation rate is 0.1 mm y^{-1}. By assuming a sediment organic P content of 2 μmol g^{-1} (the value found in sediments near the mouth of the upper gulf), a solid density of 2.7 g cm^{-3} and a sediment porosity of 30% (an approximation for non-cemented sediments; Garrels and Mackenzie, 1971), the total P accumulation rate is about 1 μmol m^{-2} d^{-1} or 0.4 Mmol d^{-1} for the total area of 400,000 km^2. In addition

to sediments, some POP could also be exported; this export could bring the gross P input to somewhat more than 0.4 Mmol d^{-1}.

A comparison between the long-term sediment P accumulation rate of 0.4 Mmol d^{-1} and the pre-human P input from coastal waters of 0.7 Mmol d^{-1} (i.e., present-day total input rate minus anthropogenic loading) gives a net P export rate from the lower gulf into the South China Sea of about 0.3 Mmol d^{-1}. However, it is likely that most of the export in the past might have taken place during the glacial period when most of the bottom of the gulf was exposed and erosion was more effective (Broecker, 1982). Hence, POP accumulation in the Holocene sediments (i.e., after the last ice age but before the recent human perturbation) could have been faster than the long-term average rate of 0.4 Mmol d^{-1}, and the export rate could have been less than 0.3 Mmol d^{-1}. If this speculation is correct, during the periods of high sea level stands, the net P export from the Gulf of Thailand into the South China Sea could have been small or even in an opposite direction.

The recently increasing anthropogenic loading of P can significantly alter the P cycle in the lower gulf. However, it is not known if the system response to this perturbation is by increasing sediment removal rate, or by increasing the export flux to the South China Sea, or both. Studies of recent sediments and sedimentation rates in the lower gulf and of material exchange across the mouth could help answer this question.

Organic Carbon Metabolism

Even though the P balance points out that the upper Gulf of Thailand is net autotrophic, the net ecosystem metabolism of the bay with respect to C is more likely to be heterotrophic. In order for the entire upper Gulf of Thailand to be a net autotrophic ecosystem with respect to C, at least 142.2 Mmol C d^{-1} must be net produced in the head-box and preserved in its sediments (i.e., as X in Fig. 2.10). This possibility is rejected because of two lines of evidence. First, the actual accumulation rate of organic C in head-box sediments is probably much less than 100 Mmol C d^{-1}. This maximum rate is calculated by assuming that all of the annual sediment discharge by all rivers at the bay head of 7×10^{12} g y^{-1} (Windom et al., 1983) is deposited only in the head box. Authigenic material, mainly $CaCO_3$, is assumed to be 30% of the detrital sediments (most of the head-box sediments collected in this study actually contain less than 10 wt% $CaCO_3$). The organic C content is assumed to be 5 wt% (more than twice the highest organic C content ever measured in head-box sediments; see Chapter 3 of this dissertation, as well as Emery and Niino, 1963). Second, in order for the 142.2 Mmol C d^{-1} to be produced, an addition of about 1.3 Mmol DIP d^{-1} are required. This requirement (designated by X in Fig. 2.7) is in addition to the 0.65 Mmol total P d^{-1} already needed to balance the horizontal transport flux. Human activities in the coastal zone can explain not more 1 Mmol P d^{-1}, with some of this being organic P rather than DIP. There is apparently no way to rationalize an additional 1.3 Mmol DIP d^{-1} source term.

The possible range of net heterotrophy with respect to C of the upper Gulf of Thailand may be indirectly estimated from P transfer (Fig. 2.7). From an assumed molar C:P ratio of 106:1 for marine organic matter, the minimum and maximum net organic C production in the head-box are +10.7 and +79.4 Mmol C d^{-1}, respectively. Note that, in reality, the upper limit of +79.4 Mmol C d^{-1} is highly unlikely, because it implies that 177.8 Mmol C d^{-1} (257.2 minus 79.4) must be loaded into the head-box from external sources as "P-free" organic matter. Yet, it imposes an extreme upper boundary for the head-box net organic C production rate. When the head-box net ecosystem production is combined with that in the rest of the bay, the upper Gulf of Thailand is a net heterotrophic ecosystem by about -132 to -63 Mmol C d^{-1} (about -14 and -7 mmol C m^{-2} d^{-1}).

One reason for the net autotrophy with respect to C in the head-box but not in the entire bay may be that most of the organic C loading is not respired immediately but is either sedimented and preserved, or exported into the mid-bay segments where it is respired. Organic materials loaded into the head-box may be comprised largely of cellulose and woody materials which require a longer time to complete degradation than the water residence time (the bulk water residence time in the head-box is about 4 days). Also, some materials discharged into the head-box, such as floating debris, are concentrated near the sea surface. Because the water mass in the head-box is vertically stratified, material carried within the thin freshwater upper layer could be transported southward at a rate that is even faster than the bulk rate integrated over the whole water column. During the sampling cruises, floating debris of different

sizes ranging from a few millimeters to several meters was observed in abundance in the head-box. That debris eventually accumulated along the river plume front which moved back and forth across the lower boundary of the head-box. Organic degradation could be very high in that zone, and thus the net organic C metabolism could change abruptly from net autotrophy to net heterotrophy.

The contradiction that the upper Gulf of Thailand is a net autotrophic ecosystem with respect to P but a net heterotrophic ecosystem with respect to C can be explained. While net P autotrophy may be due to a higher DIP utilization efficiency in marine phytoplankton than in freshwater primary producers, the net C heterotrophy occurs because of the C:P ratio difference between marine and non-marine organic matter. Organic matter loaded into the head-box has a C:P ratio that is much higher than the ratio of about 100:1 produced by the marine community. Because P in the upper gulf water mass is tightly recycled, for each mole of P recycled, organic C respiration always exceeds DIC consumption by phytoplankton. By definition, the net ecosystem organic C production is net heterotrophic.

Another important point is that the recent increase in the organic material loading into the upper gulf could make the ecosystem more heterotrophic than in the past. Anthropogenic loading of inorganic nutrient directly into the bay is very small or absent. This conclusion disagrees with the scenario used in some global geochemical models where the assumption is made that there has been a recent increase in the inorganic nutrient loading into the coastal ocean making the ecosystem more autotrophic (e.g., Peterson and Melillo, 1985). The use of this assumption at

the global scale level, however, has been recently questioned by Smith and Hollibaugh (1992).

Aside from the controversy on the net trophic status of the global coastal ecosystem, the condition found in this study is a representative of many local organically "polluted" continental shelves. Many of these environments are located in developing countries, such as those in Southeast Asia, where agricultural and municipal waste treatments are primitive (Polprasert, 1989). Large cities such as Bangkok, Manila and Jakarta, for example, are coastal cities. Each of these cities, including its suburbs, has a population of around 10 million people, which is rapidly increasing. Because of poor waste management programs, these cities discharge large amounts of organic waste into the nearby seas. This discharge can strongly effect the net ecosystem metabolism.

Nutrient Limitation of Net Ecosystem Production

It is interesting to extrapolate some of the results of this study to a discussion of the continuing controversy involving N versus P limitation. Smith (1984) argued that if the water residence time in a marine ecosystem is long, N_2 fixation can offset any N shortages, and P will limit net ecosystem production (gross primary production minus total ecosystem respiration). Smith (1984) used three semi-enclosed autotrophic embayments (Shark Bay, Christmas Island and Canton Atoll) to support the argument that the time scale for a coastal ecosystem to develop a P-limited environment is comparable to the hydrologic time-scale in the ecosystem.

Nutrient limitation of net ecosystem production is quite a different concept from that of algal growth rate or primary production. While the latter definition refers to an acceleration of rate (usually with respect to organic C) due to inorganic nutrient addition, the limitation of net production refers to the effect of nutrient addition on the net mass transfer of nutrient elements required by plants from inorganic to organic pools. Because the definition does not directly involve a time variable, nutrient limitation of net production is a mass balance concept rather than a kinetic concept. The concept of net ecosystem production used here is not restricted only to C but may be applied to any element required by biological processes, e.g. N and P, as well.

I will define the nutrient that limits net ecosystem production as the nutrient that, when added to the ecosystem in a dissolved inorganic form, increases the net transfer of all nutrient elements from inorganic to organic pools. This net transfer for each element is termed the net ecosystem production with respect to that element. For P, which has no significant internal source or sink, the nutrient limitation concept is straightforward. If P limits net ecosystem production, an additional input of DIP will increase net ecosystem production of all nutrients. For N, internal source (N_2 fixation) and sink (denitrification) are both important. The ecosystem metabolism may not respond directly to DIN addition even though the net ecosystem production is limited by N.

The above definition of nutrient limitation of net ecosystem production requires an enrichment experiment before limiting nutrients can be identified. To

extrapolate this enrichment based concept to a static dataset collected at a point in time, some additional assumptions are necessary. The net removal of an inorganic nutrient DIM via net organic production and other dissimilatory reactions may be written as:

$$\Delta M = M_{net} + R_M \tag{2.8}$$

where: ΔM = the observed net DIM removal rate, M_{net} = the net ecosystem production of organic M, and R_M = the net dissimilatory consumption of DIM. Equation (2.8) concerns only the net mass transformation among organic, dissolved inorganic, and gaseous reservoirs. This is because from the hydrologic mass balance model, only net transformation rates among reservoirs, not the individual gross reaction rates, are obtained.

The residence time of M in the DIM pool (τ_M) with respect to non-conservative mechanisms is obtained by dividing equation (2.8) by total DIM mass, $V \cdot [DIM]$;

$$\frac{1}{\tau_M} = \frac{M_{net} + R_M}{V \cdot [DIM]} \tag{2.9}$$

where: V = system volume and $[DIM]$ = DIM concentration. The inverse of residence time term ($1/\tau_M$) in equation (2.9) is the fraction of inorganic nutrient mass removed per unit time. Thus, $1/\tau_M$ is also the first derivative of the net removal rate with respect to the DIM mass, i.e. sensitivity of the rate due to DIM at the time of observation. The nutrient element that has the smallest τ_M will have a net production most sensitive to the DIM mass in the ecosystem.

For a nutrient with a non-zero R_M, the residence time of M in the DIM pool is not directly related to the net production of organic M. Yet, $1/\tau_M$ is still a measurement of the intensity at which the DIM pool must operate in order to match the fraction of nutrient required by net production not supported by R_M. If the residence times of two nutrients (i.e., N and P) are compared, the nutrient that has a shorter residence time will have a dissolved inorganic pool that is more sensitive to non-conservative uptake than that of the other nutrient. Consequently, the nutrient with a shorter residence time will have an inorganic pool that is less available for net uptake and may have a higher potential to become a true limiting nutrient than the other nutrient with a longer residence time.

By combining equations (2.9) for N and for P and rearranging the results, we get

$$\frac{\tau_P}{\tau_N} = \frac{N_{net}}{P_{net}} \cdot \frac{[DIP]}{[DIN]} + \frac{R_N}{\Delta P} \cdot \frac{[DIP]}{[DIN]} \qquad (2.10)$$

The N_{net}:P_{net} ratio can be assumed to equal the local organic N:P ratio. The [DIP]:[DIN] ratio is taken directly from the observed data. Thus, to compare τ_P with τ_N, the only unknown in equation (2.10) is the term $R_N/\Delta P$.

In the marine region of the upper Gulf of Thailand (14km and beyond), the term (N_{org}:P_{org})×(DIP:DIN) is much larger than 1 (an average of about 10; Fig. 2.11). Also in this region of the bay, the net N gas fluxes are either not significantly different from zero or directed out of the system. These two findings ensure that the τ_P:τ_N ratios are much larger than 1, and hence P is less likely than N to be the

limiting nutrient, because net ecosystem production is less sensitive to the DIP pool than to the DIN pool.

In the head-box, the situation is different from the rest of the bay. The term $(N_{org}:P_{org})\times$(DIP:DIN) in the head-box is low, an average value of about 3 (Fig. 2.11). In addition, the N mass balance model (Fig. 2.8) indicates the possibility of high N_2 fixation in the water column (a negative R_N with a net positive ΔP). Therefore, it is possible, though not yet proved, that the $\tau_P:\tau_N$ ratio in the head-box may be less than unity, and net ecosystem production may be more sensitive to DIP than DIN. In other words, N may become less likely than P to be the limiting nutrient.

Most $\tau_P:\tau_N$ ratios for estuaries and rivers are low. From $(N_{org}:P_{org})\times$(DIP:DIN) values that are mostly less than 1 (Fig. 2.11), it is likely that the calculated $\tau_P:\tau_N$ ratios are less than one, i.e. a possibly P limited ecosystem, unless there are large net N degassing fluxes out of these brackish and fresh-water zones.

<u>Possible Causes and Consequences of N:P Ratio Variation in the Upper Gulf of Thailand</u>

Evidently the river water in this study is enriched with DIN relative to DIP (Fig. 2.12a). In all rivers, an ambient DIN:DIP ratio that is clearly higher than the local PON:POP ratio, as well as slightly higher than the Redfield 16:1 ratio, suggests the possibility that P might also limit primary production by phytoplankton. Once the

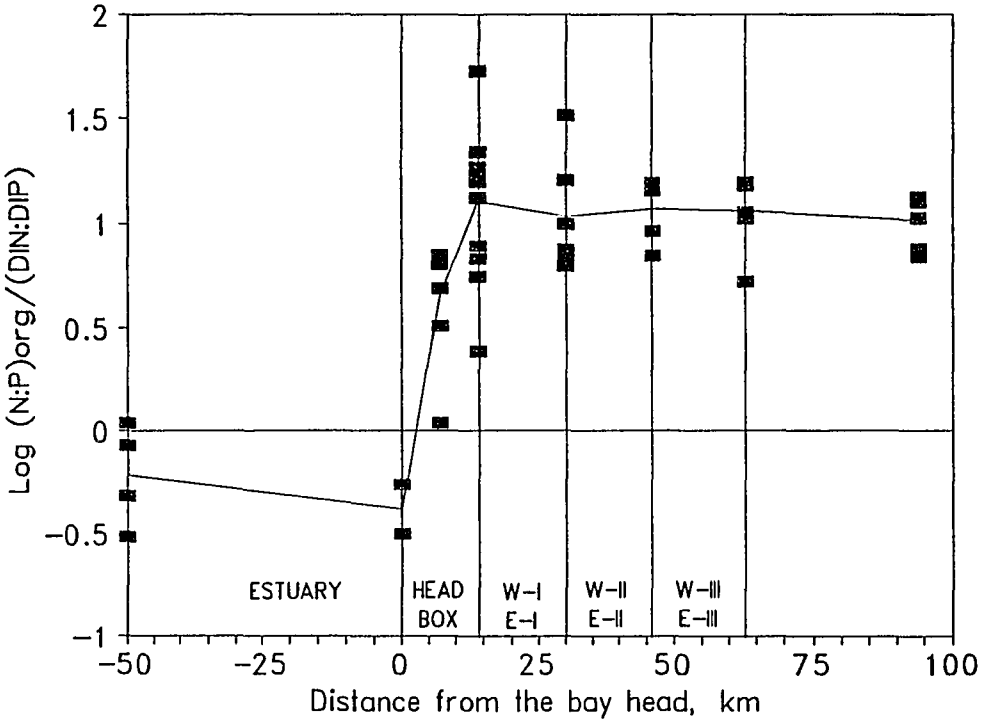

Figure 2.11. Logarithm of the relative N:P ratio between organic and inorganic pools as a function of the distance from the head of the Gulf of Thailand.

river water reaches the head-box, DIN is preferentially consumed relative to DIP and the DIN:DIP ratio decreases asymptotically from about 25 to about 3 at the interface between the head-box and Segments E-I and W-I (Fig. 2.12a). Much of the DIN consumed is probably stored in the high N:P ratio organic matter (near 30:1) found near the boundary between the head-box and Segments E-I and W-I (Figs. 2.12b and c). Because the DIN pool is much smaller than the organic N (DON+PON) pool, this preferential uptake of N by the organic reservoir may cause a DIN depleted condition with respect to phytoplankton uptake. In order to remain autotrophic, the head-box must acquire new N as DIN through sources such as N_2 fixation or anthropogenic DIN. This finding agrees with results of the N budget of the ecosystem discussed previously (Fig. 2.8).

The PON:POP ratios are low in rivers and estuaries but drastically increase in the head-box (Fig. 2.12). This trend is not consistent with the idea of switching of the nutrient that limits primary production, from P in freshwater to N in seawater. According to this idea, the PON:POP ratio would be expected to be lower in marine regions than in freshwater regions (e.g., Healey and Hendzel, 1980; Sakshaug and Olsen, 1986). Because the spatial variation in PON:POP ratio may not be explained by the concept of nutrient limitation of phytoplankton production, some alternate explanations are proposed.

A first explanation may be that the anthropogenic N and P loadings into rivers and estuaries are largely as organic sewage with a low N:P ratio, i.e. near 10. Recycling of these materials in rivers and estuaries may be slow relative to the

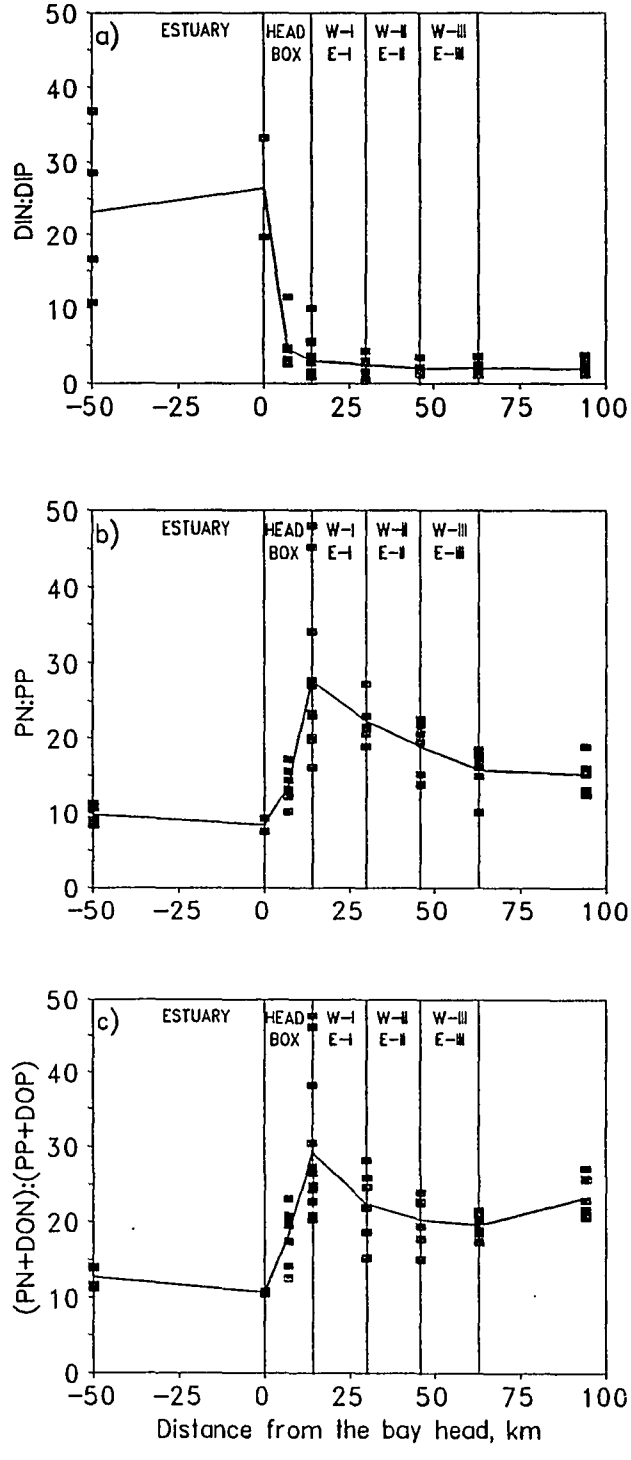

Figure 2.12. DIN:DIP (a), PN:PP (b) and (PN+DON):(PP+DOP) (c), versus distance from the head of the Gulf of Thailand.

loading rate, and thus the material still carries much of its original low N:P ratio. The second explanation may be DIP desorption from suspended particles entering marine water due to a lower ambient DIP concentration and changes in the particle's surface chemistry (Froelich, 1988). This process can raise the N:P ratio of a particle directly. The third explanation may be due the biomass of planktonic N_2 fixing cyanobacteria in the head-box may have a relatively high cellular N:P ratio than the ratio of average particles (Lindahl and Wallstrom, 1985; Downing and McCauley, 1992).

The seaward flank of the peaked PON:POP ratio gradually decreases until leveling off near the Redfield 16:1 ratio. This N:P ratio indicates a possibility that most of the suspended organic particulates away from river mouths are derived from marine plankton. A PON:POP ratio that is higher than the ambient DIN:DIP ratio for most of the bay suggests that the net primary production of these particulates may be limited by DIN availability.

Conclusion

Nitrogen and phosphorus mass balance modeling in the upper Gulf of Thailand and its estuaries reveals that river inputs account for only one half of the P requirement and only one fifth of the N requirement of the bay ecosystem. Anthropogenic nutrient loading in rivers and estuaries of the bay can explain all the P imbalance but not the N imbalance. Planktonic N_2 fixation by the dense *Trichodesmium* populations observed near the bay head is suggested as a probable significant natural N source.

Up to 90% of the P input to the bay may be organic P and the remaining fraction may be DIP. About 60% of the total P loading has an anthropogenic origin and occurs within the last 50 km stretch of the rivers where human activities are very intense. However, even with a largely organic P loading, the net ecosystem production of the bay with respect to P is autotrophic. This net autotrophy could be due to a higher DIP uptake efficiency by marine phytoplankton than that by freshwater plants and algae.

The bay net ecosystem production is heterotrophic with respect to C. This is tentatively explained by the net oxidation of C-enriched terrestrial and sewage organic matter (C:P $\approx$ 400:1) that outweighs the net primary production of marine organic matter with a C:P ratio near 100:1. Recent anthropogenic loading of organic materials into the bay causes the net ecosystem production, with respect to C, of the modern bay to be more heterotrophic than that during pre-human times. Sedimentation in the upper Gulf of Thailand removes only a small fraction of the organic material input at the bay head. Thus, the effect of this human perturbation is spread into the lower gulf and may extend outward as far as the South China Sea.

References

ASEAN Council on Petroleum 1981. Tertiary Sedimentary Basins of the Gulf of Thailand and South China Sea: Stratigraphy, Structure and Hydrocarbon Occurrences. Jakarta: ASEAN Council on Petroleum, 72 pp.

Atkinson, M. and Smith, S. V. 1983. C:N:P ratios of benthic marine plants. Limnol. Oceanogr. 28: 568-574.

Bhovichitra, M. and Manowejbhan, A. 1984. Phytoplankton in the east coast of the Gulf of Thailand. In: Tamiyavanich, S. (ed.) Proceeding of the Third Seminar on

the Water Quality and the Quality of Living Resources in Thai Waters. Bangkok: National Research Council of Thailand, pp. 229-246.

Billen, G., Lancelot, C. and Meybeck, M. 1991. N, P, and Si retention along the aquatic continuum from land to ocean. In: Mantoura, R. F. C., Martin, J.-M. and Wollast, R. (eds.) Ocean Margin Processes in Global Change. Chichester: John Wiley and Sons, pp. 19-44.

Billen, G. and Lancelot, C. 1985. Carbon-nitrogen relationships in nutrient metabolism of coastal marine ecosystems. Adv. Aquatic. Microbiol. 3: 263-322.

Boonyapiwat, S. 1984. Annual cycles and species composition of the phytoplankton in the Chao Phya Estuary and its adjacent waters. In: Tamiyavanich, S. (ed.) Proceeding of the Third Seminar on the Water Quality and the Quality of Living Resources in Thai Waters. Bangkok: National Research Council of Thailand, pp. 375-387.

Bowden, K. F. 1983. Physical Oceanography of Coastal Waters. Chichester: Ellis Horwood, 302 pp.

Broecker, W. S. 1982. Glacial to interglacial changes in ocean chemistry. Prog. Oceanogr. 11: 151-197.

Burns, N. M. and Rosa, F. 1980. In situ measurement of the settling velocity of organic carbon particles and 10 species of phytoplankton. Limnol. Oceanogr. 25: 855-864.

Capone, D. G. and Carpenter, E. J. 1982. Nitrogen fixation in the marine environment. Science 217: 1140-1142.

Carpenter, E. J. 1983. Nitrogen fixation by marine Oscillatoria (Trichodesmium) in the world's oceans. In: Carpenter, E. J. and Capone, D. G. (eds.) Nitrogen in the Marine Environment. New York: Academic Press, pp. 65-103.

Carpenter, E. J. and Romans, K. 1991. Major role of the cyanobacterium *Trichodesmium* in nutrient cycling in the north Atlantic Ocean. Science 254: 1356-1358.

Cuilen, M. R. 1985. Linear Models in Biology. Chichester: Ellis Horwood, 213 pp.

Downing, J. A. and McCauley, E. 1992. The nitrogen:phosphorus relationship in lakes. Limnol. Oceanogr. 37: 936-945.

Edmond, J. M. 1970. High precision determination of titration alkalinity and total carbon dioxide content of sea water by potentiometric titration. Deep-Sea Res. 17: 737-750.

Elder, J. W. 1959. The dispersion of marked fluid in turbulent shear flow. J. Fluid Mech. 5: 544-560.

Emery, K. O. and Niino, H. 1963. Sediments of the Gulf of Thailand and adjacent continental shelf. Geol. Soc. Am. Bull. 74: 541-554.

Environmental Health Division, 1983. Survey of the water quality in the estuary. In: Tamiyavanich, S. (ed.) Proceeding of the Third Seminar on the Water Quality and the Quality of Living Resources in Thai Waters. Bangkok: National Research Council of Thailand, pp. 62-78.

Fischer, H. B., List, E. J., Koh, R. C. Y., Imberger, J. and Brooks, N. H. 1979. Mixing in Inland and Coastal Waters. Orlando: Academic Press, 483 pp.

Fox, R. W. and McDonald, A. T. 1985. Introduction to Fluid Mechanics, Third Edition. New York: John Wiley & Sons, 741 pp.

Froelich, P. N. 1988. Kinetic control of dissolved phosphate in natural rivers and estuaries: A primer on the phosphate buffer mechanism. Limnol. Oceanogr. 33: 649-668.

Garrels, R. M. and Mackenzie, F. T. 1971. Evolution of Sedimentary Rocks. New York: W. W. Norton, 397 pp.

Graf, W. H. 1971. Hydraulics of Sediment Transport. New York: McGraw-Hill, 513 pp.

Healey, F. P. and Hendzel, L. L. 1980. Physiological indicators of nutrient deficiency in lake phytoplankton. Can. J. Fish. Aq. Sci. 37:442-453.

Howarth, R. W., Marino, R., Lane, J. and Cole, J. J. 1988a. Nitrogen fixation in freshwater, estuarine, and marine ecosystems. 1. Rates and importance. Limnol. Oceanogr. 33: 669-687.

Howarth, R. W., Marino, R. and Cole, J. J. 1988b. Nitrogen fixation in freshwater, estuarine, and marine ecosystems. 2. Biogeochemical controls. Limnol. Oceanogr. 33: 688-701.

Laws, E. A. 1981. Aquatic Pollution. New York: John Wiley and Sons, 482 pp.

Lerman, A., Mackenzie, F. T. and Geiger, R. J. 1989. Environmental chemical stress effects associated with carbon and phosphorus biogeochemical cycles. In: Levin, S. A., Harwell, M. A., Kelly, J. R. and Kimball, K. D. (eds.) Ecotoxicology: Problems and Approaches. New York: Springer-Verlag, pp. 315-350.

Lindahl, G. and Wallström, K. 1985. Nitrogen fixation (acetylene reduction) in planktic cyanobacteria in Öregrundsgrepen, SW Bthnian Sea. Arch. Hydrobiol. 104: 193-204.

Mehrbach, C., Culberson, C. H. Hawley, J. E. and Pythowicz, R. M. 1973. Measurements of the apparent dissociation constants of carbonic acid in seawater at atmospheric pressure. Limnol. Oceanogr. 18: 897-907.

Menasveta, P. 1987. Effects of water pollution on aquaculture development in Thailand. In: Sontirat, S. (ed.) Proceeding of the Fourth Seminar on the Water Quality and the Quality of Living Resources in Thai Waters. Bangkok: National Research Council of Thailand, pp. 368-378.

National Statistical Office, 1991. Statistical Yearbook Thailand, Number 38 (1991). Bangkok: National Statistical Office, 429 pp.

Neelasri, C. 1981. The mean flow in the upper part of the Gulf of Thailand during a transition period of the monsoon. In: Proceeding of the Second Seminar on the Water Quality and the Quality of Living Resources in Thai Waters. Bangkok: National Research Council of Thailand, pp. 57-63.

Nixon, S. W., Oviatt, C. A. and Hale, S. S. 1976. Nitrogen regeneration and the metabolism of coastal marine bottom communities. In: Anderson, J. M. and Macfadyen, A. (eds.) The Role of Terrestrial and Aquatic Organisms in Decomposition Processes. Oxford: Blackwell Scientific, pp. 269-283.

Officer, C. B. 1977. Longitudinal circulation and mixing relations in estuaries. In: Estuaries, Geophysics, and the Environment. Washington DC: National Academy of Science, pp. 13-21.

Paerl, H. W., Crocker, K. M. and Prufert, L. E. 1987. Limitation of N_2 fixation in coastal marine waters: Relative importance of molybdenum, iron, phosphorus, and organic matter availability. Limnol. Oceanogr. 32: 325-536.

Patarajinda, S. 1987. A study on phytoplankton occurred in red tide. In: Sontirat, S. (ed.) Proceeding of the Fourth Seminar on the Water Quality and the Quality of Living Resources in Thai Waters. Bangkok: National Research Council of Thailand, pp. 197-206.

Peierls, B. L., Caraco, N. I., Pace, M. L. and Cole, J. J. 1991. Human influence on river nitrogen. Nature 350: 386-387.

Peterson, B. J. and Melillo, J. M. 1985. The potential storage of carbon caused by eutrophication of the biosphere. Tellus 37: 117-127.

Polprasert, C. 1989. Organic Waste Recycling. Chichester: John Wiley and Sons, 357 pp.

Sakshaug, E. and Olsen, Y. 1986. Nutrient status of phytoplankton blooms in Norwegian waters and algal strategy for nutrient competition. Can. J. Fish. Aq. Sci. 43: 389-396.

Sayre, W. W. 1967. Dispersion of Mass in Open-Channel Flow. Ph.D. Thesis, Colorado State University.

Seitzinger, S. P. 1988. Denitrification in freshwater and coastal marine ecosystems: Ecological and geochemical significance. Limnol. Oceanogr. 33: 702-724.

Siripong, A. 1988. Seasonal variations of some hydrological, meteorological and oceanographical factors in southeast Asian seas and their effects on marine environment. Unpublished Manuscript, 86 pp.

Siripong, A. and Tamiyavanich, S. 1984. The variation of some physical properties of the sea water offshore of Ban Laem, Petchburi Province per tidal cycle. In: Tamiyavanich, S. (ed.) Proceeding of the Third Seminar on the Water Quality and the Quality of Living Resources in Thai Waters. Bangkok: National Research Council of Thailand, pp. 403-413.

Smith, S. V. 1984. Phosphorus versus nitrogen limitation in the marine environment. Limnol. Oceanogr. 29: 1149-1160.

Smith, S. V. and Hollibaugh, J. T. 1989. Carbon-controlled nitrogen cycling in a marine 'macrocosm': an ecosystem-scale model for managing cultural eutrophication. Mar. Ecol. Prog. Ser. 52: 103-109.

Smith, S. V. and Hollibaugh, J. T. 1993. Coastal metabolism and the oceanic organic carbon balance. Rev. Geophys. 31: 75-89.

Smith, S. V. and Kinsey, D. W. 1978. Calcification and organic carbon metabolism as indicated by carbon dioxide. In: Stoddart, D. R. and Johannes, R. E. (eds.) Coral Reefs: Research Methods. Paris: Unesco, pp. 469-484.

Smith, S. V., Kimmerer, W. J., Laws, E. A., Brock, R. E. and Walsh, T. W. 1981. Kaneohe Bay sewage diversion experiment: perspectives on ecosystem responses to nutritional perturbation. Pac. Sci. 35: 279-395.

Snedecor, G. W. and Cochran, W. G. 1980. Statistical Methods, Seventh Edition. Ames: The Iowa State University Press, 507 pp.

Sumer, B. M. 1974. Mean velocity and longitudinal dispersion of heavy particles in turbulent open-channel flow. J. Fluid Mech. 65: 11-28.

Thomann, R. V. and Mueller, J. A. 1987. Principles of Surface Water Quality Modeling and Control. New York: Harper and Row, 644 pp.

Walsh, T. W. 1989. Total dissolved nitrogen in seawater: a new-high-temperature combustion method and a comparison with photo-oxidation. Mar. Chem. 26: 295-311.

Windom, H. L., Silpipat, S., Chanpongsang, A., Smith, R. G. and Hungspreuks, M. 1984. Trace metal composition of and accumulation rates of sediments in the Upper Gulf of Thailand. Estuarine Coast. Shelf Sci. 19: 133-142.

Wollast, R. 1983. Interactions in estuaries and coastal waters. In: Bolin, B. and Cook, R. B. (eds.) The Major Biogeochemical Cycles and Their Interactions. New York: Wiley, pp. 385-407.

CHAPTER 3

COMPARISON OF BENTHIC NUTRIENT REGENERATION IN THE UPPER GULF OF THAILAND AND IN TOMALES BAY, WITH EMPHASIS ON NITROGEN CYCLING

Introduction

Sedimenting organic particles are a major source of inorganic nutrients released into porewaters of coastal sediments. Some of these regenerated nutrients in the sediment are transported back to the water column, support photosynthesis, and lead to continuing particle fallout. In many coastal environments, regeneration of nitrogen and phosphorus is particularly important, because the availability of these two nutrient elements for marine primary producers can be in limited supply (Ryther and Dunstan, 1971; Harrison et al., 1990; Howarth, 1988). However despite the fact that DIN and DIP are regenerated in sediments from organic materials which originally have a C:N:P ratio close to the uptake ratio, i.e. the Redfield Ratio of 106:16:1 (Redfield et al., 1963), the observed benthic DIC:DIN:DIP flux ratios are usually different from the C:N:P ratio of the source materials (e.g., Nixon, 1981; Dollar et al., 1991). This non-pararellism between the two ratios has consequences on local primary production as well as on the nutrient balance of the ecosystem of interest.

A bay-wide elemental mass balance study of the upper Gulf of Thailand (Chapter 2) reveals that net production of most of this system is more likely to be limited by N than by P. The model also suggests that benthic denitrification may be

responsible for significant N loss from the water-sediment system. In this chapter, N cycling in coastal sediments will be explored in detail, with the expectation that the mechanisms controlling N reactions in sediments can be delineated and quantified.

The contents of this chapter will be arranged in the following sequence:

- Review of some important factors that influence N and P cycling in marine sediments.
- Construction of sediment C, N, P stoichiometric regeneration models to be used in this study.
- Data acquisition in the Gulf of Thailand (a tropical bay) and Tomales Bay (a temperate bay) in order to evaluate the model's validity.
- Results, interpretation and evaluation of model validity.
- Extrapolation of the results of this study to a more generalized redox N cycling model for coastal sediments.

Benthic Phosphorus Regeneration

Oxidation of sediment organic matter is undoubtedly a very important source of recycled DIP in most coastal sediments (e.g., Nixon et al., 1980; Smith et al., 1981; Dollar et al., 1991; Kemp and Boynton, 1992). However, it is possible that the benthic flux ratio between DIP and calcification-corrected DIC is different from the organic P:C ratio in sediments. A DIP:DIC flux ratio that is lower than the P:C ratio of source materials might be due to various DIP reactions involving solid phases in the sediments. Some possible reactions are sorption of DIP by solid phases especially oxidized Fe minerals (Caraco et al., 1990), formation of authigenic P

minerals (Ruttenberg and Berner, 1993), and formation of refractory organic P compounds (Froelich et al., 1982).

Benthic Nitrogen Regeneration

Nitrogen cycling in marine sediments is far more complex than phosphorus cycling. Nitrogen can exist in natural environments in any oxidation state from -III to +V (Webb, 1981). The occurrence of N_2 and other forms of gaseous nitrogen further complicates the N mass balance, as the measured DIN:DIC flux ratio, even after sorption correction, may not reflect the decomposing organic N:C ratio.

Nitrogen degassing in aquatic environments is usually through biological dissimilatory NO_3^- reduction that produces gaseous nitrogen such as N_2, N_2O and NO. These nitrogen degassing mechanisms are generally referred to as "denitrification" (Knowles, 1982; Seitzinger, 1988; Koike and Sørensen, 1988). Because denitrification acquires electrons from reduced organic compounds, denitrification is frequently considered a suboxic respiration reaction.

Nitrate sources for sediment denitrification can be external as well as internal. In sediments overlain by NO_3^- seawater, such as deep-sea sediments, uptake across the sediment-water interface is usually an important NO_3^- source (e.g., Christensen et al., 1987). In some nearshore sediments, groundwater can introduce NO_3^- into the system (e.g., Capone and Slater, 1990). In addition to these external sources, NO_3^- in sediments can be formed *in situ* by oxidation of NH_4^+--the proximate DIN product of organic respiration--using O_2 as the terminal electron acceptor. This pathway is generally referred to as nitrification.

In many coastal, estuarine, and lacustrine sediments, especially those overlain by NO_3^--depleted water, calculated or observed denitrification rates can be much greater than the actual NO_3^- uptake flux across the sediment-water interface (Kaspar et al., 1985; Christensen et al., 1987; Hopkinson, 1987; Seitzinger, 1988, 1990; Dollar et al., 1991, but see also Nishio et al., 1983). This indicates that nitrification is a critically important NO_3^- source, and thus denitrification in those sediments may have nitrification as a rate limiting step.

If the coupling between net nitrification:

$NH_4^+ + 3H_2O \longrightarrow NO_3^- + 8e^- + 10H^+$,

and denitrification:

$NO_3^- + 5e^- + 6H^+ \longrightarrow 0.5N_2 + 3H_2O$,

in sediments is without a significant net NO_3^- flux across the sediment-water interface, then for each mole of N atoms emitted as $N_2(g)$, three moles of electrons created by nitrification are left behind. The overall reaction (net denitrification) is not complete until all electrons are accommodated. This makes sediment denitrification supported by an internal NO_3^- source different from that supported by external sources. In sediments dominated by internally produced NO_3^-, net denitrification does not represent a complete respiration because electrons cannot be balanced by N reactions without an ultimate electron acceptor, particularly O_2. However, both types of denitrification, regardless of the NO_3^- sources, are DIN sinks via degassing.

It is apparent that, in sediments, there are redox relationships among organic C oxidation, N reactions, and net consumption of various oxidants. In this chapter

biologically mediated N and C reactions in seemingly "oxidant limited" coastal sediments will be studied by electron balance modeling, together with the conventional conservation of mass approach (Prigogine, 1967; Helgeson, 1968). Because the experiments in this chapter were designed to study biogeochemical reactions in sediments at the functional level, the results do not necessarily represent the regional average. One must be very cautious in extrapolating the results of the individual incubations of this study to calculations of system-wide metabolism. There are many disadvantages in the summation of individual components, compared with the system-wide mass balance approach, in the estimation of net system metabolism. Some of the important disadvantages are: 1. individual incubations can be seriously biased in a patchy environment (Smith et al., 1991), 2. propagation of errors may become large, so that the estimated net system metabolism is statistically insignificant (Smith and Mackenzie, 1987), and 3. the time scale of elemental cycling in a small benthic incubator, with respect to the sediment surface area, may be much shorter than the actual time scale of cycling in the whole water column with respect to the same sediment area.

Benthic Carbon and Nitrogen Redox Models

I assume that the mass balances of C and N in sediments are controlled by three important half-cell reactions:

Reaction 1--Net organic carbon oxidation (respiration minus primary production)

$$CH_2O + H_2O \longrightarrow CO_2 + 4e^- + 4H^+$$

Reaction 2--Denitrification

$NO_3^- + 5e^- + 6H^+ \longrightarrow 0.5N_2 + 3H_2O$

Reaction 3--Net nitrification (nitrification minus ammonification)

$NH_4^+ + 3H_2O \longrightarrow NO_3^- + 8e^- + 10H^+$.

Other oxidation states of N besides N(+V) as in NO_3^-, N(0) as in N_2 gas, and N(-III) as in NH_4^+ and "organic N", are usually much less important (Seitzinger, 1988) and will be neglected.

The net electrons produced by these three steps must be accommodated by oxidants available in sediments. Normally, available oxidants are utilized in the sequence according to the net energy gained (Mackenzie and Wollast, 1977; Froelich et al., 1979).

Utilization of an aqueous oxidant usually can be estimated from the net flux of oxidant or its product across the sediment-water interface. The two most important aqueous oxidants in marine systems are O_2 and SO_4^{2-}, and the reduction of these two species can be written as:

Reaction 4--Oxygen reduction

$O_2 + 4e^- + 4H^+ \longrightarrow 2H_2O$

and, Reaction 5--Sulfate reduction

$SO_4^{2-} + 8e^- + 10H^+ \longrightarrow H_2S + 4H_2O$.

Another reduction reaction whose net progress can be estimated from the flux of products across the sediment-water interface is:

Reaction 6--CO_2 reduction (methanogenesis)

$CO_2 + 8e^- + 8H^+ \longrightarrow CH_4 + 2H_2O$.

Another CH_4 source, methanogenesis via acetate "splitting", is ignored because in marine systems CH_4 formed this way is much less abundant than CH_4 formed by CO_2 reduction (Crill and Martens, 1986; Whiticar et al., 1986). This is true because most acetate in marine sediments is oxidized by SO_4^{2-} reduction. By the time SO_4^{2-} is exhausted, only a small amount of acetate usually remains available for methanogenesis (Sansone and Martens, 1981).

The excess oxidation that cannot be accounted for by reactions 4 to 6 is assumed to be offset by the net reduction of solid mineral phases such as Fe_2O_3, FeOOH and MnO_2 (see reviews by Lovley, 1987 and Ehrlich, 1987 for more references).

<u>O_2 Reduction</u>

This respiration mode assumes all electrons generated by organic carbon oxidation (reaction 1) are taken only by O_2 reduction.

The electron balance for carbon redox is:

$$4 \cdot \xi_1 - 4 \cdot \xi_4 = 0 \qquad (3.1)$$

where ξ_i is the extent of reaction i in the system (Prigogine, 1967). Secondly, the steady state DIC balance is:

$$\xi_1 = B_{DIC} \tag{3.2}$$

where B_{DIC} is the net DIC (i.e., $CO_2+HCO_3^-+CO_3^{2-}$) efflux across the sediment-water interface, positive upward. Lastly, the steady state O_2 balance is:

$$\xi_4 = - B_{O_2} \tag{3.3}$$

where B_{O2} is the net O_2 efflux across the sediment-water interface.

By combining equations (3.1), (3.2) and (3.3), the following linear equation for the oxic respiration of organic carbon is obtained:

$$B_{O_2} = - B_{DIC} \tag{3.4}$$

The hypothesis that O_2 reduction alone is sufficient for CH_2O reduction in sediment can be tested by fitting equation (3.4) to observed B_{DIC} and B_{O2} data. The expected slope of -1 will be taken as the criterion to accept/reject the hypothesis that O_2 reduction alone is sufficient to explain organic C oxidation in sediments.

When nitrogen reactions (reactions 2 and 3) are also taken into consideration, the electron balance for the oxic respiration of carbon plus denitrification can be written as:

$$4\cdot\xi_1 - 5\cdot\xi_2 + 8\cdot\xi_3 - 4\cdot\xi_4 = 0 \tag{3.5}$$

The steady state NO_3^- balance in sediments is:

$$- \xi_2 + \xi_3 = B_{NO3\bullet} \tag{3.6}$$

where $B_{NO3\bullet}$ is the actual net NO_3^- production. Because NO_3^- adsorption by sediments is probably small (e.g., Berner, 1980), $B_{NO3\bullet}$ can be assumed to equal B_{NO3}, the observed NO_3^- efflux across the sediment-water interface, and thus:

$$- \xi_2 + \xi_3 = B_{NO3} \tag{3.7}$$

The steady state NH_4^+ balance in sediments is a function of organic N remineralization and nitrification, such that:

$$a \cdot \xi_1 - \xi_3 = B_{NH4\bullet} \tag{3.8}$$

where a is the actual N:C of decomposing organic matter and $B_{NH4\bullet}$ is the stoichiometric NH_4^+ benthic flux without sorption. Because NH_4^+ might be significantly retained by the sediment, largely via adsorption (Rosenfeld, 1979; Laima, 1992), the relationship between $B_{NH4\bullet}$ and the observed NH_4^+ efflux across sediment-water interface (B_{NH4}) assuming a linear removal will be:

$$B_{NH4\bullet} = \frac{B_{NH4}}{1 - f} \tag{3.9}$$

where f is the fraction of the produced NH_4^+ that is removed by sediment sorption.

By combining equations (3.8) and (3.9), the net NH_4^+ balance becomes:

$$a \cdot \xi_1 - \xi_3 = \frac{B_{NH4}}{1 - f} \tag{3.10}$$

The linear equation for carbon and nitrogen redox reactions with respect to O_2 reduction derived from equations (3.2), (3.3), (3.5), (3.7) and (3.10) is:

$$3 \cdot \frac{B_{NH4}}{1 - f} - 5 \cdot B_{NO3} - 4 \cdot B_{O2} = (3a + 4) \cdot B_{DIC} \qquad (3.11)$$

We may use the same statistical arguments as in the case of O_2 reduction (equation 3.4) to estimate decomposing N:C from the slope of equation (3.11) for different values of f. Note that we cannot solve for both variables a and f simultaneously by dividing equation (3.11) by B_{DIC} and performing a regression analysis for slope and intercept. By doing so, the variances for the new variables, B_{NH4}/B_{DIC} and $(-5 \cdot B_{NO3} - 4 \cdot B_{O2})/B_{DIC}$, are not uniform but approach ∞ as B_{DIC} approaches 0, and approach 0 as B_{DIC} approaches ∞. Therefore one assumption for a regression analysis is violated.

A realistic range for f, the removal constant for NH_4^+ by sediments, can be estimated from published data on sorbed NH_4^+ on solid particles, and on dissolved NH_4^+ in porewater. The normal NH_4^+ content of marine sediments is about 400 $\mu g\ g^{-1}$ (Muller, 1977; Rosenfeld, 1979; Laima, 1992). To maximize the value of f, all particulate NH_4^+ is assumed to be sorbed NH_4^+. With the sedimentation rate of about 1 $g\ cm^{-1}\ y^{-1}$ for both the Gulf of Thailand (this study) and Tomales Bay (Snidvongs et al., ms.) sediments, the maximum NH_4^+ removal by particle adsorption is about 1 $mmol\ m^{-2}\ d^{-1}$. The NH_4^+ concentration in porewater that is in equilibrium with this adsorption can be estimated by a linear adsorption isotherm. To maximize the concentration, the lowest adsorption coefficient for coastal sediments of about 0.2 (Rosenfeld, 1979; Blackburn, 1986; Seitzinger et al., 1991) will be used. With a deep sediment porosity of about 0.5, NH_4^+ removal due to porewater burial is at most

about 2 mmol m^{-2} d^{-1}. If the average NH_4^+ efflux across the sediment-water interface is 2 mmol m^{-2} d^{-1}, the maximum value for f should be about (1+2)/(1+2+2) = 0.6.

Justification of the O_2 + NO_3^- reduction model can be made by comparing the best-fit a with a reasonable range of organic N:C ratios, such as the Redfield N:C ratio of 16:106.

<u>O_2 + SO_4^{2-} Reduction</u>

If organic carbon oxidation in sediments is not balanced by O_2 reduction or O_2 + NO_3^- reduction, SO_4^{2-} reduction (reaction 5) is added, and the new electron balance, without N reactions, would be:

$$4\cdot\xi_1 - 4\cdot\xi_4 - 8\cdot\xi_5 = 0. \qquad (3.12)$$

The steady state DIC and O_2 balances for this model are exactly the same as in the previous O_2 model, i.e. equations (3.2) and (3.3). The steady state SO_4^{2-} balance in the sediments is:

$$\xi_5 = - B_{SO4}. \qquad (3.13)$$

where B_{SO4} is the net SO_4^{2-} production by the sediments.

Because the sorption of SO_4^{2-} by particles is small (Li and Gregory, 1974), the net SO_4^{2-} production is assumed to equal the net SO_4^{2-} efflux across the sediment-water interface (B_{SO4}). Moreover, for each mole SO_4^{2-} added or removed from the solution the total alkalinity (TA) is decreased or increased by 0.5 equivalents. This enables us to estimate B_{SO4} using the TA flux after correcting for $CaCO_3$ reactions and nutrient effects (Berner et al., 1970). Hence,

$$\xi_5 = - B_{SO4} = \frac{B_{TA}}{2}. \tag{3.14}$$

By combining equations (3.2), (3.3), (3.12) and (3.14), the equation:

$$B_{TA} - B_{O2} = B_{DIC} \tag{3.15}$$

for $O_2 + SO_4^{2-}$ respiration can be derived. A similar statistical argument as in the oxic respiration model (equation 3.4) can also be applied here to test the hypotheses that the best-fit slope equals 1.

The electron balance for the $O_2 + SO_4^{2-}$ reduction of organic carbon oxidation and denitrification is:

$$4 \cdot \xi_1 - 5 \cdot \xi_2 + 8 \cdot \xi_3 - 4 \cdot \xi_4 - 8\xi_5 = 0. \tag{3.16}$$

Mass balances for DIC, O_2, NO_3^-, NH_4^+, and SO_4^{2-} were given by equations (3.2), (3.3), (3.7), (3.10), and (3.14), respectively. Therefore:

$$3 \cdot \frac{B_{NH4}}{1 - f} - 5 \cdot B_{NO3} - 4 \cdot B_{O2} + 4 \cdot B_{TA} = (3a + 4) \cdot B_{DIC}. \tag{3.17}$$

The slope term of equation (3.17) can be estimated by an appropriate statistical technique. The estimated slope is compared with theoretical stoichiometry, determined by the decomposing organic N:C ratio, in order to test the hypothesis that $O_2 + SO_4^{2-} + NO_3^-$ reduction is an appropriate respiration model for organic carbon respiration in sediments.

$O_2 + SO_4^{2-} + CO_2$ Reduction

If the combination of O_2 and SO_4^{2-} reduction and denitrification is still not sufficient to account for all the electrons generated by organic carbon oxidation, CO_2 reduction to CH_4 (reaction 6) is included in the array of reactions. The electron balance without NO_3^- reduction is therefore:

$$4\cdot\xi_1 - 4\cdot\xi_4 - 8\cdot\xi_5 - 8\cdot\xi_6 = 0. \tag{3.18}$$

The steady state O_2 and SO_4^{2-} balances for the model will be the same as in the O_2 + SO_4^{2-} model (equations 3.3 and 3.14). However, with the generation of CH_4, B_{DIC} is no longer an indicator for organic carbon decomposition; instead, dissolved inorganic phosphorus (B_{DIP}) will be used. Because a significant fraction of regenerated DIP can be retained in the sediment, such as by adsorption (Krom and Berner, 1981; Caraco et al., 1990) and authigenic formation of fluorapatite (Ruttenberg and Berner, 1993), observed DIP flux at the sediment-water interface (B_{DIP}) will be less than the DIP production (B_{DIP^*}). The steady state DIP balance corrected for a linear removal by sediments is:

$$b\cdot\xi_1 = \frac{B_{DIP}}{1 - g} \tag{3.19}$$

where b is the P:C ratio of decomposing organic material and g is the fraction of regenerated DIP removed by the sediments. The DIC balance will be a function of organic carbon degradation (reaction 1) and CO_2 reduction (reaction 6):

$$\xi_1 - \xi_6 = B_{DIC} \cdot \tag{3.20}$$

The linear diagenetic equation without N reactions derived from equations (3.3), (3.14), (3.18), (3.19) and (3.20) is:

$$2 \cdot B_{DIC} + B_{O2} - B_{TA} = \frac{1}{b} \cdot \frac{B_{DIP}}{1 - g}. \tag{3.21}$$

The statistical approach to test the hypothesis that organic carbon oxidation in sediments is coupled with O_2 + SO_4^{2-} + CO_2 reduction is similar to the approach used in previous redox models.

A calculation similar to one used to calculate f can be done for the maximum value for g. The maximum content of adsorbed DIP in well oxidized marine sediments is about 2 μmol g^{-1} (Krom and Berner, 1980; Strom and Biggs, 1982; S. Vink, personal communication). Therefore, for the sedimentation rate of 1 g cm^{-2} y^{-1}, DIP removal by sediment adsorption is about 0.06 mmol m^{-2} d^{-1}. With the smallest reported adsorption coefficient of about 1 (Krom and Berner, 1980) and sediment porosity of 0.5, the removal of DIP by porewater is at most about 0.03 mmol m^{-2} d^{-1}. The average observed DIP efflux across the sediment-water interface in this study is about 0.2 mmol m^{-2} d^{-1}; therefore the maximum value for g is about (0.06+0.03)/(0.06+0.03+0.2) = 0.3.

The electron balance if nitrogen redox reactions are included is:

$$4\cdot\xi_1 - 5\cdot\xi_2 + 8\cdot\xi_3 - 4\cdot\xi_4 - 8\cdot\xi_5 - 8\cdot\xi_6 = 0. \qquad (3.22)$$

Finally the linear equation for carbon and nitrogen diagenesis in the sediment, when O_2, SO_4^{2-} and CO_2 reductions are included, can be derived from equations (3.3), (3.7), (3.10), (3.14), (3.19), (3.20) and (3.22) as:

$$3\cdot\frac{B_{NH4}}{1-f} - 5\cdot B_{NO3} - 4\cdot B_{O2} + 4\cdot B_{TA} - 8\cdot B_{DIC} = (\frac{3a-4}{b})\cdot\frac{B_{DIP}}{1-g}. \qquad (3.23)$$

Methods

Benthic Flux Measurements in the Upper Gulf of Thailand

Benthic flux measurements were performed at seven stations in the Upper Gulf of Thailand (Fig. 3.1) between 21 and 25 September 1991. These stations were chosen such that they represented two major benthic environments: 1) the "offshore" environment, where sediments are dominated by coarse-grained biogenic $CaCO_3$, with relatively low organic content (Stations 1, 2 and 3); and 2) the near-river benthic environments, where sediments were poorly sorted and organic contents are generally higher (Station 5 and 6). The remaining two stations--Station 4 and 7--were intermediate between these two major sediment types.

Flux chambers were made from cylindrical opaque PVC pipes with a cross sectional area of 127 cm^2. The total length of the chamber was 35 cm. The chamber caps were made from PVC plumbing pipe caps. Each chamber cap had two small holes fitted with Tygon tubing. The external end of each tube was connected to a 140 ml polyethylene syringe. One syringe was the sampling syringe and the other one

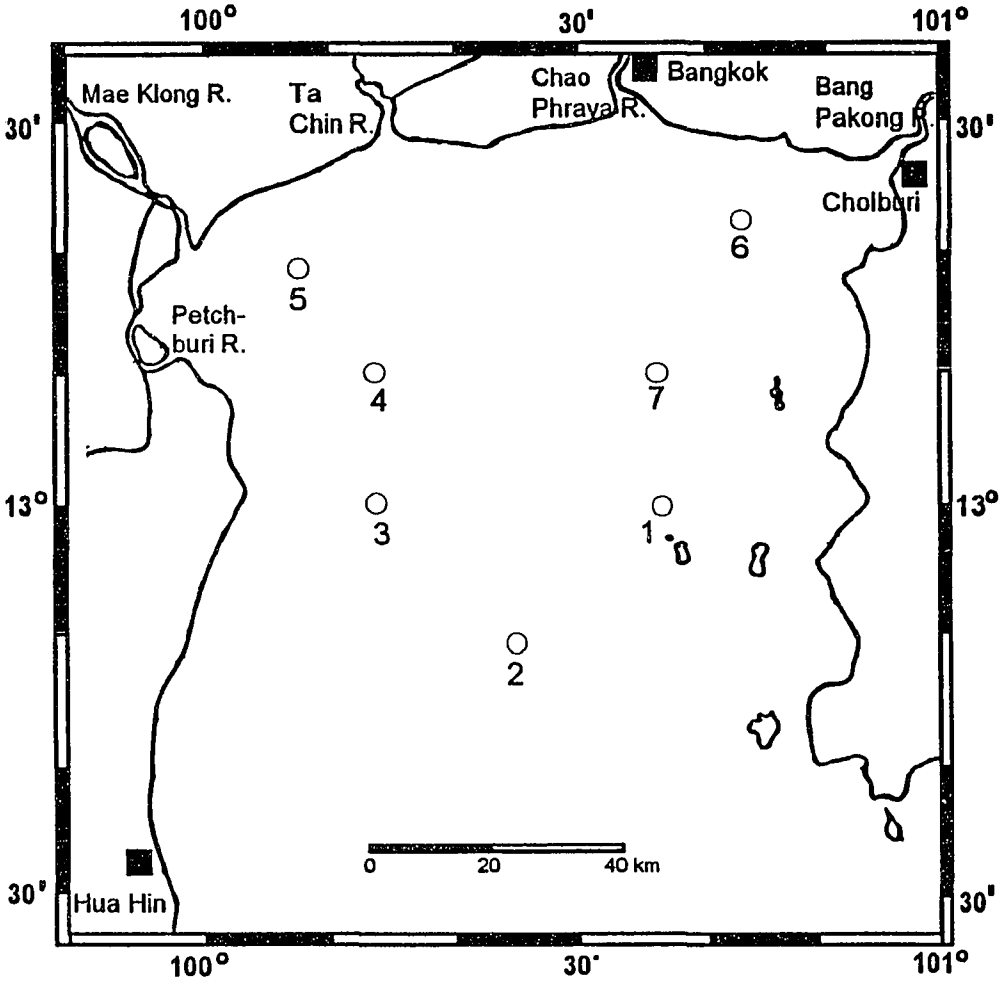

Figure 3.1. The study area in the upper Gulf of Thailand and seven benthic study stations.

was the compensator for volume change due to water sampling. Syringes and tubings were wrapped with black electrician tape to minimize photosynthetic effects on nutrient concentration.

Three benthic flux chambers were used at each experimental site. The chambers were deployed with the cap off and were pushed 10-20 cm into the sediments. The exact height of the head space of each chamber was individually measured. After about 15-20 minutes, the chamber was capped and the experiment started. At the beginning of the experiment, one syringe at each chamber's cap was filled to the 140 ml mark with bottom seawater. The other syringe was left at the 0 ml mark. Syringes and tubes were carefully checked for air bubbles that might be trapped inside. In addition to the benthic chambers, bottom water was incubated *in situ* in a 500 ml dark polyethylene bottle in order to correct for the uptake or release due to activity in the water column. Bottom water at the time when the experiment began was collected and served as the initial reference condition.

After about 8 hours, the water inside each chamber was withdrawn into the empty syringe by a diver. Because there was no water mixing mechanism in the flux chambers, the water in the chamber was mixed before each sampling by gently pumping water in and out by the action of the two syringes.

The concentration change of all chemical constituents included in this study could be readily observed after the 8 hour incubations. A preliminary study with the flux chambers used in this study found that further incubation beyond 8 hours

sometimes created anoxic conditions inside the chamber, thus severely changing the chemical condition at and above the sediment-water interface (Berner, 1979).

Once a water sample was on board the boat, it was transferred from the syringe into a clean plastic beaker via Tygon tubing. Care was taken not to introduce air bubbles into the water. The O_2 concentration and temperature were immediately measured by a YSI digital oxygen meter and a digital thermometer. The measurement resolutions were 0.01 mg O_2 l^{-1} and 0.1°C, respectively. The pH was measured according to techniques described in Chapter 2 of this dissertation.

Water samples were filtered and analyzed for total alkalinity and DIC following the procedures given in Chapter 2. The concentrations of DIP, $NO_3^-+NO_2^-$ and NH_4^+ in filtered samples were determined manually by the spectrophotometric methods described in Parsons et al. (1984). The measurement precision was better than 0.01 μM for DIP and better than 0.05 μM for $NO_3^-+NO_2^-$ and NH_4^+. All alkalinity and nutrient analyses of water samples were completed at the Marine Science Department, Chulalongkorn University in Bangkok within two weeks after the cruise. The used filter membranes were saved for analysis of suspended particulate C, N and P by the methods described in the following section on sediment analysis.

Benthic efflux (B_M) of a constituent M in mmol m^{-2} d^{-1} from the sediment was calculated by:

$$B_M = \frac{([M]_{Ch,t} - [M]_{B,t}) \times (h + 0.013) \times 24}{t}$$

where $[M]_{Ch,t}$ and $[M]_{B,t}$ are concentrations of M in μM in chamber and in bottle at time t in hours after the experiment started, h is the chamber head space height in meters, and 0.013 is the head space correction for syringes and tubing attached to the chamber.

Net $CaCO_3$ precipitation by benthic organisms, mainly echinoderms, bivalves, and solitary corals, will affect TA and DIC fluxes observed at the sediment-water interface. Because most $CaCO_3$ found in the upper Gulf of Thailand sediments comes from benthic organisms, with very few planktonic skeletons, the effect of net $CaCO_3$ precipitation on TA and DIC fluxes was corrected using the ^{210}Pb sedimentation rate multiplied by $CaCO_3$ content of deep sediments collected near the flux measurement stations (see the section below). This calculation implies that $CaCO_3$ sedimentation represents *in situ* production, and that no $CaCO_3$ is horizontally transported into or away from production site. The effect of nutrients on TA flux was corrected according to Dickson (1981).

The upper Gulf of Thailand dataset is small, containing only 21 data points for each chemical flux. Analysis of this dataset using a conventional regression model can be strongly biased by even a few outliers. Hence, visual observation will be used for the Gulf of Thailand flux data to justify the goodness of fit between observed data and the theoretical slope determined by different oxidant reduction models, i.e. equations (3.4), (3.11), (3.15), (3.17), (3.21) and (3.23).

Analyses of Gulf of Thailand Sediments

At each benthic flux measurement station, a sediment core was collected by divers using a 1.2 m long, 7.5 cm inner diameter PVC pipe. The core was brought on board and immediately cut into sections 3 to 5 cm in length. These sections were subsequently compressed by a screw-driven stainless steel squeezer in order to extract the porewater. All sample preparation and porewater extraction steps were performed under normal atmosphere. Porewater chemistry will be the topic of Chapter 4 of this dissertation, and more details on the chemical methods can be found in that chapter. The thickness of each compressed sediment slab was measured before storage in a plastic container in a freezer. All porewater extraction was accomplished within 5 hours after each core was collected.

In the laboratory, sediment samples were weighed before and after drying at $\approx$80°C in an oven. The original porosity of each sediment section (ϕ) was computed by:

$$\phi = \frac{wt.loss + ml.porewater}{44 \times sect.thick}$$

where *wt. loss* = weight loss in g after drying at 80°C, *ml. porewater* = ml. of total porewater extracted by the squeezer, 44 = cross sectional area in cm^2 of the core, and *sect. thick* = the thickness of the original section in cm.

The density of the bulk solids (ρ_{ss}) in g cm^{-3} was estimated by:

$$\rho_{ss} = \frac{dry\ wt.}{slab\ vol. - wt.loss}$$

where *dry wt.* = the final dry weight of the slab in g, *slab vol.* = slab volume in cm^3 after squeezing and *wt. loss* = weight loss in g after drying at 80°C. The salt effect on the dry weight (less than 5%) was neglected.

Dried sediment samples were ground into a fine powder with a porcelain mortar and pestle. The excess ^{210}Pb activity profile in sediments was determined by a gamma spectrometry procedure outlined by Kim and Burnett (1983). To avoid the surface mixed layer effect, which was previously observed for the same study by Windom et al. (1984) to be as deep as 10 cm from the sediment-water interface, only sections below the 10 cm mark were used. The sedimentation rate in mass units (i.e., g cm^{-2} y^{-1}) was estimated, according to Robbins (1978), by dividing the ^{210}Pb decay constant by the slope of the plot for the logarithm of excess ^{210}Pb (dpm g^{-1}) versus depth in accumulated mass units (g cm^{-2}). The slope was estimated using the geometric mean regression (Ricker, 1973) as discussed by Snidvongs et al. (ms.).

The total carbon (organic C plus carbonate C) and nitrogen contents of sediments and suspended particles were analyzed by a Carlo Erba NA1500 Nitrogen Analyzer with the CO_2 trap removed. Samples were combusted at 1020°C. The total phosphorus content was determined by combusting sediment and suspended solid samples at 550°C in a muffle furnace. The residues were hydrolyzed in a 10% HCl solution. The pH of the sample solution was then adjusted to about 3 (using pH

paper) by adding saturated $NaHCO_3$ solution. The total molybdate-reactive phosphate in solution was determined manually by the method of Parsons et al. (1984).

The organic carbon fraction of the sediment was estimated by slowly adding 10% HCl solution into the ground sediment sample until CO_2 effervescence could not be seen. The samples were subsequently dried in an oven at 80°C and re-ground into fine powder. This carbonate free sample was analyzed for carbon and reactive phosphate by the same methods as for unacidified samples. The organic carbon in an acidified sample was standardized against P and then multiplied by the P content of the unacidified fraction to get the organic C content of the original sediment sample. The $CaCO_3$-C content was taken as the difference between the total and organic carbon fractions.

Tomales Bay Benthic Flux Dataset

A long-term benthic flux dataset from Tomales Bay, California, was given to me by Dr. S. V. Smith. Fluxes of O_2, DIC, TA, $NO_3^-+NO_2^-$, and NH_4^+ across the sediment-water interface at three locations--6, 10, and 16 km from the bay mouth (Fig. 3.2)--were measured approximately every two months between June 1987 and July 1992 by hemispherical transparent domes which covered a bottom area of 0.2 m^2 (three to six replicates per site). Detailed description of the sampling methods are given in Dollar et al. (1991).

Because the Tomales Bay dataset is large, more than 300 data points, regression analysis can be performed with only slight effects due to outliers. The hypothesis that the best-fit slope is not significantly different from the expected slope

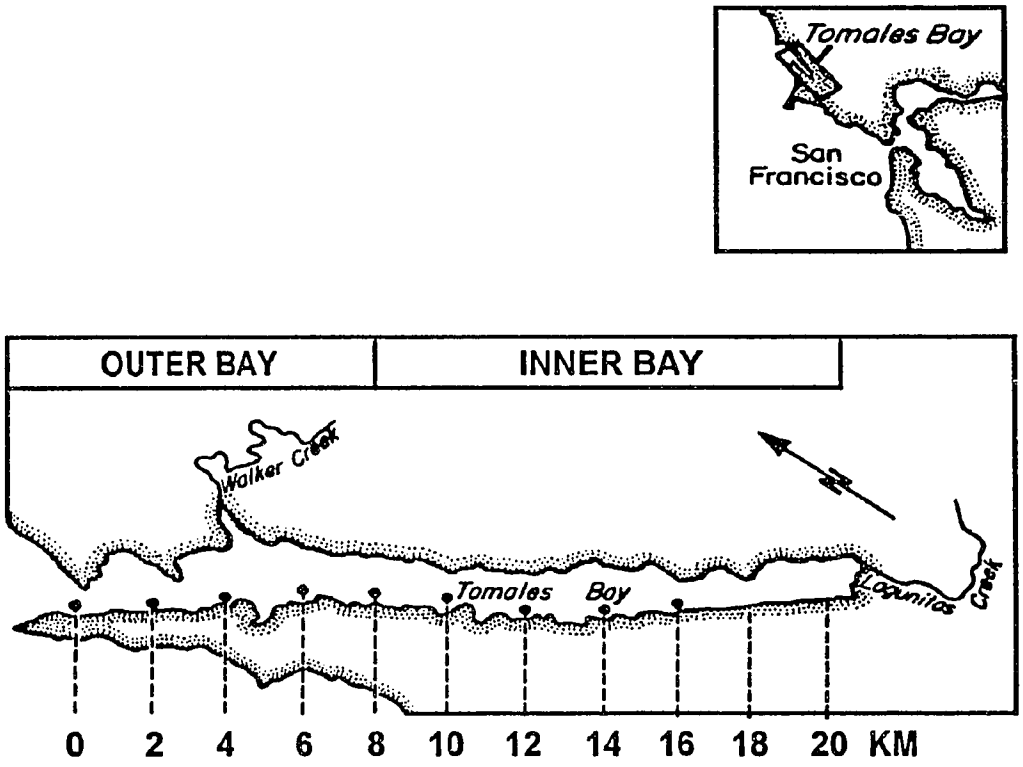

Figure 3.2. The study area in Tomales Bay and three benthic flux study stations located at 6, 10, and 16 km from the bay mouth.

can be tested. The statistical approach used to test the hypothesis and the program listing are given in Appendix C.

Results

Gulf of Thailand

The average benthic fluxes for DIC, O_2, TA, DIP, $NO_3^-+NO_2^-$ and NH_4^+ at seven stations are tabulated in Table 3.1. Because NO_2^- fluxes were always very low in comparison with NO_3^- fluxes, for brevity, the variable "$NO_3^-+NO_2^-$" will be subsequently referred to in this chapter as NO_3^-.

The absolute fluxes of DIC, O_2, TA and DIP (Table 3.1) were higher at the near-river stations (5 and 6) and the intermediate stations (4 and 7) than at the outer stations (1, 2 and 3; Fig. 3.1). Conversely, the NO_3^- fluxes were lower at Stations 5, 6 and 7 than at Stations 2 and 3. The NO_3^- fluxes at Stations 1 and 4 were about the same. The fluxes of NH_4^+ across the sediment-water interface showed no recognizable geographic trend among these seven locations.

The organic particle delivery rate at the sediment-water interface at each site was estimated indirectly by adding the ultimate organic carbon removal (^{210}Pb sedimentation rate $\times$ organic content of deep sediments) to the net carbon oxidation in the sediments (benthic DIC efflux corrected for $CaCO_3$ reactions). This assumes a steady state for organic carbon mass in "active" surface sediment and ignores all effects of DOC and DIC in porewater. The results are shown in Table 3.2. Evidently the organic carbon input at the two near-river stations, 5 and 6, was much higher than other locations, indicating influence from terrestrial inputs.

Table 3.1. The average among three replicates of observed benthic fluxes (+ = out; - = into sediments) of 6 constituents at seven locations in the upper Gulf of Thailand in September 1991. All fluxes are in mmol m^{-2} d^{-2} except TA fluxes which are in meq m^{-2} d^{-2}. Standard errors of the mean are given in parentheses.

Station	DIC	O2	TA	DIP	$NO_3^-+NO_2^-$	NH_4^+
1	10.0	-12.9	-1.6	0.07	0.60	1.75
	(2.2)	(2.0)	(0.9)	(0.04)	(0.04)	(0.65)
2	12.2	-11.2	1.9	0.03	1.08	0.92
	(4.4)	(3.2)	(1.2)	(0.05)	(0.09)	(0.93)
3	13.9	-16.6	-0.9	0.05	1.11	2.89
	(2.6)	(3.5)	(1.0)	(0.05)	(0.05)	(0.94)
4	31.6	-29.9	1.8	0.23	0.77	2.78
	(2.3)	(1.9)	(1.5)	(0.01)	(0.21)	(0.71)
5	39.8	-29.8	13.7	0.37	-0.07	1.42
	(0.9)	(2.2)	(1.2)	(0.09)	(0.14)	(0.68)
6	46.2	-31.8	16.8	0.72	0.42	3.68
	(2.6)	(3.8)	(3.2)	(0.07)	(0.10)	(0.54)
7	39.0	-32.4	7.8	0.23	-0.08	0.84
	(2.7)	(0.7)	(0.4)	(0.09)	(0.37)	(0.44)

Table 3.2. Estimation of organic carbon input by settling particles at the sediment-water interface at seven locations in the upper Gulf of Thailand in September 1991. Deep sediment organic contents are the average of the three deepest sections of each core. Standard errors of the mean are given in parentheses.

Station	^{210}Pb Sediment. rate A g cm^{-1} y^{-1}	Deep sediment org.C B wt.%	Ultimate C removal A × B	DIC efflux mmol C m^{-2} d^{-1}	Total org. C input
1	0.35 (0.33)	0.37 (0.01)	3.0 (2.8)	10.0 (2.2)	13.0 (3.6)
2	0.14 (0.12)	0.28 (0.02)	0.9 (0.8)	12.2 (4.4)	13.1 (4.4)
3	0.21 (0.14)	1.20 (0.35)	5.8 (4.2)	13.9 (2.6)	19.7 (4.9)
4	0.88 (0.53)	0.68 (0.20)	13.7 (10.7)	31.6 (2.3)	45.3 (10.9)
5	0.86 (0.56)	1.02 (0.26)	20.0 (14.0)	39.8 (0.9)	59.8 (14.0)
6	1.10 (0.74)	1.50 (0.27)	37.7 (26.2)	46.2 (2.6)	83.9 (26.3)
7	0.42 (0.36)	0.36 (0.19)	3.5 (3.0)	39.0 (2.7)	42.5 (4.0)

The plot of calcification-corrected DIC versus O_2 fluxes in Fig. 3.3 reveals that O_2 reduction could explain the organic carbon respiration in sediments at Stations 1, 2 and 3. All these stations were "offshore" stations (Fig. 3.1). At intermediate and near-river stations--4, 5, 6 and 7--O_2 fluxes were stable at about 25-30 mmol m^{-2} d^{-1}. This leveling off effect was not because the O_2 in the flux chambers was exhausted, because at the end of all experiments, more than 0.5 mg l^{-1} (usually more than 1 mg l^{-1}) of O_2 remained in the water. There is a possibility that the observed effect might be due to the lack of continuous mixing that prohibited vertical O_2 exchange within the chambers. However, further analyses in this chapter will demonstrate that this leveling off effect can be explained by the suboxic respiration model.

Addition of denitrification did not significantly improve the goodness of fit between model and observed data (Fig. 3.4). Organic carbon oxidation in sediments at Stations 4, 5, 6, and 7 was still much larger than that accounted for by O_2 reduction and denitrification.

Inclusion of SO_4^{2-} reduction had a strong impact on the results (Figs. 3.5 and 3.6). It is clearly seen that organic carbon oxidation at all stations in the Gulf of Thailand could be balanced by the reduction of O_2 and SO_4^{2-}. All other reduction reactions, such as denitrification and methanogenesis, appear to be unimportant in the overall redox reaction in these sediments.

Due to the absence of significant methanogenesis in the Gulf of Thailand sediments, a linear correlation between $CaCO_3$ corrected DIC and sorption corrected

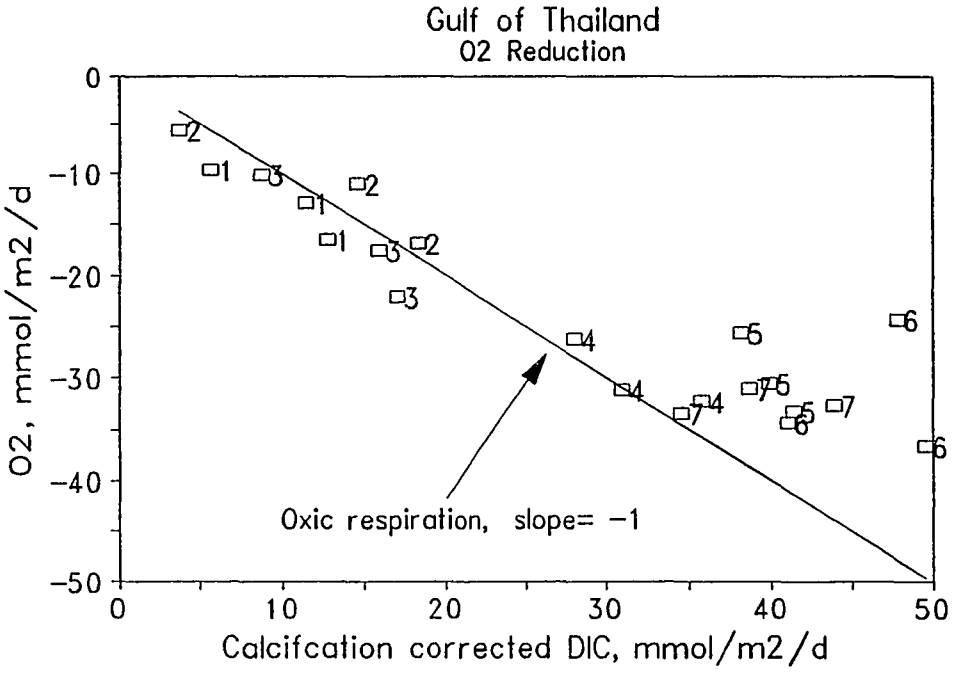

Figure 3.3. Calcification-corrected DIC flux (i.e., net organic C oxidation) versus O_2 reduction in the upper Gulf of Thailand sediments. The linear relationship expected for complete organic C respiration by O_2 reduction (equation 3.4, see text) is shown. The numbers near each data point label are station numbers.

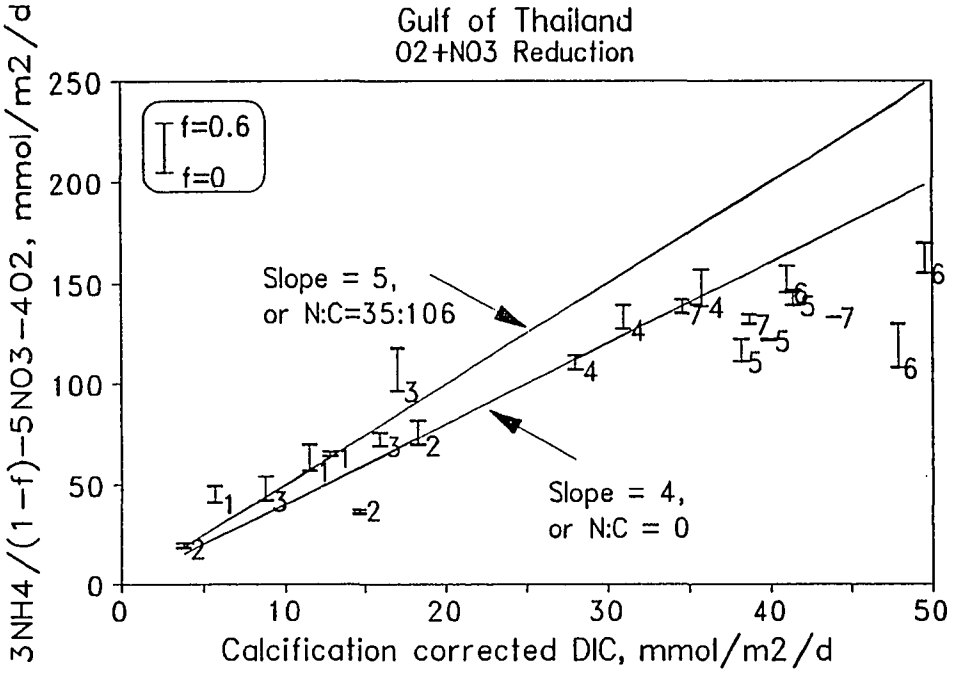

Figure 3.4. Observed net organic C oxidation versus O_2 reduction and denitrification combined in the upper Gulf of Thailand sediments. The range given for each data point represents sediment NH_4^+ sorption coefficients between 0 and 0.6. The linear relationships expected for complete organic C respiration by O_2 reduction and denitrification combined (equation 3.11, see text) for the decomposing N:C ratios of 0 and 35:106 are shown. The numbers near each data point are station numbers.

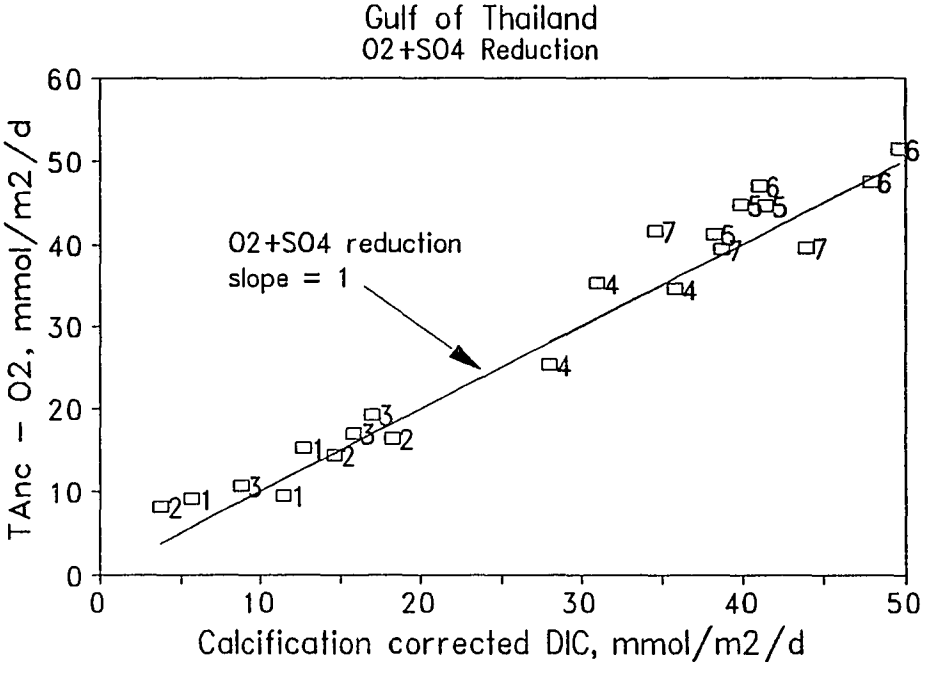

Figure 3.5. Observed net organic C oxidation versus the sum of O_2 and SO_4^{2-} reduction in upper Gulf of Thailand sediments. The linear relationship expected for the complete organic C respiration by O_2 and SO_4^{2-} reduction (equation 3.15, see text) is shown. The numbers near each data point are station numbers.

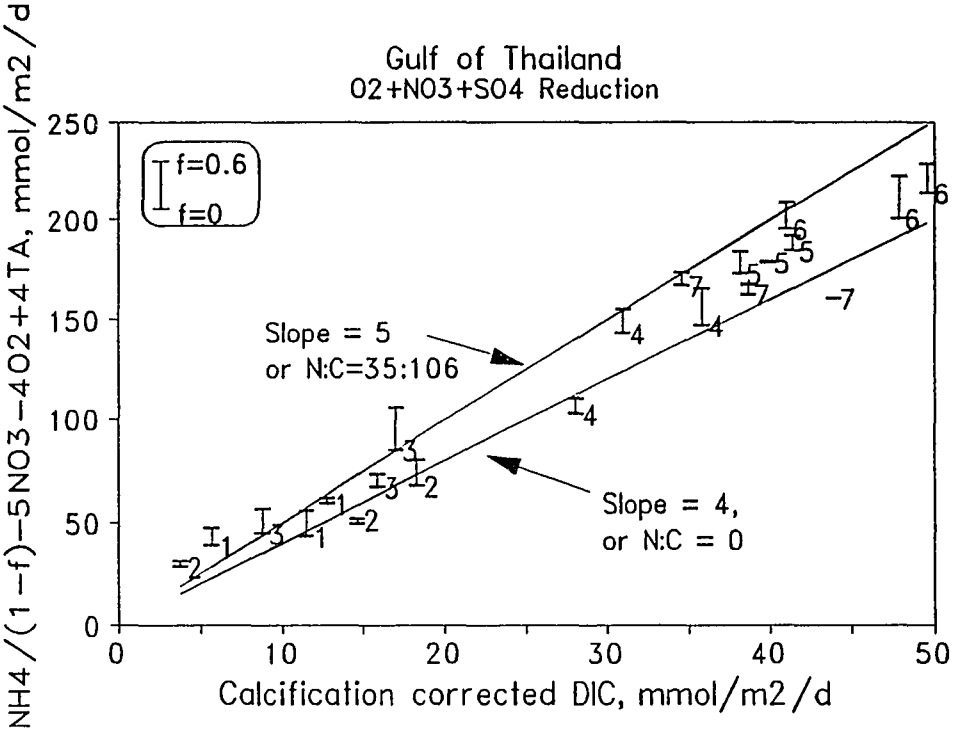

Figure 3.6. Observed net organic C oxidation versus the sum of O_2, NO_3^-, and SO_4^{2-} reduction in upper Gulf of Thailand sediments. The linear relationships expected for the complete organic C respiration by O_2, NO_3^-, and SO_4^{2-} reduction (equation 3.17, see text) for the decomposition of organic matter with the N:C ratios of 0 and 35:106 are shown. The numbers near each data point are station numbers.

DIP fluxes is expected. Such a plot (Fig. 3.7) indicates that this expectation can generally be applied at all stations, except Station 6. At Station 6, the observed DIP flux was about 0.3 mmol m^{-2} d^{-1} higher than the rate predicted by the Redfield P:C ratio of 1:106. This deviation indicates that mechanisms responsible for C and P regeneration at Station 6 might be different than those at other locations.

The sediment P:C ratios at Stations 5 and 6 were all less than the ambient planktonic P:C ratio (Fig. 3.8). By taking the difference between the sediment and plankton P:C ratio and standardizing the results against the local organic C input rate (Table 3.2), the "leaching P", or preferentially released P relative to C from particles, at each station can be estimated. The "leaching P" estimated this way for Station 6 of 0.3 mmol m^{-2} d^{-1} matches well with the observed excess DIP flux across the sediment-water interface (Fig. 3.7). The estimated P leaching rate of 0.2 mmol m^{-2} d^{-1} for Station 5 may be slightly too high, but it is still within the range of chamber-to-chamber measurement variation (Fig. 3.7).

The mechanism of P leaching from sediment particles was not studied here. However, it may be related to DIP desorption from particles. Bottom water at the two near-river stations 5 and 6 had lower O_2 concentrations than at other stations; this might suggest more reduced sediments. Under a sufficiently reduced environment, Fe(III) in FeOOH and Fe_2O_3 can be reduced to Fe(II). As the oxidized iron minerals are consumed, the capacity of sediments to sorb DIP is decreased (Schindler, 1985; Caraco et al., 1989, 1990).

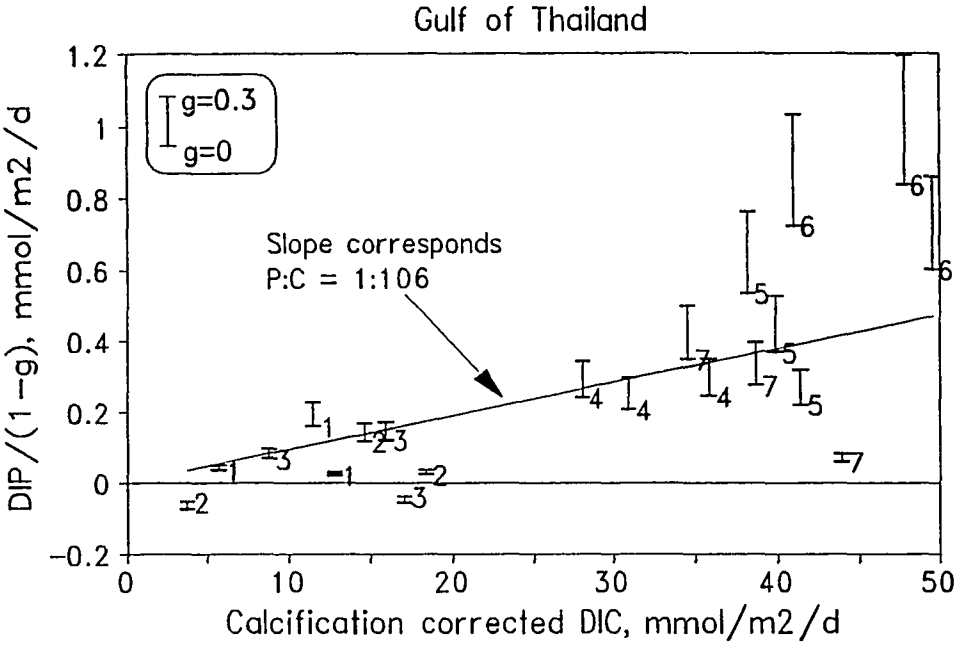

Figure 3.7. The fluxes of calcification-corrected DIC versus sorption-corrected DIP for upper Gulf of Thailand sediments. The range given for each data point represents sediment DIP removal coefficients between 0 and 0.3. The linear relationship expected for the organic matter with the P:C ratio of 1:106 is shown. The numbers near each data point are station numbers.

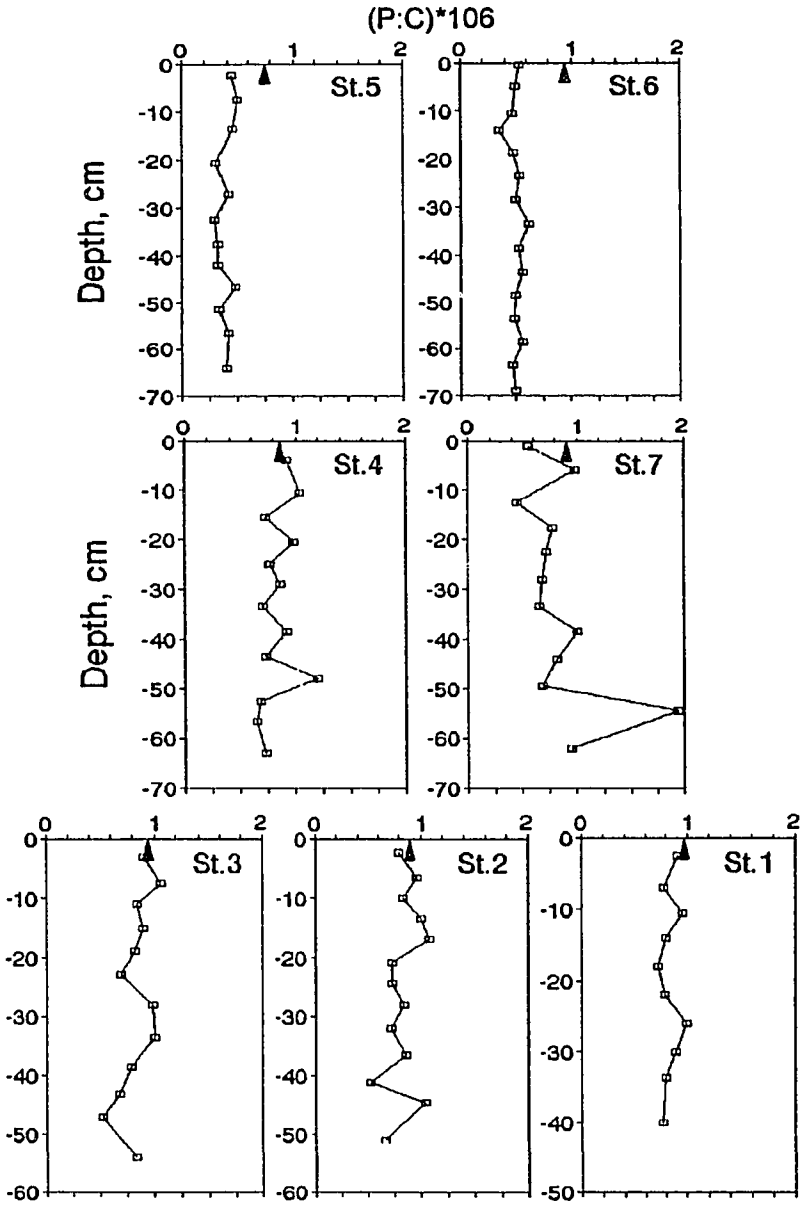

Figure 3.8. Organic P:C ratio of sediments at 7 sampling stations in the upper Gulf of Thailand. The seston P:C ratio at each site is indicated by the triangle.

The second factor that may favor DIP desorption is the sharp decrease in water-column DIP concentration as a particle moves from the riverine to the marine environment (Froelich, 1988). In some cases the DIP concentration near the Chao Phraya rivermouth dropped by more than 10 times over distances of less than 10 km (Umnuay, 1984; Appendix B).

Groundwater could also be another source of excess DIP in sediments at Station 6. Porewater salinity at this station is 2-3‰ less than bottom water salinity (about 29‰). This indicates that up to 10% of the porewater may be groundwater. Even though all known groundwater in the vicinity is in confined aquifers 50 m or more below ground (Piancharoen, 1976; Sharma, 1986), there might be openings in the overlying stratum. The piezometric level of the shallowest aquifer, the Bangkok Aquifer, is well above sealevel. Thus there is enough head to create localized groundwater springs. The DIP enrichment effect seen only at Station 6, and not at any other stations, supports the idea of a localized freshwater spring.

The sediment N:C ratio is lower than the ambient plankton N:C ratio at all seven locations in this study (Fig. 3.9) and indicates the more labile nature of particulate N relative to C. The net nitrogen remineralization estimated from the N:C ratio difference is usually quite different from the observed DIN ($NO_3^-+NO_2^-+NH_4^+$) flux at the same location (Table 3.3). The differences indicate that the sediments at Stations 1, 2 and 3 were minor DIN sources while the sediments at the other four stations were DIN sinks. The positive "missing N" in Table 3.3 could be assumed to be net denitrification (i.e., sediment denitrification rate is larger than sediment N_2

Table 3.3. Nitrogen balance of the sediments at seven stations in the upper Gulf of Thailand. All fluxes are in mmol m^{-2} d^{-1}. The N:C ratios are atomic ratios. Standard errors are given in parentheses.

Station	Seston N:C	Deep sediment org. N:C	Expected DIN	Observed DIN	Missing N
1	0.139 (0.012)	0.074 (0.004)	1.56 (0.67)	2.35 (0.63)	-0.79 (0.92)
2	0.124 (0.011)	0.056 (0.009)	1.59 (1.60)	2.00 (0.93)	-0.41 (1.85)
3	0.118 (0.001)	0.058 (0.010)	1.98 (0.68)	4.00 (0.94)	-2.02 (1.16)
4	0.142 (0.016)	0.129 (0.013)	4.69 (1.28)	3.51 (0.74)	1.18 (1.48)
5	0.178 (0.026)	0.123 (0.014)	8.17 (1.43)	1.35 (0.69)	6.82 (1.59)
6	0.255 (0.073)	0.133 (0.012)	16.40 (2.52)	4.09 (0.55)	12.31 (2.58)
7	0.156 (0.019)	0.132 (0.036)	6.19 (1.04)	0.76 (0.57)	5.43 (1.19)

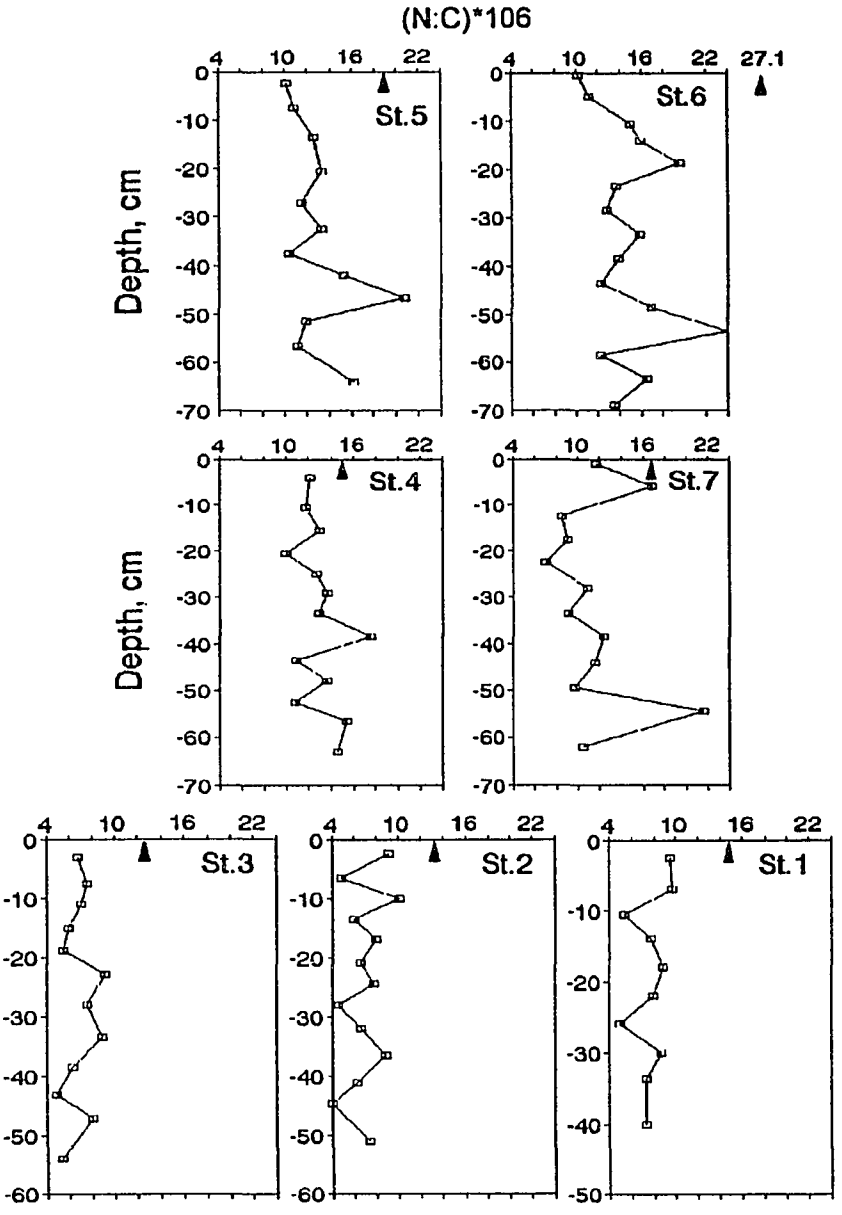

Figure 3.9. Organic N:C ratio of sediments at seven sampling stations in the upper Gulf of Thailand. The seston N:C ratio at each site is indicated by the triangle.

fixation rate) while the negative "missing N" could be due to net N_2 fixation in the sediments.

The net denitrification and nitrification rates can be deduced from ξ_2 and ξ_3 (reactions 2 and 3), respectively. Because CH_4 formation is insignificant in the Gulf of Thailand sediments of this study, there are two ways to estimate ξ_3: 1) from the B_{DIC} and N:C decomposition ratio by solving equations (3.2) and (3.10); or 2) from the B_{DIP} and N:P decomposition ratio by solving equations (3.10) and (3.19). Subsequently, ξ_2 can be derived by substituting the value obtained for ξ_3 in equation (3.7). These two approaches were used by Dollar et al. (1991) to calculate denitrification in Tomales Bay sediments.

Calculated net nitrification and denitrification are shown in Table 3.4. In all cases the differences between the net nitrification and denitrification, i.e. the net NO_3^- flux across sediment-water interfaces, were small. This indicates that the coupling between these two nitrogen reactions in these sediments is tight. Note that DIP based nitrification and denitrification rates may be less reliable at Station 6 because of unusual P behavior in sediments at this station.

To demonstrate the variation of sediment denitrification rates among approaches and locations, the results of each individual model--the missing PN (Table 3.3), DIP based denitrification (Table 3.4) and DIC based denitrification (Table 3.4)--are plotted against the average rates at each station (Fig. 3.10). The results from all stations, except that from Station 6, show good agreement among the

Table 3.4. Calculated net nitrification and denitrification in sediments at seven locations in the upper Gulf of Thailand in September 1991. Rates are calculated from DIP and DIC by using sestons C:N:P ratio at each station. Coefficients for NH_4^+ and DIP removal by sediments (*f* and *g*) are both assumed to be 0.2. All rates are in mmol N m^{-2} d^{-1}. Standard errors (due to flux measurement) are given in parentheses.

Calculated from:	DIP		DIC	
Station	Net nitri.	Denitri.	Net nitri.	Denitri.
1	-0.76 (1.20)	-1.37 (1.20)	-0.68 (0.88)	-1.29 (0.88)
2	-0.57 (1.53)	-1.65 (1.53)	0.69 (1.33)	-0.39 (1.33)
3	-2.63 (1.51)	-3.74 (1.51)	-1.52 (1.24)	-2.63 (1.24)
4	1.13 (0.92)	0.40 (0.95)	1.29 (0.96)	0.56 (0.98)
5	5.72 (1.99)	5.79 (1.99)	4.24 (0.86)	4.30 (0.87)
6	9.82 (1.51)	9.40 (1.51)	2.37 (0.78)	1.96 (0.78)
7	3.53 (1.82)	3.61 (1.86)	4.84 (0.68)	4.92 (0.77)

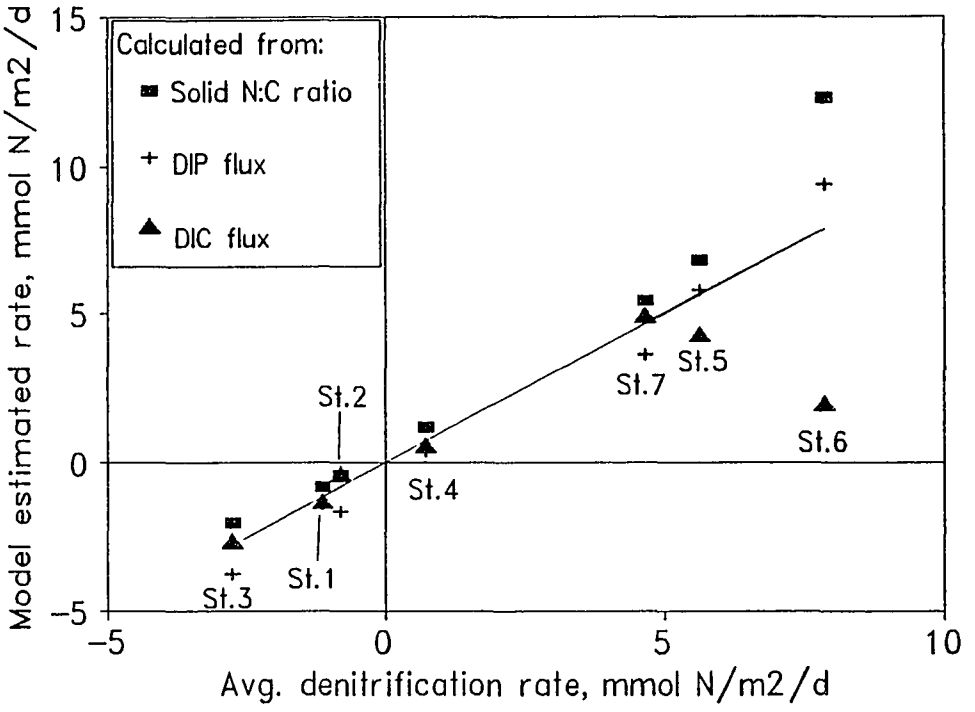

Figure 3.10. Denitrification rated rates estimated for the upper Gulf of Thailand sediments by: 1) the N:C ratio difference between sestons and deep sediments and the ^{210}Pb sedimentation rate, 2) the observed DIN and DIP fluxes and the assumed decomposing N:P ratio of 16:1, and 3) the observed DIN and DIC fluxes and the assumed decomposition N:C ratio of 16:106.

three estimation approaches. The average sediment denitrification rates derived from the three approaches are slightly lower than the whole system denitrification rates estimated from N in water column in the generally same areas (Fig. 2.9). Some possible explanations were already discussed in Chapter 2.

Interestingly, denitrification rates at Stations 1, 2 and 3 are slightly negative, suggesting net N_2 fixation. At Stations 4 to 7, where planktonic N_2 fixation was possibly high (Chapter 2), there was positive net denitrification in sediments.

The wide variation among the three estimation approaches at Station 6 could be a result of groundwater nutrient input. A small additional NH_4^+ flux due to groundwater (most DIN in groundwater is probably NO_3^-; Oberdorfer et al., 1990; Valiela et al., 1990) could lead to a slight underestimation of nitrification rate (ξ_3, equation 3.10). The effect of groundwater DIC on ξ_3 (via ξ_1, equation 3.2) could be smaller than the NH_4^+ effect because the groundwater DIC:NH_4^+ ratio is usually smaller than that in seawater and porewater (Oberdorfer et al., 1990). The underestimated ξ_3, when combined with groundwater NO_3^- flux, would result in equation (3.7) giving even further underestimates of the DIC-derived denitrification rate (ξ_2).

The extent of organic C oxidation (ξ_1) based on DIP flux (equation 3.19) could be overestimated because of the groundwater DIP effect. However, when this overestimated DIP-derived ξ_1 is substituted into equation (3.10), it is compensated by the groundwater NH_4^+ effect and the resulting DIP derived ξ_3 would be less underestimated than the DIC-derived ξ_3 described in the last paragraph. When this

DIP-derived ξ_3 is subsequently substituted into equation (3.7), the final DIP-derived denitrification rate (ξ_2), even though possibly too low, is still higher than the DIC-based ξ_2. These groundwater effects could well explain why, at Station 6, the DIC-derived denitrification rate is lower than the DIP-derived rate (Fig. 3.10). Furthermore, denitrification rate calculated from missing N is not affected by groundwater nutrient input and thus it makes sense that the missing N-derived rate is highest among the results of the three approaches (Fig. 3.10).

Tomales Bay

The time series of the mean among replicates of benthic O_2, DIC, TA, DIP, NH_4^+, and NO_3^- fluxes at each sampling station in Tomales Bay between June 1987 and July 1992 is shown in Figs. 3.11 to 3.16. Because $CaCO_3$ is not important in Tomales Bay sediments (less than 2 wt.% calcite as determined by powdered X-ray diffraction; unpublished data), it is not necessary to correct the observed DIC and TA fluxes. In other words, these two benthic fluxes can be taken directly as the net organic C respiration and SO_4^{2-} reduction rates in sediments.

The best fit slope of the relationship between DIC and O_2 fluxes (-0.50; Fig. 3.17) is significantly greater than -1 as expected from the stoichiometry of oxic respiration of organic carbon (equation 3.4). In Fig. 3.18 the slopes between observed B_{DIC} and total O_2 + NO_3^- reduction for f = 0 and 0.6 (2.21 and 2.52) are both significantly less than 4.45. The hypothesis that O_2 + NO_3^- reduction can explain the organic carbon reactions in Tomales Bay sediments is therefore rejected.

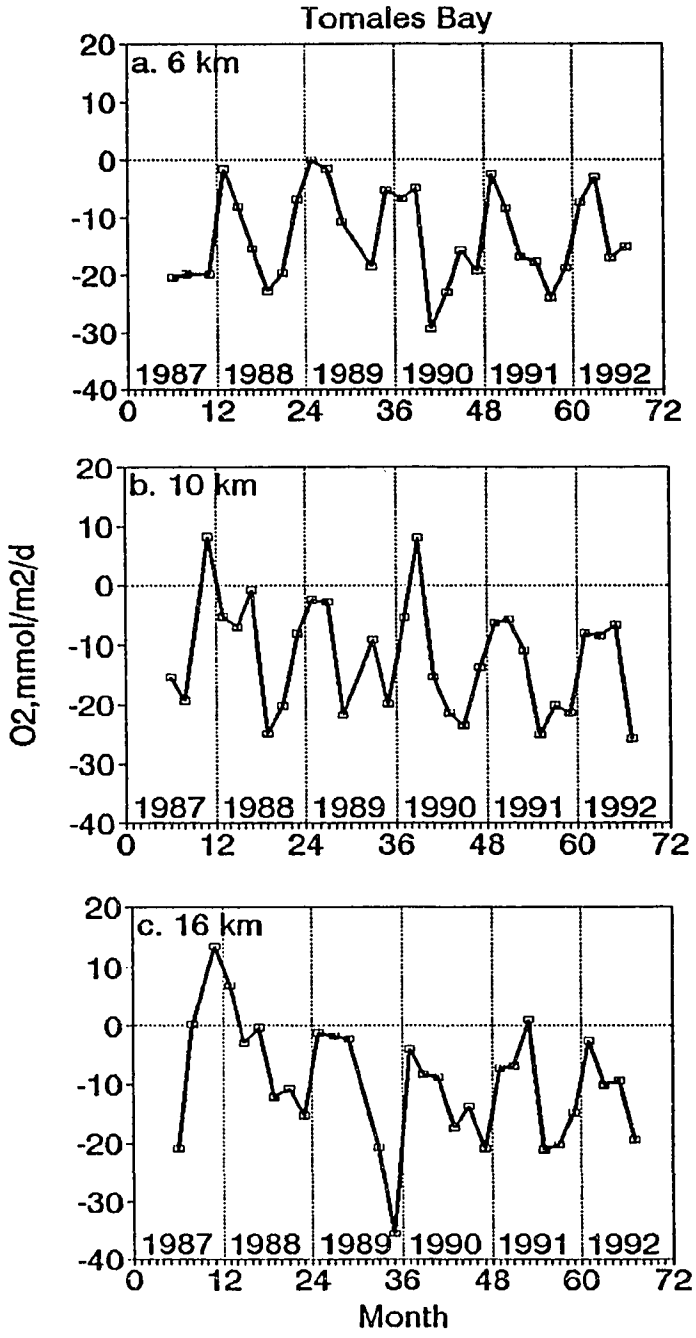

Figure 3.11. The average among replicates of benthic O_2 flux between June 1987 and July 1992 for stations 6, 10, and 16 km from the mouth of Tomales Bay.

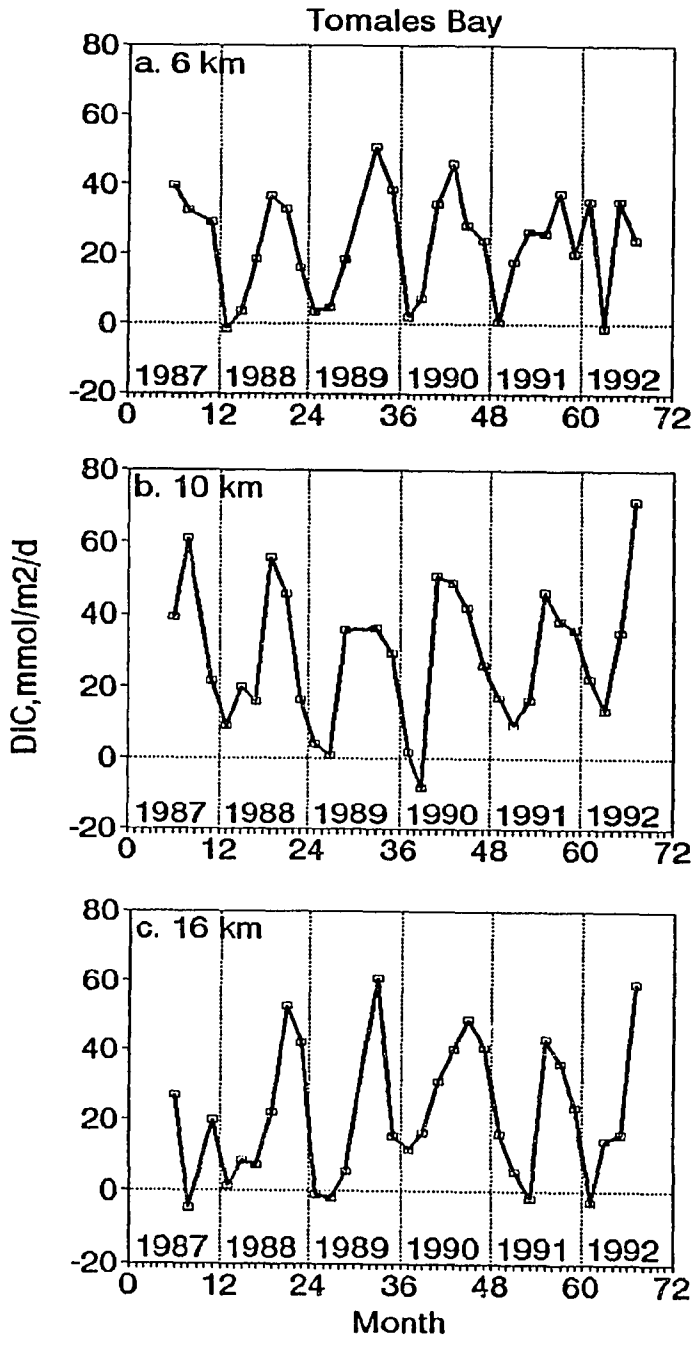

Figure 3.12. Same as Fig. 3.11 but for DIC.

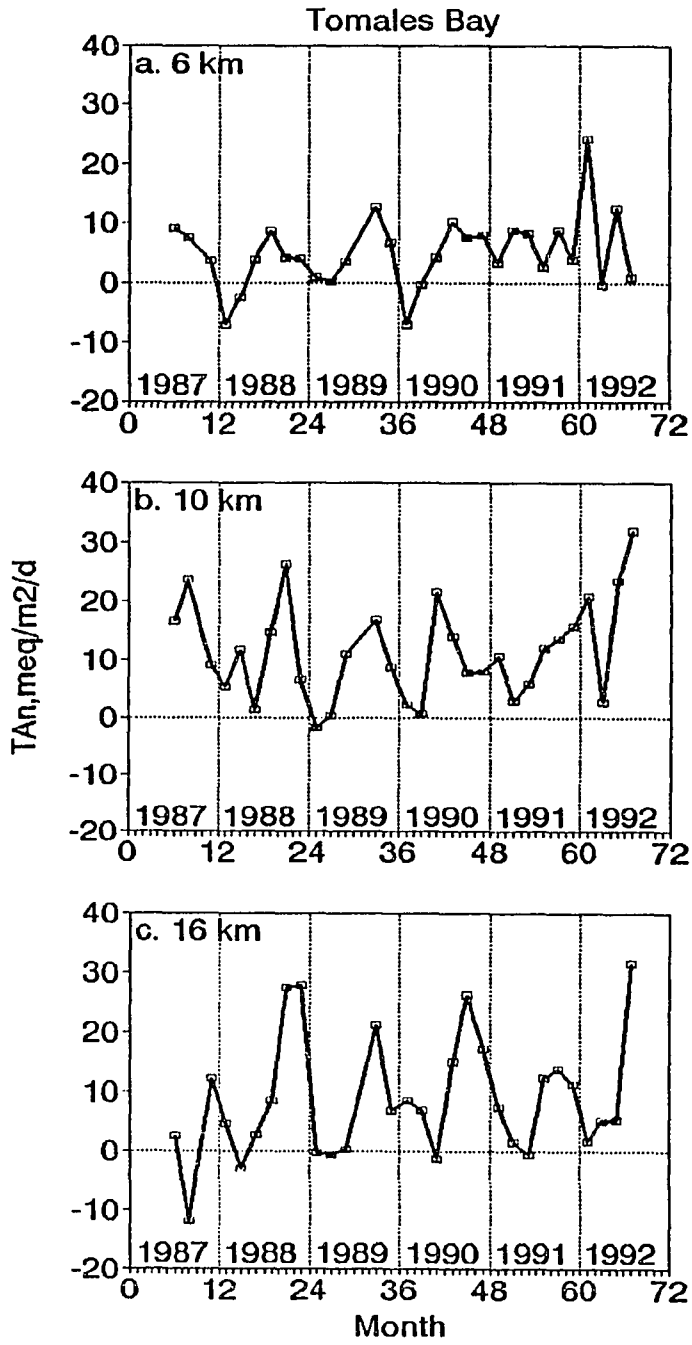

Figure 3.13. Same as Fig. 3.11 but for TA.

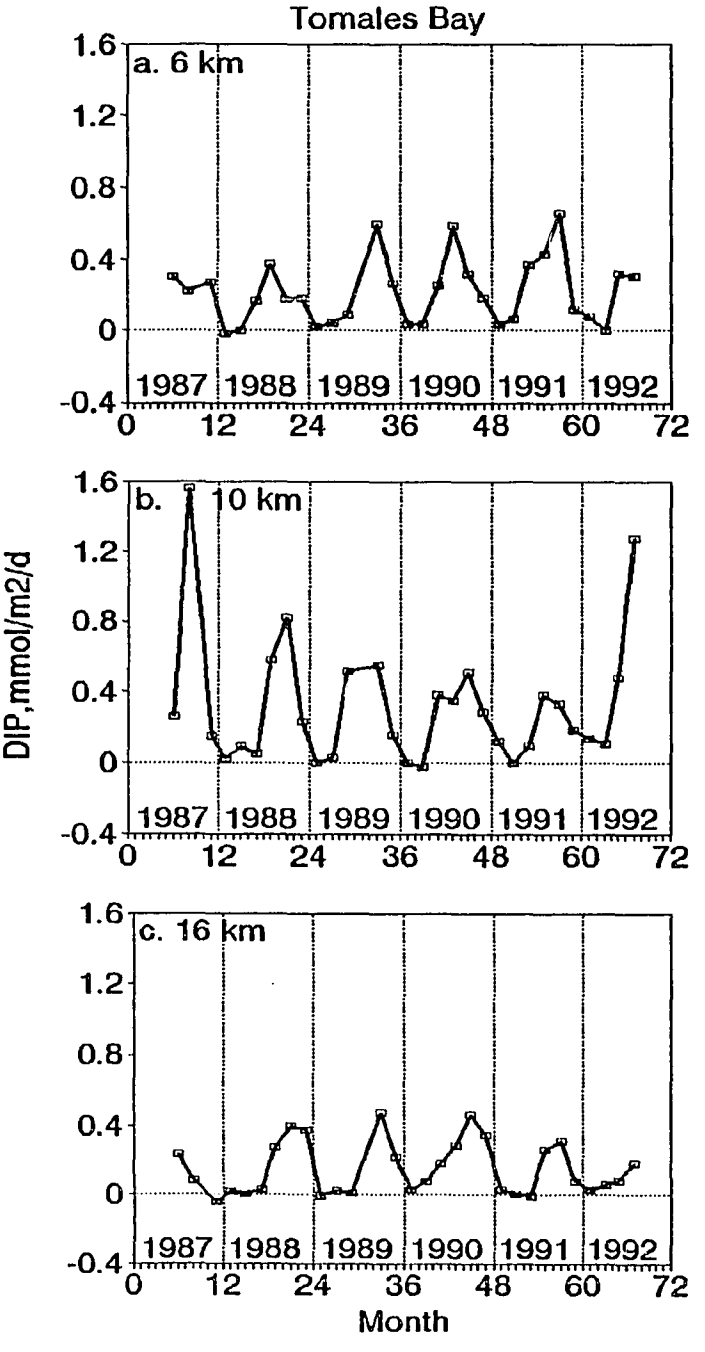

Figure 3.14. Same as Fig. 3.11 but for DIP.

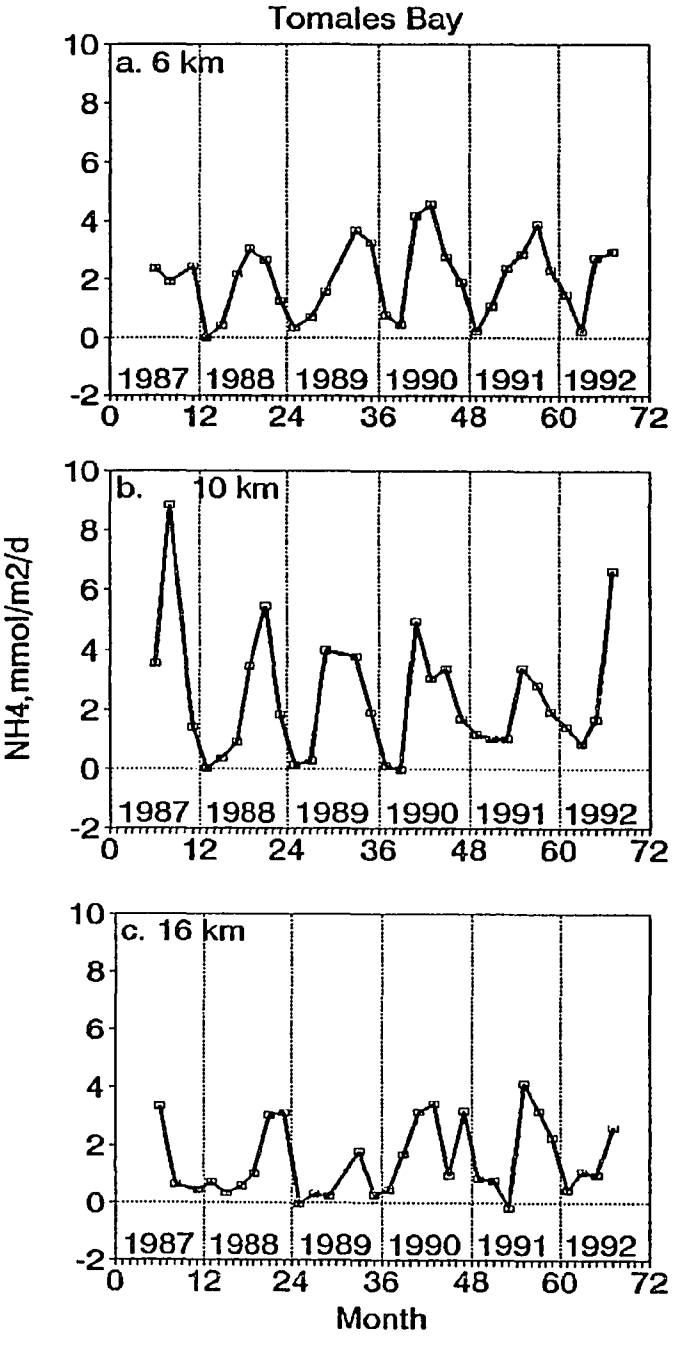

Figure 3.15. Same as Fig. 3.11 but for NH_4^+.

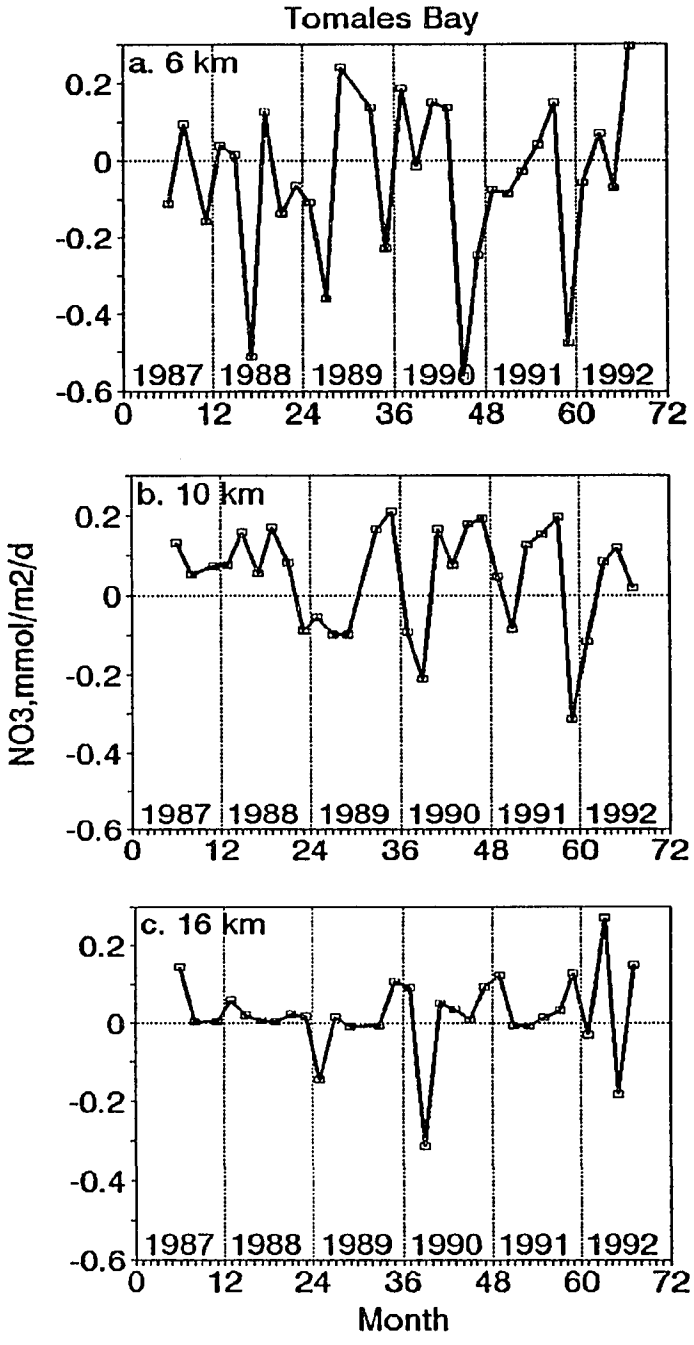

Figure 3.16. Same as Fig. 3.11 but for NO_3^-.

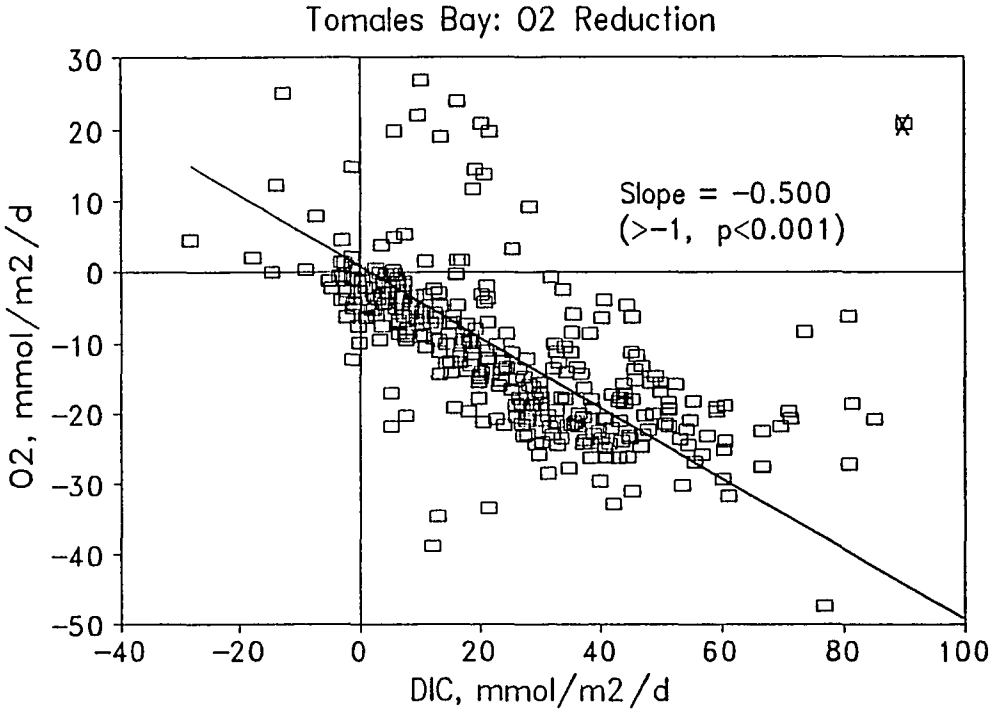

Figure 3.17. Observed net organic C oxidation versus O_2 reduction in Tomales Bay sediments. The slope of the best-fit linear regression is compared with the theoretical slope of -1 expected for complete organic C respiration by O_2 reduction (equation 3.4, see text). The data point marked by × is the outlier detected with $p<0.0001$ that it is real (see Appendix C).

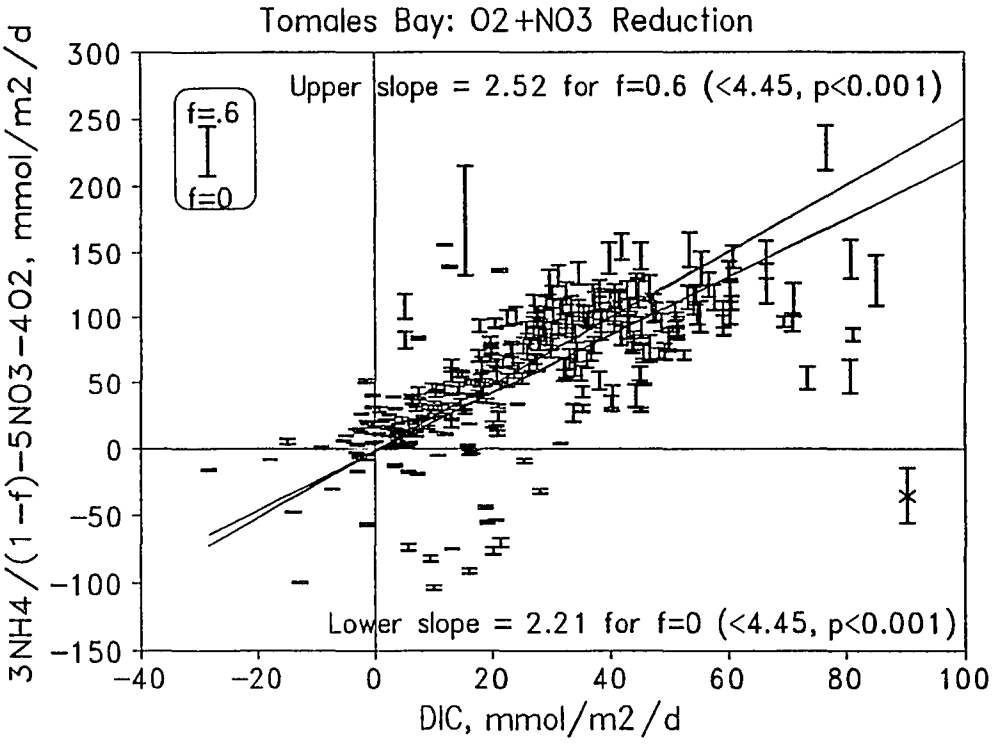

Figure 3.18. Observed net organic C oxidation versus the sum of O_2 and NO_3^- reduction in Tomales Bay sediments. The range given for each data point represents sediment NH_4^+ removal coefficients between 0 and 0.6. The best-fit slope for each sorption coefficient is compared with the theoretical slope of 4.45 expected for complete organic C respiration by O_2 and NO_3^- reduction (equation 3.11, see text) for the decomposition of organic matter with the N:C ratio of 16:106. The data marked by × is the outlier detected with $p<0.0001$ that it is real (see Appendix C).

The balance of the redox reactions in the sediments is much improved with the addition of SO_4^{2-} reduction (Figs. 3.19 and 3.20). Yet, the significant differences between both slopes and their theoretical values indicate additional oxidants, besides seawater O_2, SO_4^{2-} and NO_3^-, are needed.

When CO_2 reduction is added to the diagenetic model, the results appear to be quite satisfactory (Figs. 3.21 and 3.22). To some extent, however, the apparent agreement between the best-fit slopes and slopes predicted by the Redfield Ratio (Figs. 3.21 and 3.22) results from the large variation in the estimation of DIP production rate in sediments. The precision of the $O_2 + SO_4^{2-} + CO_2$ reduction model can be demonstrated by comparing model predicted CH_4 production rate (ξ_6) and observed CH_4 flux across the sediment-water interface (Rust, 1993). This analysis provides a mean calculated CH_4 flux of 4.5 mmol m^{-2} d^{-1} with a standard deviation of 21.3 mmol m^{-2} d^{-1}, assuming organic C:P ratio of 106:1 and g of 0.2. This mean calculated CH_4 flux is 1-2 orders of magnitude larger than the range of CH_4 fluxes across the sediment-water interface in Tomales Bay observed by Rust (1993). Moreover, many of the individual calculated CH_4 fluxes were unrealistically high or low, or even negative; these anomalies indicate poor resolution of the stoichiometric model in this study with respect to methanogenesis. If NH_4^+ and DIP retaining factors (f and g) were determined, the resolution of the model (equation 3.23) could be significantly improved; it might then be possible to estimate net methanogenesis in Tomales Bay sediments.

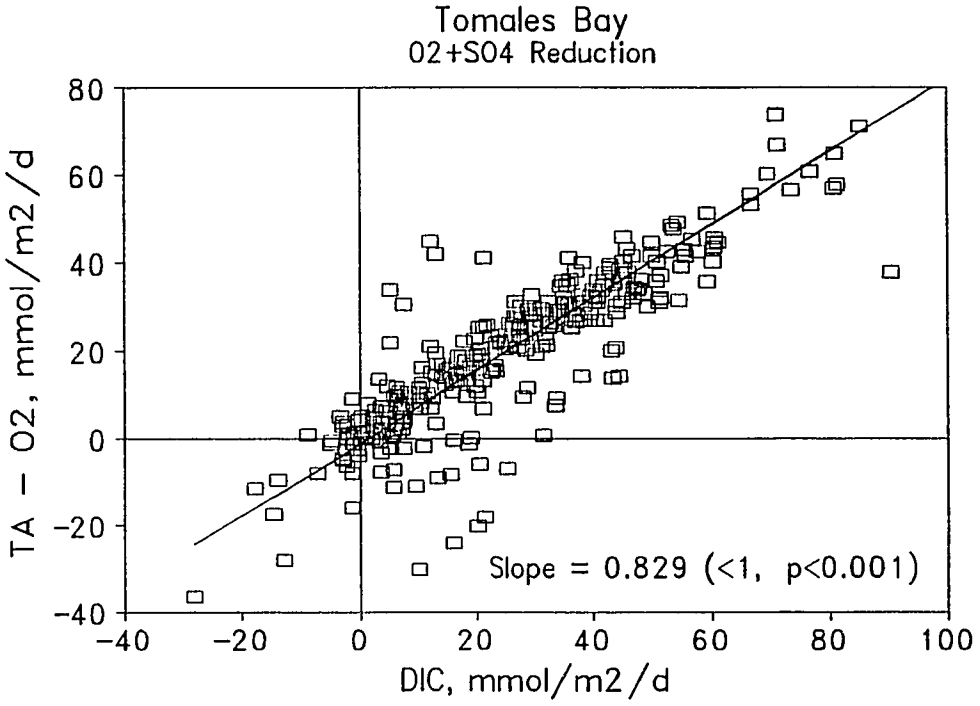

Figure 3.19. Observed net organic C oxidation versus the sum of O_2 and SO_4^{2-} reduction in Tomales Bay sediments. The best-fit slope is compared with the theoretical slope of 1 expected for complete organic C respiration by O_2 and SO_4^{2-} reduction (equation 3.15, see text).

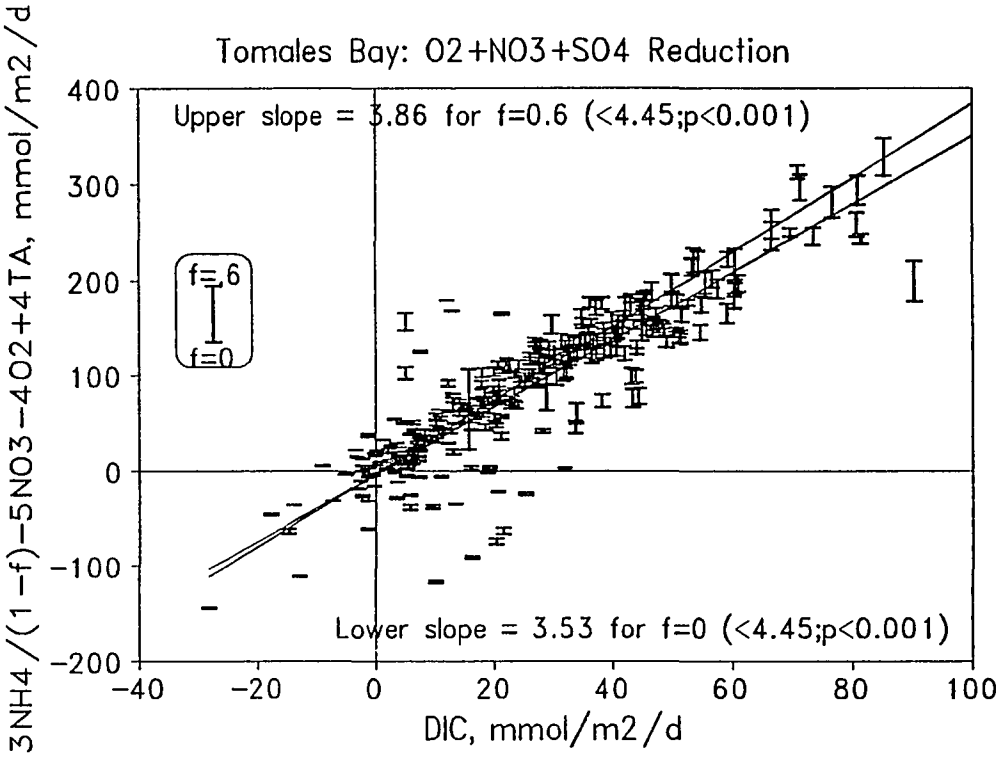

Figure 3.20. Observed net organic C oxidation versus the sum of O_2, NO_3^-, and SO_4^{2-} reduction in Tomales Bay sediments. The range given for each data point represents sediment NH_4^+ removal coefficients between 0 and 0.6. The best-fit slope for each sorption coefficient is compared with the theoretical slope of 4.45 expected for complete organic C respiration by O_2, NO_3^- and SO_4^{2-} reduction (equation 3.17, see text) for the decomposition of organic matter with the N:C ratio of 16:106.

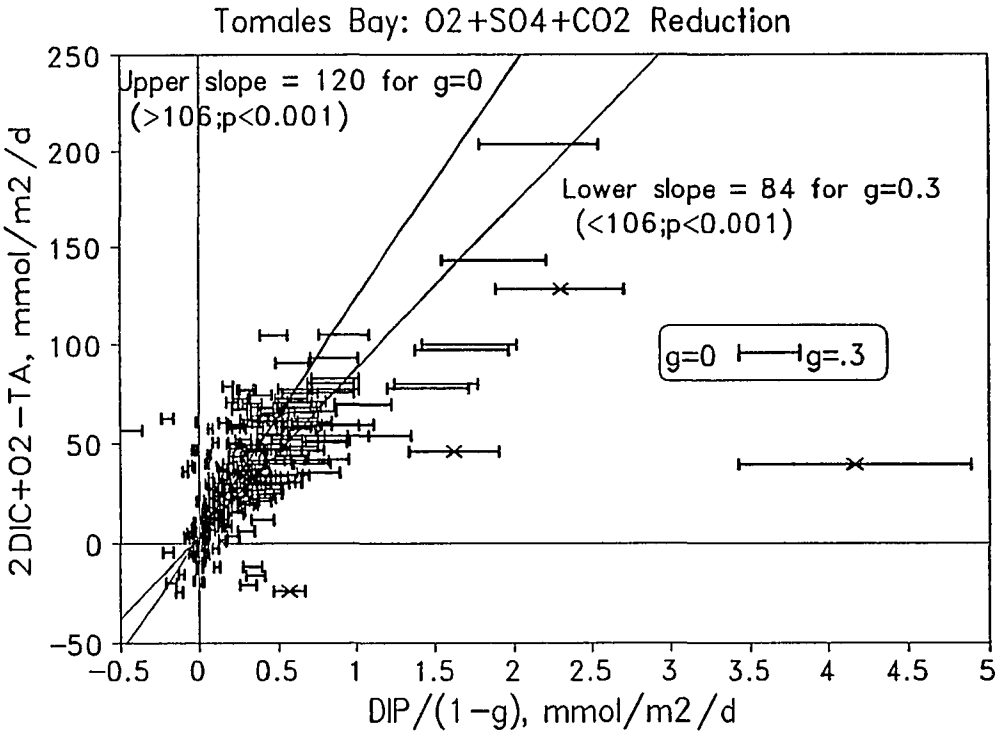

Figure 3.21. Benthic DIP flux as an indicator of the net organic C oxidation (when methanogenesis is included) versus the sum of O_2, SO_4^{2-}, and CO_2 reduction in Tomales Bay sediments. The range given for each data point represents sediment DIP removal coefficients between 0 and 0.3. The best-fit slopes for these sorption coefficients correspond to the decomposition of organic matter with the C:P ratio of 120:1 and 84:1 (equation 3.21, see text). Both of them are significantly different from 106 ($p<0.001$). Data marked by X are outliers detected with $p<0.0001$ that they are real (see Appendix C).

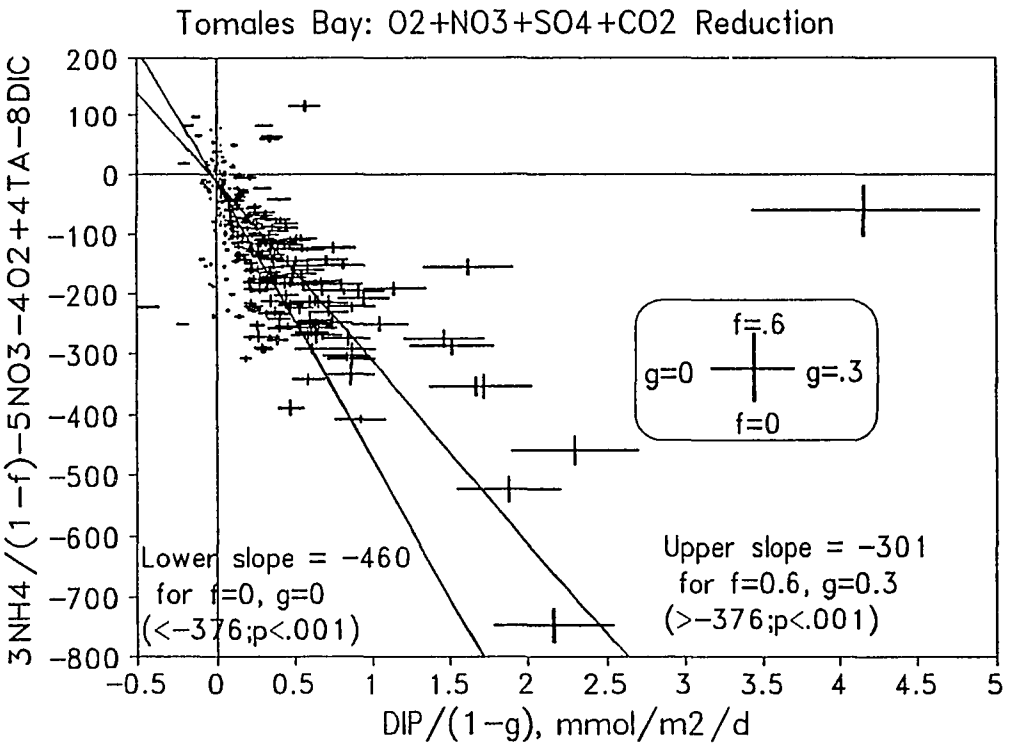

Figure 3.22. Benthic DIP flux as an indicator of the net organic C oxidation (when methanogenesis is included) versus the sum of O_2, NO_3^-, SO_4^{2-}, and CO_2 reduction in Tomales Bay sediments. The vertical and horizontal error bars represent uncertainties due to NH_4^+ and DIP removals by sediments. The best-fit slopes for each removal extreme are significantly different from -376, which corresponds to the decomposition of organic matter with the C:N:P ratio of 106:16:1 (equation 3.23, see text).

Let us go back to Fig. 3.20 and estimate how much additional oxidant is needed in order to balance redox reactions in Tomales Bay sediments. If the median NH_4^+ sorption coefficient (*f*) of 0.3 is chosen, the best-fit slope will be 3.77 and the y-intercept will be 0.07. By solving this linear regression equation for the average DIC flux of 25.1 mmol m^{-2} d^{-1} and subtracting the result from the theoretical value for decomposing organic N:C ratio of 16:106--which is: $(3\times16/106+4)\times25.05 = 111.5$ meq m^{-2} d^{-1}--it leaves 17.2 meq m^{-2} d^{-1} of electrons (about 15% of the total electrons generated) unaccounted for by O_2 + SO_4^{2-} + NO_3^- reduction.

Net methanogenesis in Tomales Bay sediment ranges from 0 to 0.2 mmol m^{-2} d^{-1} (Rust, 1993); this can accept up to 1.6 meq m^{-2} d^{-1} of the unaccommodated electrons discussed above. Reduction of oxidized metals, namely Fe(III) and Mn(IV), are estimated based on an average particle accumulation rate of about 1 g cm^{-2} y^{-1} for the bay (Snidvongs et al., ms.). Dollar et al. (1991) found that the Fe(II) contents of the bay and stream sediments were about 1 and 0.6 wt%, respectively. According to Dollar et al. (1991), this 0.4 wt% difference can be assumed to be formed in the bay sediment *in situ* by Fe(III) reduction. Therefore Fe(III) reduction rate estimated this way is about 2 mmol m^{-2} d^{-1}, which is also 2 meq m^{-2} d^{-1} electrons consumed. If the Fe content of the average shale of about 4 wt% (Li, 1981) is assumed for Tomales Bay sediments, the reduction of all Fe will consume 20 meq m^{-2} d^{-1} electrons. This reduction rate may be regarded as an upper limit for electron consumption. Lastly, Mn(IV) reduction is also estimated by assuming an average shale Mn of 840 ppm (Li,

1981) for Tomales Bay sediments. From this assumption, Mn(IV) reduction rate is about 0.8 meq m^{-2} d^{-1}.

Reduction of these three minor oxidants in Tomales Bay sediments can accommodate 3 to 22 meq m^{-2} d^{-1} of electrons (Table 3.5). The range covers the 17.2 meq m^{-2} d^{-1} needed. In addition to these reduction reactions, another factor that can influence the observed electron transfer in coastal sediments is groundwater seepage. Groundwater can contain significant amounts of DIC, NO_3^- and TA. These chemical constituents can lead the model to overestimate organic C oxidation rate, underestimate NO_3^- reduction rate and overestimate SO_4^{2-} reduction rate. To correct for groundwater effects, discharge data for three geological regions around Tomales Bay and the average concentration of DIC, NO_3^- and TA in groundwater in each region reported by Oberdorfer et al. (1991) were used.

It is shown in Table 3.5 that the excess electrons unaccounted for by O_2 + SO_4^{2-} + NO_3^- reduction (17.2 meq m^{-2} d^{-1} for decomposing organic N:C ratio of 16:106) can possibly be balanced by minor reduction reactions and groundwater effects. One implication of this electron balance is that organic diagenesis in Tomales Bay sediments is controlled by conventional processes, even though many of them are yet to be quantified.

The net nitrification and denitrification rates at each location in Tomales Bay were estimated from the benthic DIC or DIP fluxes and an assumed organic N:P ratio of 16:1. The organic C:P ratio was estimated by varying the ratio until the variance between DIC-predicted, and DIP-predicted denitrification was at a minimum. This

Table 3.5. Minor mechanisms in Tomales Bay sediments that may be responsible for excess electrons unaccounted for by the net uptakes of O_2, SO_4^{2-} and NO_3^- from the water column.

Reactions	Rate mmol m^{-2} d^{-1} Min	Max	Electrons consumed meq m^{-2} d^{-1} Min	Max
Minor reduction reactions*				
$CO_2 \rightarrow CH_4$	0	0.2	0	2
Fe(III) → Fe(II)	2	20	2	20
Mn(IV) → Mn(II)	0.4		0.8	
Total minor reduction			**2.8**	**23**
Groundwater inputs**				
DIC	0.8	3	3.1	12
NO_3^-	0.04	0.14	0.2	0.7
TA	0.5	2	-0.5	-2
Total groundwater effects			**2.8**	**11**
Grand total***			**5.6**	**34**

* Maximum and minimum rates for each reaction are discussed in text

** Maximum and minimum groundwater discharges are estimated by Darcy's Law and by soil moisture budget (Oberdorfer et al., 1991).

*** Excess electrons unaccounted for by net O_2, SO_4^{2-} and NO_3^- uptakes from the water column 17.2 meq m^{-2} d^{-1}.

iterative technique is chosen because it is not very sensitive to outliers. The decomposing organic C:N:P ratios that gave the best agreement between the two approaches for the 6 km, 10 km and 16 km sediments were 84:16:1, 63:16:1 and 116:16:1, respectively. Time series of the estimated denitrification rates are shown in Fig. 3.23. Nitrification is not shown in the figure, because the difference between nitrification and denitrification is always very small compared with the rates themselves.

Discussion

Nitrogen Cycling in Coastal Marine Sediments: Some Conceptual Models

Some insights about the coupling between nitrification and denitrification in sediments can be deduced from the observed benthic NO_3^- flux (Christensen et al., 1987; Henriksen and Kemp, 1988; Hansen and Blackburn, 1991). Although the absolute magnitude of NO_3^- fluxes is usually small and contributes little to the net N budget, the relative magnitudes of NO_3^- fluxes with time should reflect the temporal net balance of nitrogen reactions in sediments. Because the NO_3^- flux is a variable that is measured directly, the net difference between nitrification and denitrification in sediments, although small relative to each reaction rate, is known with a reasonable precision. If the observed NO_3^- fluxes are plotted against the calculated nitrification or denitrification rates, some internal kinetics that control these nitrogen reactions can be postulated. For the sake of simple discussion here, groundwater nutrient input is set aside. If the NO_3^- pool in sediments is in a quasi steady state (relative to the time scale of fluctuations in the nitrification and denitrification rates), NO_3^- flux across the

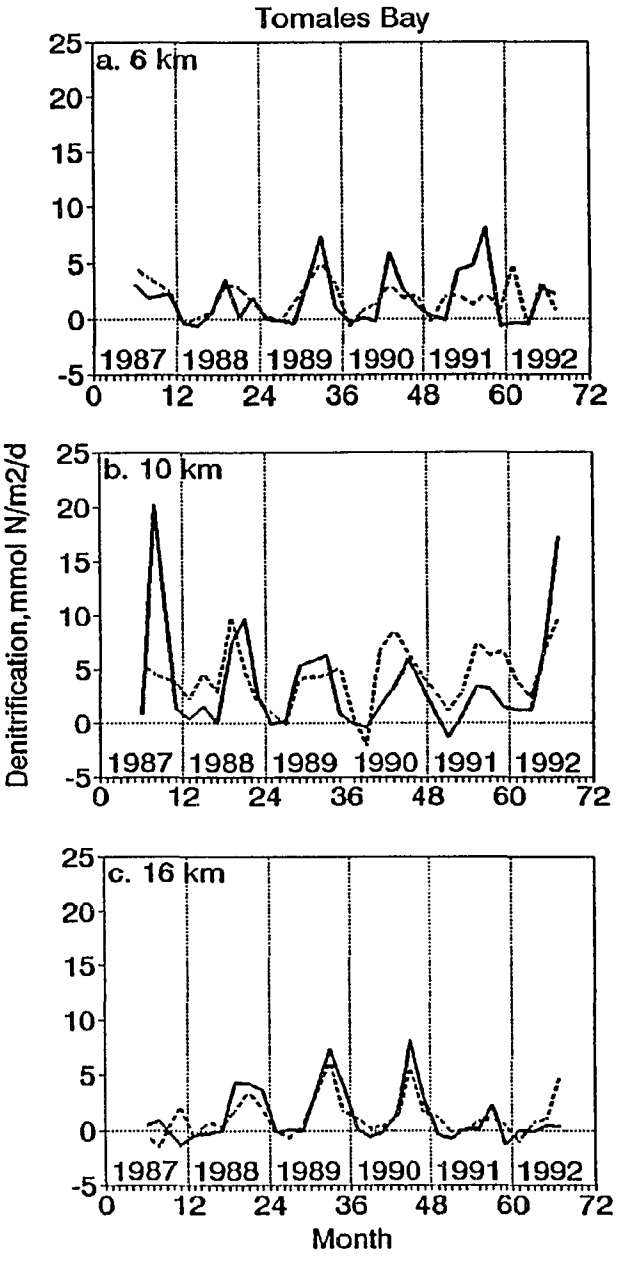

Figure 3.23. Model denitrification rates in Tomales Bay sediments at 6, 10, and 16 km from the bay mouth. Solid lines were estimated from the benthic DIP fluxes and assumed decomposition N:P ratio of 16:1. Dashed lines were estimated from the benthic DIC fluxes and the decomposition of organic matter with the C:N ratios of 84:16, 63:16, and 116:16 for 6, 10, and 16 km sediments, respectively (see text).

sediment-water interface equals nitrification minus denitrification rates. Net NO_3^- flux out of the sediment implies a nitrification rate that is faster than the denitrification rate, and thus the net N_2 degassing from the sediments is limited by the denitrification step. Zero NO_3^- flux means nitrification equals denitrification and possibly nitrification limits N_2 degassing. Net NO_3^- flux into the sediment implies a nitrification rate that is slower than denitrification. However, under the last condition, the direction of NO_3^- flux alone is not sufficient to establish which step; among nitrification, denitrification or NO_3^- uptake across the sediment-water interface, is the rate limiting step.

Kinetics of nitrogen reactions in coastal sediments are probably controlled by two important internal mechanisms: 1) nitrogen cycling and 2) electron cycling. These two cycles in coastal sediments are generalized as flowcharts in Figs. 3.24 and 3.25. In both flowcharts, four groups of benthic organisms will be considered: 1) aerobic macro- and micro-organisms, 2) nitrifying microbes, 3) denitrifying microbes, and 4) ammonifying microbes. The last two groups are both NO_3^- reducers but they produce different N products. These organisms are assigned to either O_2 reduction or NO_3^- reduction zones (or microzones) according to their roles in N redox.

In the diagram in Fig. 3.24, aerobic respiration is the most important source of "new" NH_4^+. Ammonification also produces NH_4^+ but by recycling N from NO_3^-. Although strictly speaking, NH_4^+ is also regenerated from organic N by ammonifiers and denitrifiers as they utilize organic matter for energy, the magnitude of "new" NH_4^+ produced by these anaerobic N respirations is negligible compared with the

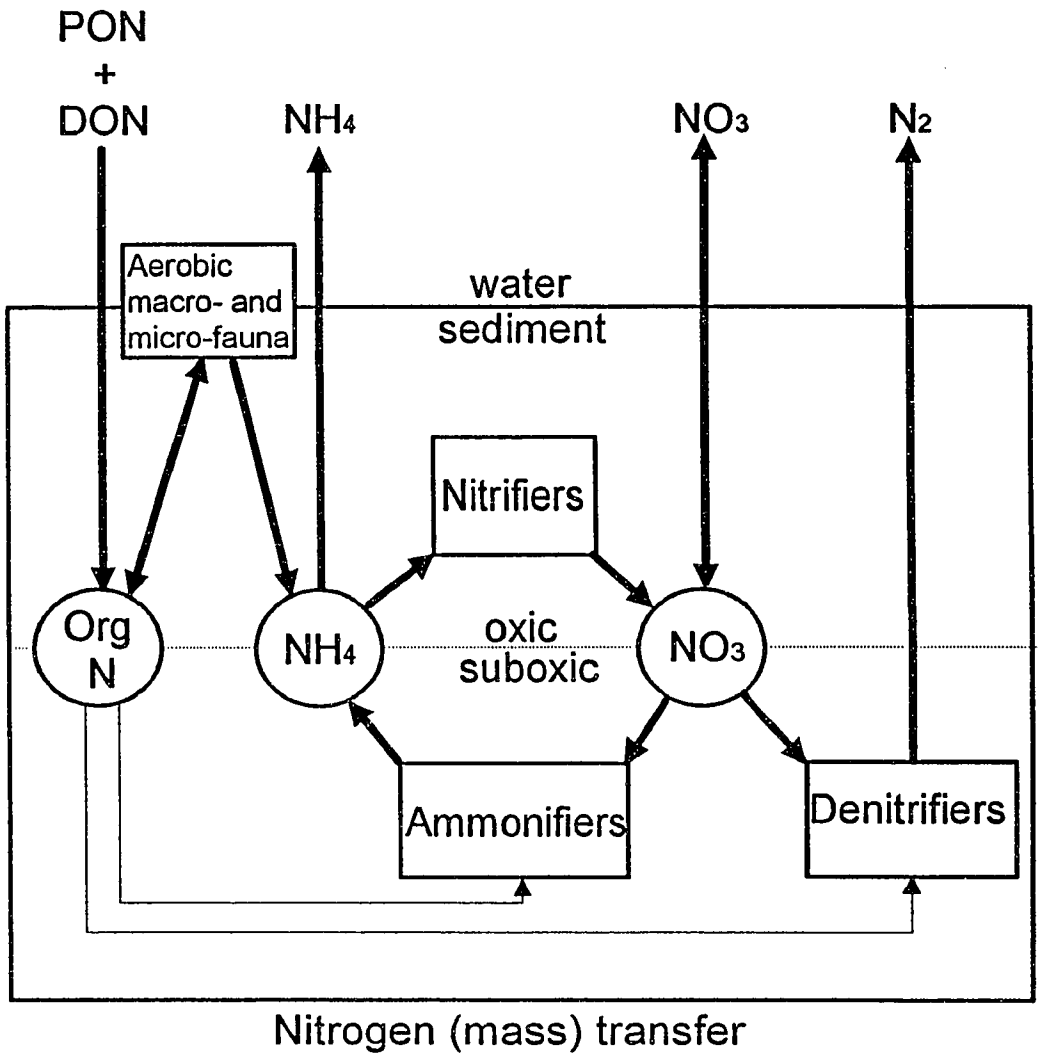

Figure 3.24. A diagram for nitrogen mass cycling in coastal sediments. Groups of organisms that are involved in the cycling are shown by rectangular boxes. Non-living N pools are shown by circular boxes. Transfer paths shown by thin lines are less important, although they are given in the diagram for the sake of completeness.

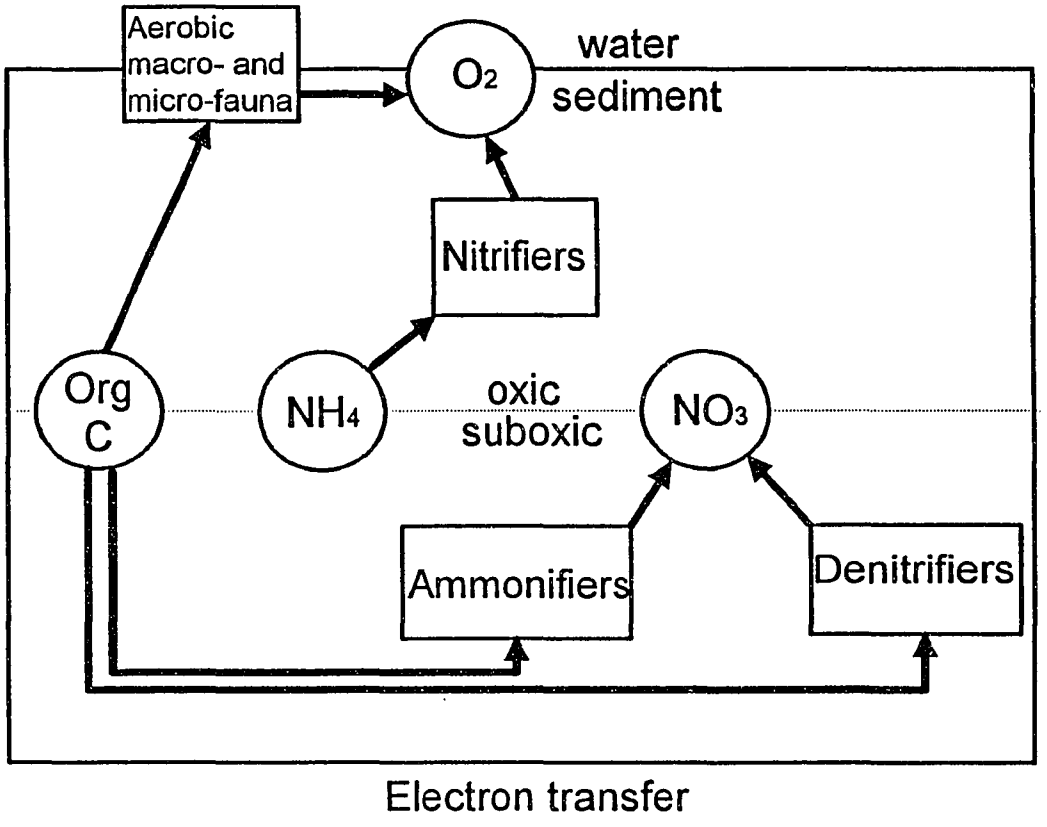

Figure 3.25. A diagram for electron transfers in the C and N redox cycle in coastal sediments. Groups of organisms that are involved in the cycling are shown by rectangular boxes. Non-living C, N, and O pools are shown by circular boxes.

organic N breakdown by aerobic pathways. At steady state, gross NH_4^+ yield in sediments is balanced by the release of NH_4^+ into the water column and by consumption by nitrifying microorganisms. Because most coastal sediments release NH_4^+, it is rare that nitrification would be limited by NH_4^+.

Electron transfers by the N reaction system in coastal surface sediments are shown in Fig. 3.25. Among the two oxidants in this diagram, O_2 input across the sediment-water interface is far more critical than NO_3^- input, because in most coastal sediments NO_3^- is produced *in situ* by nitrifying microorganisms using O_2 (Seitzinger, 1988, 1990). In addition, the Michaelis constants for O_2 uptake (i.e., O_2 concentration such that the uptake rate is one half the maximum uptake rate) by nitrification are much less than by aerobic respiration (Henriksen and Kemp, 1988), indicating a lower affinity for O_2 by nitrifiers than aerobic organisms. The sediment nitrification could be easily limited by O_2.

Dissimilatory NO_3^- reduction reactions could also be limited by organic C (Knowles, 1982; Bradley et al., 1992; Brettar and Rheinheimer, 1992). Although a shortage of bulk organic C is unlikely in surface coastal sediments, denitrification and ammonification might be limited by certain simple organic molecules which are preferred by microorganisms. Many studies on organic-rich sewage sludge have found that addition of simple organic molecules, such as acetate, methanol, and methane can accelerate the net denitrification rate by the nitrification-denitrification system (Carley and Mavinic, 1991; Hanaki and Polprasert, 1989). These findings suggest that denitrification cannot utilize all organic compounds, but may be restricted

to certain compounds. Because simple organic molecules can also be consumed by oxic respiration at a rate at least equal to that by suboxic respirations (Lee, 1992), in well oxidized sediments, it is possible that the organic molecules preferred by NO_3^- reducers might be available in limited supply.

Although both denitrification (producing N_2) and ammonification (producing NH_4^+) reduce NO_3^-, the conditions that favor the reactions are not the same. In a strongly anaerobic habitat where the electron activity is high, ammonification is favored because of its capacity to take up eight moles of electrons per mole of NO_3^- instead of the five taken up by denitrification (Tiedje et al., 1982; Jørgensen, 1989). Denitrification will dominate the system when suitable reduced organic C substrates are limited, because denitrification yields more energy per unit substrate than ammonification (Tiedje et al., 1982; Brettar and Rheinheimer, 1992).

Previous studies have confirmed that the net outcome of the N reactions in marine sediments depends on both the organic carbon delivery rate and the redox condition. Hopkinson (1987) found that NO_3^- fluxes out of Georgia Bight sediments were highest in summer, when the organic deposition rate was probably highest. This result is in contrast to many temperate coastal systems, such as inner Tomales Bay (this study and Dollar et al., 1991), Narrangansett Bay (Nixon et al., 1976) and Chesapeake Bay (Kemp and Boynton, 1992), where net NO_3^- fluxes are usually zero during the high organic input period due to the limitation of nitrification. However, the Georgia Bight porewaters studied by Hopkinson (1987) in the upper 30 cm were oxidized, and NO_3^- concentrations in porewater were always high even during the

months of high benthic respiration. This is very much different from the other three temperate coastal embayments mentioned above, where sediments were possibly less oxic during the period of high organic input. The effects of organic matter quality as the energy source for N reactions in these temperate coastal sediments are not known.

Benthic macrofauna can play physical roles in the N mass transfer in surface sediments. One of the effects is bioturbation, which could make new substrates and oxidants available for nitrogen reactions. At the same time, bioturbation prevents accumulation of metabolic products that can inhibit the reactions (Aller, 1982). Fragmentation of organic particles by macrofauna also increases surface areas for microbial colonization (Lee, 1992).

Bioturbation activity by benthic fauna has a strong effect on the redox condition of sediments (Aller and Aller, 1992). The coupling between nitrification and denitrification is thought to be independent of the bulk redox condition of the sediment (e.g., electron activity per unit sediment area), but this coupling depends on the aerobic/anaerobic microzone in sediments created by burrows and tubes of benthic fauna (Hylleberg and Henriksen, 1980; Jenkins and Kemp, 1984; Aller, 1988). A decline in the benthic fauna population or a reduction in their burrowing activity, e.g. in temperate sediments in winter time (Kemp et al., 1990), can lead to a more homogeneous sediment, a condition that does not favor nitrification.

<u>Nitrogen Reactions in the Upper Gulf of Thailand Sediments</u>

The plot between denitrification rate and NO_3^- flux for the Gulf of Thailand clearly indicates a generally negative trend (Fig. 3.26). Denitrification rates at

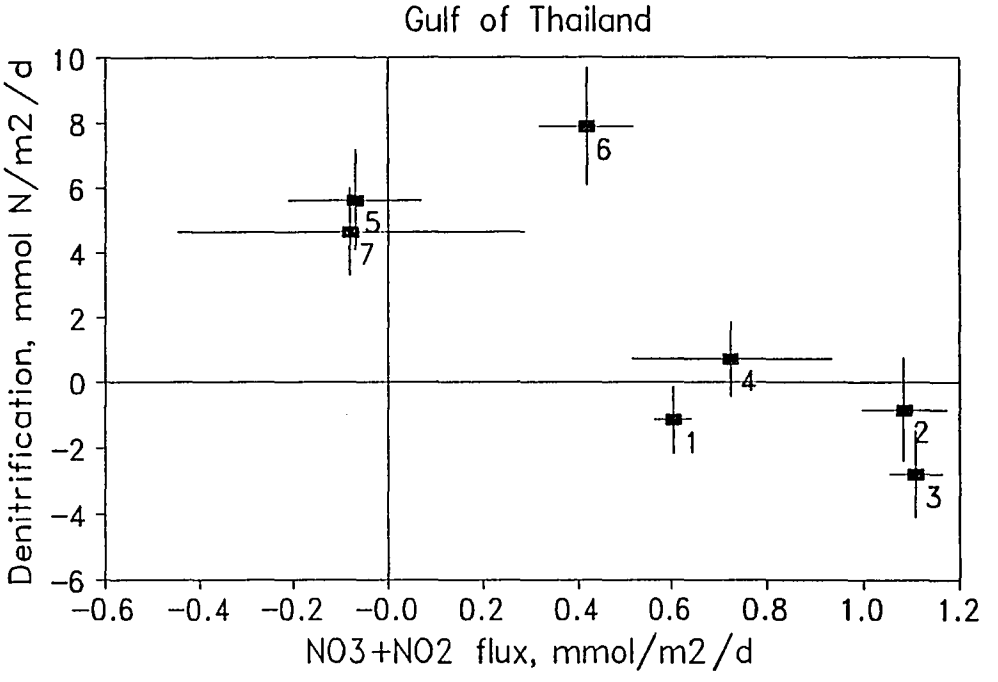

Figure 3.26. The observed benthic NO_3^- effluxes versus model sediment denitrification rates--average of the three methods (Fig. 3.10)--at seven benthic study stations in the upper Gulf of Thailand. Error bars represent standard errors of the mean rates among three replicates at each locations.

Stations 1 to 4 were near zero or slightly negative (net N_2 fixed?). Upward NO_3^- fluxes at these four locations were high; thus denitrification was apparently not limited by NO_3^- or by the nitrification step. Instead, organic carbon was more likely to be at least partially the rate limiting factor. This condition is reasonable for offshore locations (Stations 1, 2, and 3) where organic inputs (Table 3.2) were relatively low. This hypothesis could also explain the relatively high denitrification (Table 3.4; Fig. 3.26) and the lack of NO_3^- flux at Stations 5 and 7 (Table 3.1; Fig. 3.26). At both stations organic input rates were high (Table 3.2), and NO_3^- reduction and nitrification could proceed at the same rate. This seems to be the condition where net N_2 degassing in the sediment was operating at its highest efficiency.

There were net upward fluxes of NO_3^- at Stations 4 and 6 despite the high delivery rates of organic C to sediments at these locations (Table 3.2). Some of the excess NO_3^- flux at Station 6 might be due to groundwater input, but this explanation might not be applicable for Station 4. An alternative explanation would be that the organic molecules preferred by the two NO_3^- reduction reactions (denitrification and ammonification) were less available. A high input of bulk organic carbon at these two stations would not guarantee that the preferred organic molecules were in abundant. The bulk organic matter delivered to the sediments at both of these locations is probably high in terrestrial materials. Many of these could be complex organic molecules, e.g. humic and fulvic substances, which might not be readily available for NO_3^- reduction. Oxic respiration in these sediments was also high and could out-compete N reactions for organic molecules.

Besides organic C quantity and quality, surface mixing of the Gulf of Thailand sediments can favor oxic respiration over NO_3^- reduction. Macrofauna were abundant at every location in this study, implying rapid bioturbation rates. Moreover, bottom trawlers operating intensively in the upper Gulf of Thailand might help accelerate surface sediment mixing. According to a survey in 1985, there were about 1000 trawlers working in the bay (National Statistical Office, 1987). About 10% of the bay bottom could be trawled daily. Although there was no measurement of surface sediment mixing rate in this study, the detection of excess ^{234}Th (half-life = 24 days) as deep as 9 cm in some cores in the Gulf of Thailand (unpublished data) is evidence that rapid mixing was probably occurring.

Nitrogen Reactions in Tomales Bay Sediments

The Tomales Bay dataset is used to apply a kinetic analysis of NO_3^- flux and denitrification rate by assuming no groundwater nutrient input. Because the observed NO_3^- fluxes across the sediment-water interface in Tomales Bay are very small (Fig. 3.16), they can be easily affected by the groundwater NO_3^- inputs which might be as large as the fluxes themselves (Table 3.5). The following analyses are therefore only examples of how to apply the N and electron transfer models (Figs. 3.24 and 3.25) to some "real" time series data. The analysis would be much more realistic if groundwater input rates could be estimated.

The plots of the monthly average data for sediments at 6 km, 10 km, and 16 km from the bay mouth are shown in Fig. 3.27. The temporal differences between net nitrification and denitrification rates that correspond to the relationships in Fig.

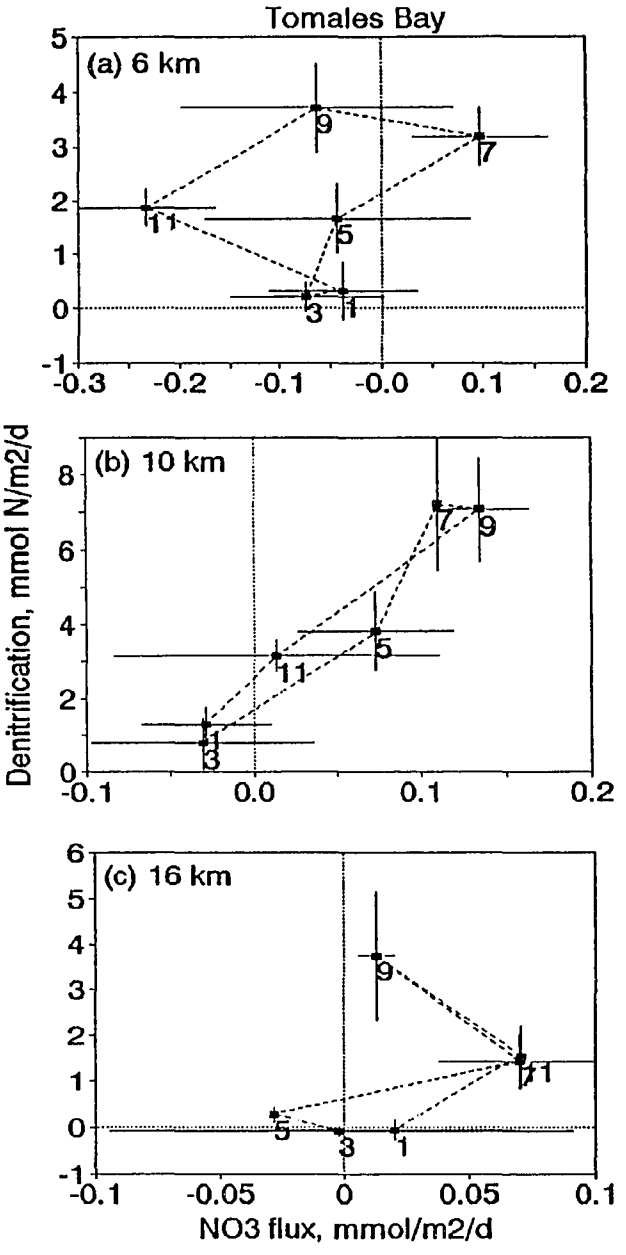

Figure 3.27. Benthic NO_3^- effluxes versus model denitrification rates for Tomales Bay sediments at 6, 10, and 16 km from the bay mouth. All data are averaged by month from 1987 to 1992. Error bars represent standard error of the mean. The numbers are the month of a year (i.e., January=1, February=2, etc.).

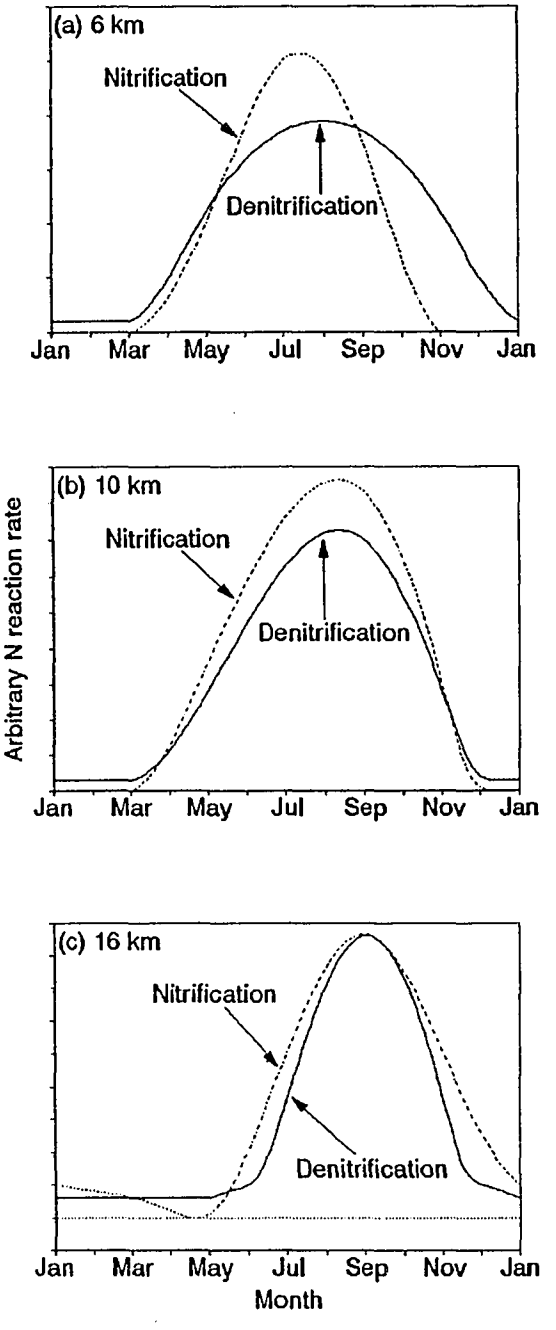

Figure 3.28. Monthly rates of denitrification and net nitrification in Tomales Bay sediments such that the patterns in Fig. 3.27 are produced. Vertical axis scale is proportionally exaggerated so that the difference between the two N reactions can be seen.

3.27 are given in Fig. 3.28. Temperature is possibly the primary factor controlling the general trend of seasonal rate of each N reaction. However, there are also several other controlling factors, such as the supply rates of O_2 (the ultimate oxidant) and of organic C (the ultimate reductant) to sediments.

In outer bay sediments, 6 km from the bay mouth (Figs. 3.27a and 3.28a), both net nitrification and denitrification rates are low in winter but denitrification is faster than net nitrification and sediments take up NO_3^-. In spring, the net nitrification rate increases faster than the denitrification rate and eventually exceeds denitrification in mid-summer. This may be due partly to the increasing population of benthic fauna which irrigate oxygenated water through sediments. An opposing effect of O_2 in sediments is the increase in organic C consumption, reducing its availability for denitrification. In the fall season, nitrification in the sediments declines more rapidly, leading to the largest NO_3^- net uptake observed for the bay sediments in order to support denitrification. The low correlation between sediment nitrification and denitrification for outer bay sediments at the 6 km site, compared with those at the other two inner bay stations, suggests that the coupling between these two nitrogen reactions is relatively less tight. Moreover, water column NO_3^- can be a significant, although small, NO_3^- source for N_2 degassing in late summer and fall seasons. Upwelling of deep-water in the nearby Bodega Bay could be an important source of NO_3^- for Tomales Bay water.

Net nitrification and denitrification in inner bay sediments 10 km from the bay mouth (Figs. 3.27b and 3.28b) follow each other more closely than those in outer bay

sediments at the 6 km site. However, at 10 km, net nitrification in the spring through the fall always proceeds at a rate faster than denitrification. This can be a result of the conditions in sediments that are more appropriate for nitrification than denitrification. One possibility is that O_2 supply to the sediments is enhanced in the summer by bioturbation thus accelerating the nitrification rate. At the same time, oxic respiration out-competes denitrification for organic substrates and the latter reaction can not keep up with nitrification.

Nitrification and denitrification coupling in sediments 16 km from the bay mouth, which is also a part of the inner bay, is slightly different from that at 10 km. Although the coupling in 16 km sediments is also tight (i.e., there is very small NO_3^- flux in or out), nitrogen reactions are not accelerated until late spring. This may be a consequence of lower O_2 availability for nitrification in sediments in early spring due to the decay of terrestrial organic materials brought in during the winter peak stream discharge (Hollibaugh et al., 1988; Smith et al., 1991). Another characteristic of the nitrogen reactions in sediments at the 16 km site is the lack of net NO_3^- flux across the sediment-water interface during the time when nitrification and denitrification rates are highest. This can be an effect of anoxia due to the decay of sedimenting organic particulates and organic material associated with seagrass and macroalgae communities developed in the inner bay during summer (Smith et al., 1991).

Conclusion

Smith and Hollibaugh (1989) concluded from their whole bay DIN and DIP (as the net organic C production "currency") mass balances that the net N sink in

Tomales Bay is probably controlled by net system respiration (net heterotrophy). This hypothesis was further explored in this study. It was found that the net DIN sinks via N_2 degassing in the Gulf of Thailand and Tomales Bay sediments were controlled principally by two factors: 1) quantity and quality of organic materials delivered; and 2) the O_2 supply rate to sediments relative to organic material input. Direct uptake of NO_3^- from the water column was, on an annual average, a very small N source for N_2 degassing. Most NO_3^- in Tomales Bay sediments were generated *in situ* via nitrification. The relative rates between nitrification and denitrification in sediments varied seasonally and had strong effects on the bay N cycle.

Denitrification in most sediments in the upper Gulf of Thailand was apparently not limited by nitrification but could possibly be limited by quantity and quality of sediment organic materials. Surface sediment mixing rates could be high and N reactions in sediment were apparently not limited by O_2.

References

Aller, R. C. 1982. The effect of macrobenthos on chemical properties of marine sediment and overlying water. In: McCall, P. L. and Tevesz, M. J. S. (eds.) Animal-Sediment Relations. New York: Plenum, pp. 53-102.

Aller, R. C. 1988. Benthic fauna and biogeochemical processes in marine sediments: The role of burrow structures. In: Blackburn, T. H. and Sørensen, J. (eds.) Nitrogen Cycling in Coastal Marine Environments. Chichester: Wiley, pp. 301-338.

Aller, R. C. and Aller, J. Y. 1992. Meiofauna and solute transport in marine muds. Limnol. Oceanogr. 37: 1018-1033.

Berner, R. A. 1979. Kinetics of nutrient regeneration in anoxic marine sediments. In: Ahrens, L.H. (ed.) Origin and Distribution of the Elements. Oxford: Pergamon Press, pp. 279-292.

Berner, R. A. 1980. Early Diagenesis: A Theoretical Approach. Princeton: Princeton University Press, 241 pp.

Berner, R. A., Scott, M. R. and Thomlinson, C. 1970. Carbonate alkalinity in the pore waters of anoxic marine sediments. Limnol. Oceanogr. 15: 544-549.

Blackburn, T. H. 1986. Nitrogen cycle in marine sediments. Ophelia 26: 65-76.

Bradley, P. M., Fernandez, M. and Chapelle, F. H. 1992. Carbon limitation of denitrification rates in an anaerobic groundwater system. Environ. Sci. Tech. 26: 2237-2381.

Brettar, I. and Rheinheimer, G. Influence of carbon availability on denitrification in the central Baltic Sea. Limnol. Oceanogr. 37: 1146-1163.

Capone, D. G. and Slater, J. M. 1990. Interannual patterns of water table height and groundwater derived nitrate in nearshore sediments. Biogeochemistry 10: 277-288.

Caraco, N., Cole, J. and Likens, G. E. 1989. Evidence for sulfate-controlled phosphorus release from sediments of aquatic systems. Nature 341: 316-318.

Caraco, N., Cole, J. and Likens, G. E. 1990. A comparison of phosphorus immobilization in sediments of freshwater and coastal marine systems. Biogeochemistry 9: 277-290.

Carley, B. N. and Mavinic, D. S. 1991. The effects of external carbon loading on nitrification and denitrification of a high-ammonia land fill leachate. Res. J. Water Pollut. Control Fed. 63: 51-59.

Christensen, J. P., Murray, J. W., Devol, A. H. and Codispoti, L. A. 1987. Denitrification in continental shelf sediments has major impact on the oceanic nitrogen budget. Global Biogeochem. Cycles 1: 97-116.

Crill, P. M. and Marten, C. S. 1986. Methane production from bicarbonate and acetate in an anoxic marine sediment. Geochim. Cosmochim. Acta 50: 2089-2097.

Dickson, A. G. 1981. An exact definition of total alkalinity and a procedure for the estimation of alkalinity and total inorganic carbon from titration. Deep-Sea Res. 28: 609-623.

Dollar, S. J., Smith, S. V., Vink, S. M., Obrebski, S. and Hollibaugh, J. T. 1991. Annual cycle of benthic nutrient fluxes in Tomales Bay, California, and contribution of the benthos to total ecosystem metabolism. Mar. Ecol. Prog. Ser. 79: 115-125.

Ehrlich, H. L. 1987. Manganese oxide reduction as a form of anaerobic respiration. Geomicrobiol. J. 5: 423-431.

Froelich, P. N. 1988. Kinetic control of dissolved phosphate in natural rivers and estuaries: A primer on the phosphate buffer mechanism. Limnol. Oceanogr. 33: 649-668.

Froelich, P. N., Klinkhammer, G. P., Bender, M. L., Luedtke, N. A., Heath, G. R., Cullen, D., Dauphin, P., Hammond, D., Hartman, B. and Maynard, V. 1979. Early oxidation of organic matter in pelagic sediments of the eastern equatorial Atlantic: suboxic diagenesis. Geochim. Cosmochim. Acta 43: 1075-1090.

Froelich, P. N., Bender, M. L., Luedtke, N. A., Heath, G. R. and DeVries, T. 1982. The marine phosphorus cycle. Am. J. Sci. 282: 475-511.

Hanaki, K. and Polprasert, C. 1989. Contribution of methanogenesis to denitrification with an upflow filter. J. Water Pollut. Control Fed. 61: 1604-1611.

Hansen, L. S. and Blackburn, T. H. 1991. Aerobic and anaerobic mineralization in marine sediment microcosms. Mar. Ecol. Prog. Ser. 75: 283-291.

Harrison, P. J., Hu, M. H., Yang, Y. P. and Lu, X. 1990. Phosphate limitation in estuarine and coastal waters of China. J. Exp. Mar. Biol. Ecol. 140: 79-87.

Helgeson, H. C. 1968. Evaluation of irreversible reactions in geochemical processes involving minerals and aqueous solutions--I. Thermodynamic relations. Geochim. Cosmochim. Acta 32: 853-877.

Henriksen, K. and Kemp, W. M. 1988. Nitrification in estuarine and coastal marine sediments. In: Blackburn, T. H. and Sørensen, J. (eds.) Nitrogen Cycling in Coastal Marine Environments. Chichester: Wiley, pp. 207-249.

Hollibaugh, J. T., Cole, B. E., Dollar, S. J., Hager, S. W., Vink, S. M., Kimmerer, W. J., Obrebski, S., Smith, S. V., Valentino, M. and Walsh, T. W. 1988. Tomales Bay, California: a macrocosm for examining biogeochemical coupling at the land-sea interface. Eos 69: 843-845.

Hopkinson, C. S. 1987. Nutrient regeneration in shallow-water sediments of the estuarine plume region of the nearshore Georgia Bight, USA. Mar. Biol. 94: 127-142.

Howarth, R. W. 1988. Nutrient limitation of net primary production in marine ecosystems. Ann. Rev. Ecol. 19: 89-110.

Hylleberg, J. and Henriksen, K. 1980. The central role of bioturbation in sediment mineralization and element re-cycling. Ophelia, Suppl. 1: 1-16.

Jenkins, M. C. and Kemp, W. M. 1984. The coupling of nitrification and denitrification in two estuarine sediments. Limnol. Oceanogr. 29: 609-619.

Jørgensen, K. S. 1989. Annual pattern of denitrification and nitrate ammonification in estuarine sediment. Appl. Environ. Microbiol. 55: 1841-1847.

Kaspar, H. F., Asher, R. A. and Boyer, I. C. 1985. Microbial nitrogen transformations in sediments and inorganic nitrogen fluxes across the sediment/water interface on the South Island west coast, New Zealand. Estuarine Coast. Shelf Sci. 21: 245-255.

Kim, K. H. and Burnett, W. C. 1983. Gamma-ray spectrometric determination of uranium-series nuclides in marine phosphorites. Anal. Chem. 55: 1796-1800.

Kemp, W. M., Sampou, P., Caffrey, J., Mayer, M., Henriksen, K. and Boynton, W. R. 1990. Ammonium recycling versus denitrification in Chesapeake Bay sediments. Limnol. Oceanogr. 35: 1545-1563.

Kemp, W. M. and Boynton, W. R. 1992. Benthic-pelagic interactions: nutrient and oxygen dynamics. In: Smith, D. E., Leffler, M. and Mackiernan, G. (eds.) Oxygen Dynamics in the Chesapeake Bay: A Synthesis of Recent Research. College Park: Maryland Sea Grant, pp. 149-221.

Knowles, R. 1982. Denitrification. Microbiol. Rev. 46: 43-70.

Koike, I. and Sørensen, J. 1988. Nitrate reduction and denitrification in marine sediments. In: Blackburn, T. H. and Sørensen, J. (eds.) Nitrogen Cycling in Coastal Marine Environments. Chichester: Wiley, pp. 251-273.

Krom, M. D. and Berner, R. A. 1980. Adsorption of phosphorus in anoxic marine sediments. Limnol. Oceanogr. 25: 797-806.

Krom, M. D. And Berner, R. A. 1981. The diagenesis of phosphorus in a nearshore marine sediment. Geochim. Cosmochim. Acta 45: 207-216.

Laima, M. J. C. 1992. Extraction and seasonal variation of NH_4^+ pools in different types of coastal marine sediments. Mar. Ecol. Prog. Ser. 82: 75-84.

Lee, C. 1992. Control on organic carbon preservation: The use of stratified water bodies to compare intrinsic rates of decomposition in oxic and anoxic systems. Geochim. Cosmochim. Acta 56: 3323-3335.

Li, Y.-H. and Gregory, S. M. 1974. Diffusion of ions in sea water and in deep-sea sediments. Geochim. Cosmochim. Acta 38: 703-714.

Li, Y.-H. 1981. Geochemical cycles of elements and human perturbation. Geochim. Cosmochim. Acta 45: 2073-2084.

Lovley, D. R. 1987. Organic matter mineralization with the reduction of ferric iron: a review. Geomicrobiol. J. 5: 375-399.

Mackenzie, F. T. and Wollast, R. 1977. Thermodynamic and kinetic controls of global chemical cycles of the elements. In: Stumm, W. (ed.) Global Chemical Cycles and Their Alterations by Man. Berlin: Dahlem Konferenzen, pp. 45-49.

Muller, P. J. 1977. C/N ratios in Pacific deep-sea sediments: Effect of inorganic ammonium and organic nitrogen compounds sorbed by clays. Geochim. Cosmochim. Acta 41: 765-776.

National Statistical Office, 1987. 1985 Marine Fishery Census of Thailand. Bangkok: National Statistical Office, Publication E-Cr-MarF-No. 1-87, 328 pp.

Nishio, T., Koike, I. and Hattori, A. 1983. Estimates of denitrification and nitrification in coastal and estuarine sediments. Appl. Environ. Microbiol. 45: 444-450.

Nixon, S. W. 1981. Remineralization and nutrient cycling in coastal marine ecosystems. In: Neilson, B. J. and Cronin, L. E. (eds.) Estuaries and Nutrients. Clifton, NJ: Humana Press, pp. 111-138.

Nixon, S. W., Oviatt, C. A. and Hale, S. S. 1976. Nitrogen regeneration and the metabolism of coastal marine bottom communities. In: Anderson, J. M. and Macfadyen, A. (eds.) The Role of Terrestrial and Aquatic Organisms in Decomposition Processes. Oxford: Blackwell Scientific, pp. 269-283.

Nixon, S. W., Kelly, J. R., Furnas, B. N., Oviatt, C. A. and Hale, S. S. 1980. Phosphorus regeneration and the metabolism of coastal marine bottom communities. In: Tenore, K. and Coull, B. C. (eds.) Marine Benthic Dynamics. Columbia: University of South Carolina Press, pp. 219-242.

Oberdorfer, J. A., Valentino, M. A. and Smith, S. V. 1990. Groundwater contribution to the nutrient budget of Tomales Bay, California. Biogeochemistry 10: 199-216.

Parsons, T. R., Maita, Y. and Lalli, C. M. 1984. A Manual of Chemical and Biological Methods for Seawater Analysis. Oxford: Pergamon Press, 173 pp.

Piancharoen, C. 1976. Ground water and land subsidence in Bangkok, Thailand. In: Proceedings of the Second Symposium on Land Subsidence. Anaheim, California: Int. Assoc. Hydrol. Sci. Publ. 121, pp. 355-364.

Prigogine, I. 1967. Introduction to Thermodynamics of Irreversible Processes, Third Edition. New York: Interscience, 147 pp.

Redfield, A. C., Ketchum, B. H. and Richard, F. A. 1963. The influence of organisms on the composition of seawater. In: Hill, M. N. (ed.) The Sea. New York: Wiley and Sons, pp. 27-77.

Ricker, W. E. 1973. Linear regression in fishery research. J. Fish. Res. Bd. Can. 30: 409-434.

Robbins, J. A. 1978. Geochemical and geophysical applications of radioactive lead. In: Nriagu, J. O. (ed.) The Biogeochemistry of Lead in the Environment. Amsterdam: Elsevier, pp. 285-393.

Rosenfeld, J. K. 1979. Ammonium adsorption in nearshore anoxic sediments. Limnol. Oceanogr. 24: 356-364.

Rust, T. M. 1993. The Relative Importance of Processes Controlling the Distribution of Methane in Tomales Bay, California. M.S. Thesis, University of Hawaii, 76 pp.

Ruttenberg, K. C. and Berner, R. A. 1993. Authigenic apatite formation and burial in sediments from non-upwelling, continental margin environments. Geochim. Cosmochim. Acta 57: 991-1007.

Ryther, J. H. and Dunstan, W. M. 1971. Nitrogen, phosphorus, and eutrophication in the coastal marine environment. Science 171: 1008-1013.

Sansone, F. J. and Marten, C. S. 1981. Methane production from acetate and associated methane fluxes from anoxic coastal sediments. Science 211: 707-709.

Schindler, D. W. 1985. Coupling of elemental cycles by organisms: evidence from whole-lake chemical perturbations. In: Stumm, W. (Ed.) Chemical Processes in Lakes. New York: Wiley, pp. 225-250.

Seitzinger, S. P. 1988. Denitrification in freshwater and coastal marine ecosystems: Ecological and geochemical significance. Limnol. Oceanogr. 33: 702-724.

Seitzinger, S. P. 1990. Denitrification in aquatic sediments. In: Revsbech, N. P. and Sørensen, J. (eds.) Denitrification in Soil and Sediment. New York, Plenum Press, pp. 301-322.

Seitzinger, S. P., Gardner, W. S. and Spratt, A. K. 1991. The effect of salinity on ammonium sorption in aquatic sediments: implications for benthic nutrient recycling. Estuaries 14: 167-174.

Sharma, M. L. 1986. Role of Groundwater in Urban Water Supplies of Bangkok, Thailand, and Jakarta, Indonesia. Honolulu: East-West Environ. Policy Inst. Alumni Paper No. 6, 123 pp.

Smith, S. V. and Hollibaugh, J. T. 1989. Carbon-controlled nitrogen cycling in a marine 'macrocosm': an ecosystem-scale model for managing cultural eutrophication. Mar. Ecol. Prog. Ser. 52: 103-109.

Smith, S. V. and Mackenzie, F. T. 1987. The ocean as a net heterotrophic system: implication from the carbon biogeochemical cycle. Global Biogeochem. Cycles 1: 187-198.

Smith, S. V., Kimmerer, W. J., Laws, E. A., Brock, R. E. and Walsh, T. W. 1981. Kaneohe Bay sewage diversion experiment: perspectives on ecosystem responses to nutritional perturbation. Pac. Sci. 35: 279-395.

Smith, S. V., Hollibaugh, J. T., Dollar, S. J. and Vink, S. 1991. Tomales Bay metabolism: C-N-P stoichiometry and ecosystem heterotrophy at the land-sea interface. Estuarine Coast. Shelf Sci. 33: 223-257.

Snidvongs, A., McMurtry, G. M. and Smith, S. V. ms. ^{210}Pb and ^{137}Cs in sediments and soils of Tomales Bay watershed, Northern California. Submitted to Geochim. Cosmochim. Acta.

Strom, R. N. and Biggs, R. B. 1982. Phosphorus distribution in sediments of the Delaware River estuary. Estuaries 5: 95-101.

Tiedje, J. M., Sexstone, A. J., Myrold, D. D. and Robinson, J. A. 1982. Denitrification: ecological niches, competition and survival. Antonie van Leeuwenhoek 48: 569-583.

Umnuay, G. 1984. The behavior of some trace elements in the Chao Phraya River estuary. In: Tamiyavanich, S. (ed.) Proceeding of the Third Seminar on the Water Quality and the Quality of Living Resources in Thai Waters. Bangkok: National Research Council of Thailand, pp. 304-334.

Valiela, I., Costa, J., Foreman, K., Teal, J. M. Howes, B. and Aubrey, D. 1990. Transport of groundwater-borne nutrients from watersheds and their effects on coastal waters. Biogeochemistry 10: 177-197.

Webb, K. L. 1981. Conceptual models and processes of nutrient cycling in estuaries. In: Neilson, B. J. and Cronin, L. E. (eds.) Estuaries and Nutrients. Clifton, NJ: Humana Press, pp. 25-46.

Whiticar, M. J., Faber, E. and Schoell, M. 1986. Biogenic methane formation in marine and freshwater environments: CO_2 reduction *vs.* acetate fermentation--Isotope evidence. Geochim. Cosmochim. Acta 50: 693-709.

Windom, H. L., Silpipat, S., Chanpongsang, A., Smith, R. G. and Hungspreuks, M. 1984. Trace metal composition of and accumulation rates of sediments in the Upper Gulf of Thailand. Estuarine Coast. Shelf Sci. 19: 133-142.

CHAPTER 4

INTERACTION BETWEEN BENTHIC RESPIRATION AND CALCIUM CARBONATE DISSOLUTION IN SEDIMENTS: AN *IN SITU* KINETIC MODEL

Introduction

Although surface seawater is usually supersaturated with respect to most $CaCO_3$ minerals (e.g., Li et al., 1969; Broecker et al., 1979), the saturation state of porewater in many coastal sediments is different from that of overlying water (Aller, 1982; Morse et al., 1985; Walter and Burton, 1990). Reduction in the degree of $CaCO_3$ saturation in surface sediments is usually associated with organic respiration via O_2 reduction (Moulin et al., 1985) and the early stages of SO_4^{2-} reduction (Aller, 1982; Morse and Mackenzie, 1990). However, as SO_4^{2-} reduction continues, its effect on total alkalinity (TA) may become stronger than the effects on dissolved inorganic carbon (DIC, which equals $H_2CO_3+HCO_3^-+CO_3^{2-}$); thus CO_3^{2-} concentration is proportionally increased. Eventually porewater of deep sediments may again become supersaturated with respect to carbonate minerals (Aller, 1982; Reaves, 1986; Morse and Mackenzie, 1990; Walter and Burton, 1990).

The degree of partitioning of respiratory CO_2 during $CaCO_3$ dissolution has been studied in a number of coastal systems. Moulin et al. (1985) reported that in a sedimentary system dominated by aerobic respiration, organic carbon reduction was tightly coupled with $CaCO_3$ dissolution, i.e. each mole of CO_2 produced by respiration dissolved 1 mole of $CaCO_3$. However, in the reducing environment of a

coral reef, Tribble et al. (1990) found that the coupling ratio between $CaCO_3$ dissolution and SO_4^{2-} reduction was only 1:4. Sansone et al. (1990) suggested that $CaCO_3$ dissolution in anoxic carbonate frameworks may involve FeS formation, and the net reaction can be limited by Fe^{2+} supply. This Fe limitation, however, may be less severe in iron-enriched terrigenous sediments.

The degree of coupling between oxic (near surface) or suboxic (deeper layers) respiration and $CaCO_3$ dissolution in coastal sediments can have important consequences for the global carbon cycle. Tight coupling implies that respiratory CO_2 can react with "old" $CaCO_3$ and remain in solution as alkalinity. Thus, net CO_2 degassing by the coastal ocean over a short time scale may not necessarily equal the actual net system respiration. This possibility is not valid over longer time scales, but it can be important over a time scale that is less than the age of surface sediments where porewaters are undersaturated with respect to $CaCO_3$ dissolution (i.e., few decades).

In this study, sediment porewater chemistry in the upper Gulf of Thailand was analyzed for the saturation state with respect to different magnesian calcite phases. Carbonate chemistry results of this study have been reported elsewhere (Snidvongs, in press). To avoid redundancy, this chapter will emphasize mathematical modeling of the analytical data. A model will be developed to quantify the degree of coupling between oxic or suboxic (i.e. SO_4^{2-} reduction) respiration and $CaCO_3$ reactions. This model will utilize the fact that different respiration reactions and $CaCO_3$ dissolution produce different TA:DIC ratios in porewaters. Another modeling technique will be

used to describe calcite dissolution kinetics *in situ* from porewater chemistry and benthic fluxes across the sediment-water interface. Only important chemical data related to the models will be briefly described in this chapter.

Methods

Core Sampling and Chemical Analyses

Seven sediment cores were retrieved from the upper Gulf of Thailand in September 1991, one from each benthic flux station described in Chapter 3 (Figs. 3.1 and 4.1). The details of the sampling equipment and techniques used were given in Chapter 3. As soon as a core was brought on shipboard, it was cut into 3 to 5 cm sections. The pH at the center of each section was immediately measured by a Cole-Palmer flat surface pH electrode connected to a custom made digital electrometer (the measurement precision was ± 0.1 mV or about 0.002 pH unit). A seawater+Tris buffer (Smith and Kinsey, 1978) was used as the routine pH standard. This secondary standard was standardized at least twice daily against the NBS pH 4 and 7 standard buffer solutions (Fisher Scientific). Sediment temperature was measured by a digital thermometer (± 0.1°C). All pH measurements were accomplished within one hour after the core was collected.

Porewater in each sediment section was extracted by a screw-driven, stainless steel squeezer under a normal atmosphere. The extracted porewater was in-line filtered through Whatman GF/C glass fiber filters (1 μm pore size). Water samples were stored at room temperature in 30 ml polyethylene bottles.

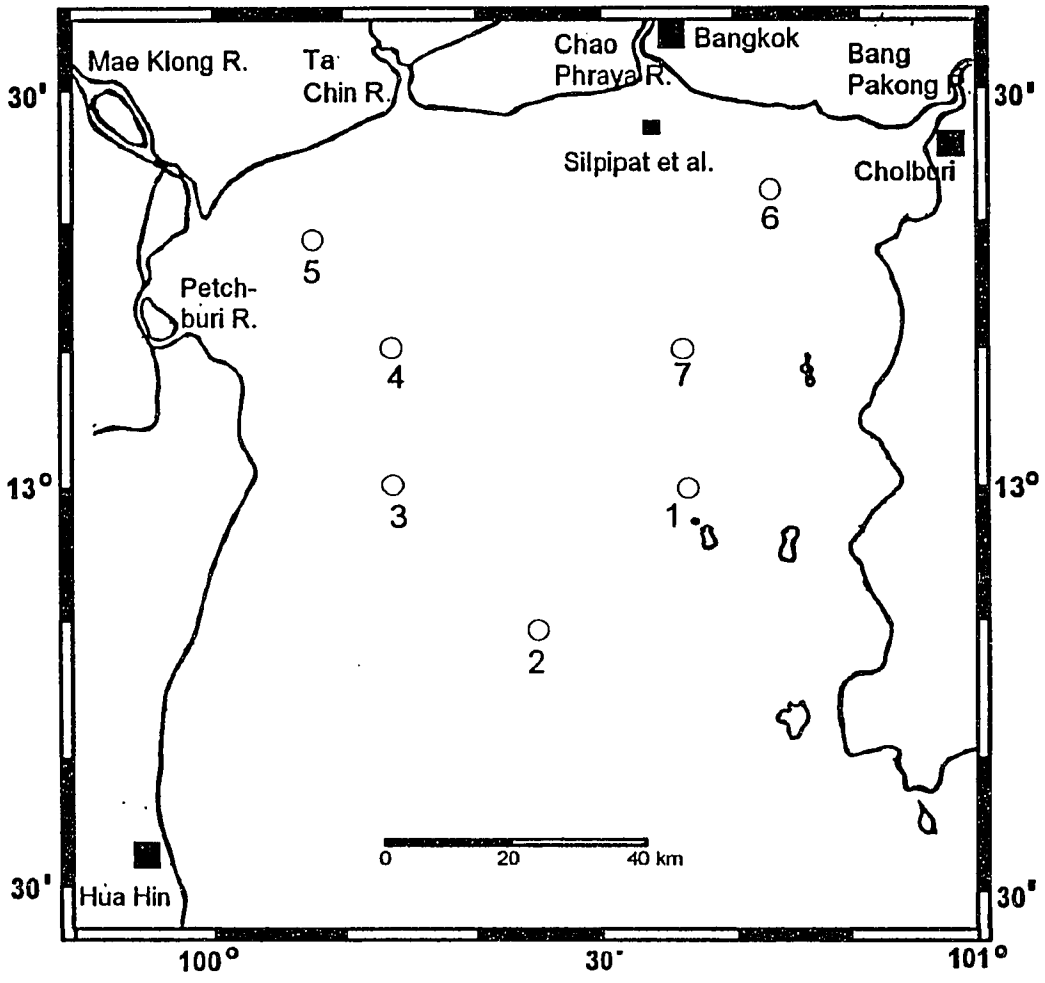

Figure 4.1. Core sampling stations in the upper Gulf of Thailand. The long-term sediment study station of Silpipat et al. (1984) is indicated by a square.

Total alkalinity (TA) of porewater samples was analyzed by a Gran plot titration (Edmond, 1970) at Chulalongkorn University campus in Bangkok within two weeks after the cores were collected. The technique was modified for small volume samples (<5 ml) by using a Gilmont micrometer burette as an acid dispenser.

Dissolved Ca and Mg concentrations in all samples were measured on quantitatively diluted samples using a Pye Unicam atomic absorption spectrophotometer (air/C_2H_2 flame for Ca and N_2O/C_2H_2 flame for Mg). Measurement precisions for Ca and Mg are 0.1 and 0.5 mM, respectively. DIP concentrations in some porewaters were analyzed on diluted samples following the method of Parsons et al. (1984). Measurement precision for DIP was between 0.01 and 0.1 μM, depending on the degree of dilution. Salinity of porewater was determined using an American Optical refractometer ($\pm$ 1 ‰).

Organic carbon and $CaCO_3$ content of sediments were analyzed by the methods fully described in Chapter 3. In brief, HCl and non-HCl treated sediment samples were analyzed for C using a Carlo Erba NA1500 Elemental Analyzer, and the results were taken as $CaCO_3$-C and organic-C + $CaCO_3$-C contents, respectively.

The concentration of DIC and CO_3^{2-} were calculated from *in situ* pH and carbonate alkalinity (CA) using apparent dissociation constants of Mehrbach et al. (1973). For a first approximation, CA was obtained from TA minus borate alkalinity (BA). Total boron was calculated from salinity and Lyman's apparent borate dissociation constant (Skirrow, 1975).

First approximations of DIC concentration (i.e., without SO_4^{2-} reduction correction) are plotted against TA. If the relationship between the two variables can be fitted by a single line for the whole core, oxic conditions will be assumed for the entire core. Under oxic conditions, the production of weak acids and weak bases is small and further corrections for CA is unnecessary. However, in some cores, the DIC-TA relationship breaks down into two discontinuous lines which could reflect the switching of respiration modes between O_2 and SO_4^{2-} reduction. In the SO_4^{2-} reducing environments, the production of NH_3 and H_2S can alter the CA of porewater. To maximize the NH_3 effect, NH_3 production is assumed to be 0.15 times the net DIC production below the assumed oxic/anoxic boundary (the actual organic N:C ratio in these sediments is much less than the Redfield N:C Ratio; see Fig. 3.6). Nitrification and subsequent denitrification are ignored in the SO_4^{2-} reducing environment. NH_3 dissociation is calculated using the apparent equilibrium constant of Johansson and Wedborg (1980). Sulfide alkalinity (SA) is calculated for two scenarios: a) when all reduced S is consumed by the solid mineral phase (represented in this paper by FeS), i.e. SA = 0; and b) when all reduced S remains in solution. The apparent sulfide dissociation constants of Goldhaber and Kaplan (1975) are used to calculate SA. All other effects on alkalinity, besides carbonate, borate, sulfide and ammonia, are trivial and ignored. These alkalinity adjustments are necessary for the calculation of the net extent of SO_4^{2-} reduction. They also correct for the effects of weak acids and weak bases on the $CaCO_3$ saturation state of anoxic porewater (Tribble, 1993). Without these CA corrections, DIC concentrations in the Gulf of Thailand anoxic porewater

could be overestimated by as much as 10 %, but in most cases the error is less than 5 % (e.g., Thorstenson and Mackenzie, 1974).

<u>$CaCO_3$ Saturation State</u>

The stoichiometric ion activity product for an x mol% Mg calcite (IAP_x) is defined as (e.g., Thorstenson and Plummer, 1977):

$$IAP_x = a_{Ca}^{1-x}\, a_{Mg}^{x}\, a_{CO3} \tag{4.1}$$

where a_{Ca}, a_{Mg} and a_{CO3} are activities of Ca^{2+}, Mg^{2+} and CO_3^{2-}, and x is the mole fraction of $MgCO_3$ in calcite. Activities of these ions were calculated from their concentrations in mol kg^{-1} using Pitzer ion activity coefficients for seawater listed in Table 1.5 of Morse and Mackenzie (1990). Subsequently, the degree of saturation of porewater with respect to an x mol% Mg calcite (Ω_x) is defined by:

$$\Omega_x = \frac{IAP_x}{K_x} \tag{4.2}$$

where K_x is the solubility constant for x mol% magnesian calcite. A porewater is said to be supersaturated with respect to x mol% Mg calcite if Ω_x is greater than 1, and undersaturated if Ω_x is less than 1. In this study, for the description of saturation state profiles in sediment porewaters, K_x values from Plummer and Mackenzie (1974) will be used. According to Bischoff et al. (1987), the Plummer and Mackenzie's K_x values are probably more appropriate for natural biogenic calcites in the marine environment than other estimates which are based on cleaned or synthetic samples.

Results

The upper Gulf of Thailand sediments contain between 0 and 25 wt.% $CaCO_3$ (Fig. 4.2) and 0.2 to 2 wt.% organic-C (Fig. 4.3). In most cores except #6, there are generally decreasing trends of $CaCO_3$ content with depth. The non-$CaCO_3$ fraction of the sediments is yellowish in color. After samples are heated in a muffle furnace, the color turns to brick red, indicating the possibility of iron-enriched phases in these sediments.

Vertical profiles of TA and DIC (SO_4^{2-} reduction corrected) concentration in sediment porewater are shown in Figs. 4.4 and 4.5. Statistical testing for TA and DIC concentration gradients in the sediment zones near the core bases revealed that none of those gradients were significantly different from zero (t-test, $p<0.05$; Table 4.1). Therefore diffusional transport of TA and DIC between the surface sediments

Table 4.1. Concentration gradients (in mmol m^{-1} for DIC and meq m^{-1} for TA) at the core bases. 95% confidence intervals of the slope (Snedecor and Cochran, 1980) are given in parentheses.

Stations:	1	2	3	4	5	6	7
DIC	0.11	0.31	-0.12	1.40	0.93	1.41	1.96
	(6.71)	(1.88)	(2.96)	(3.37)	(3.49)	(2.82)	(2.63)
TA	-0.33	0.27	-0.51	-0.12	0.65	0.21	1.06
	(7.80)	(1.62)	(5.51)	(3.14)	(2.71)	(1.39)	(1.97)

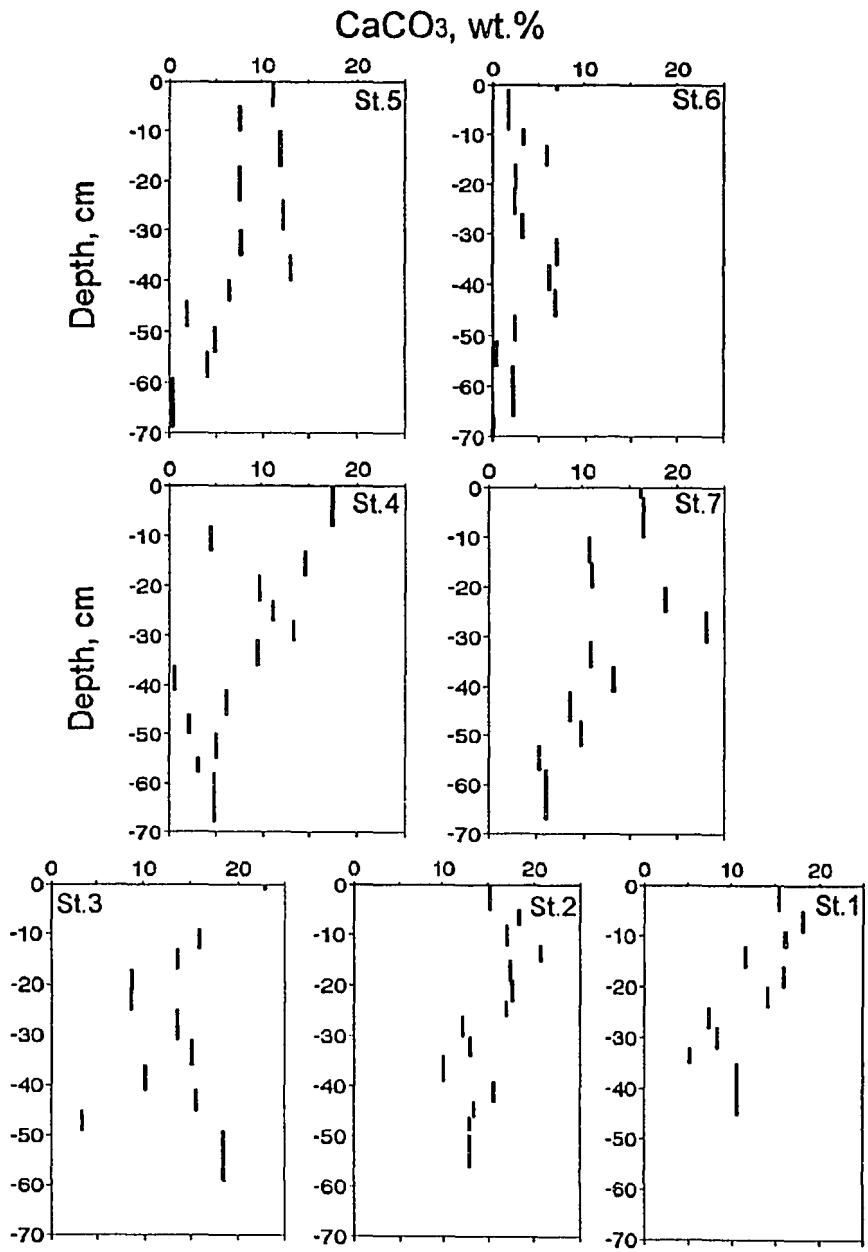

Figure 4.2. $CaCO_3$ content (in weight percent) of seven sediment cores from the upper Gulf of Thailand.

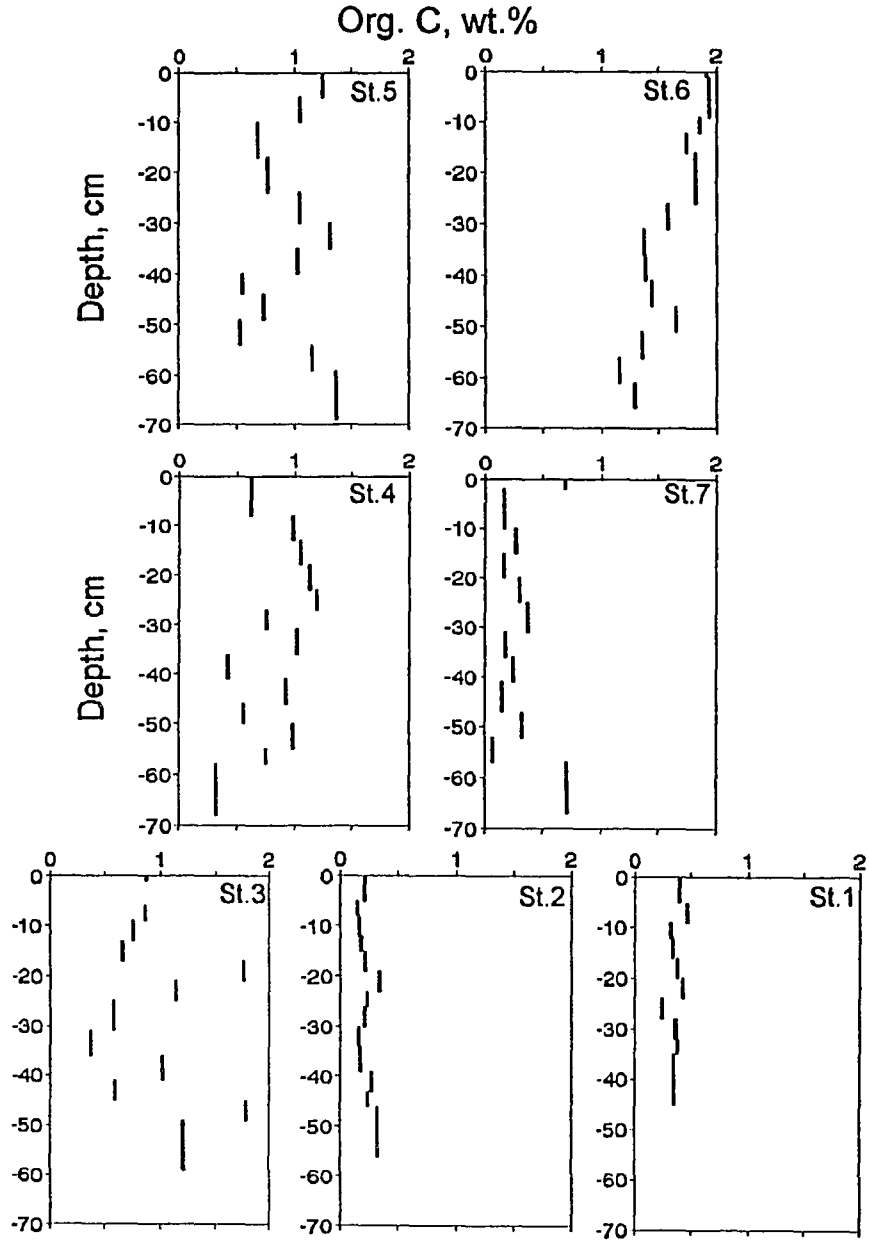

Figure 4.3. Organic carbon content (in weight percent) of seven sediment cores from the upper Gulf of Thailand.

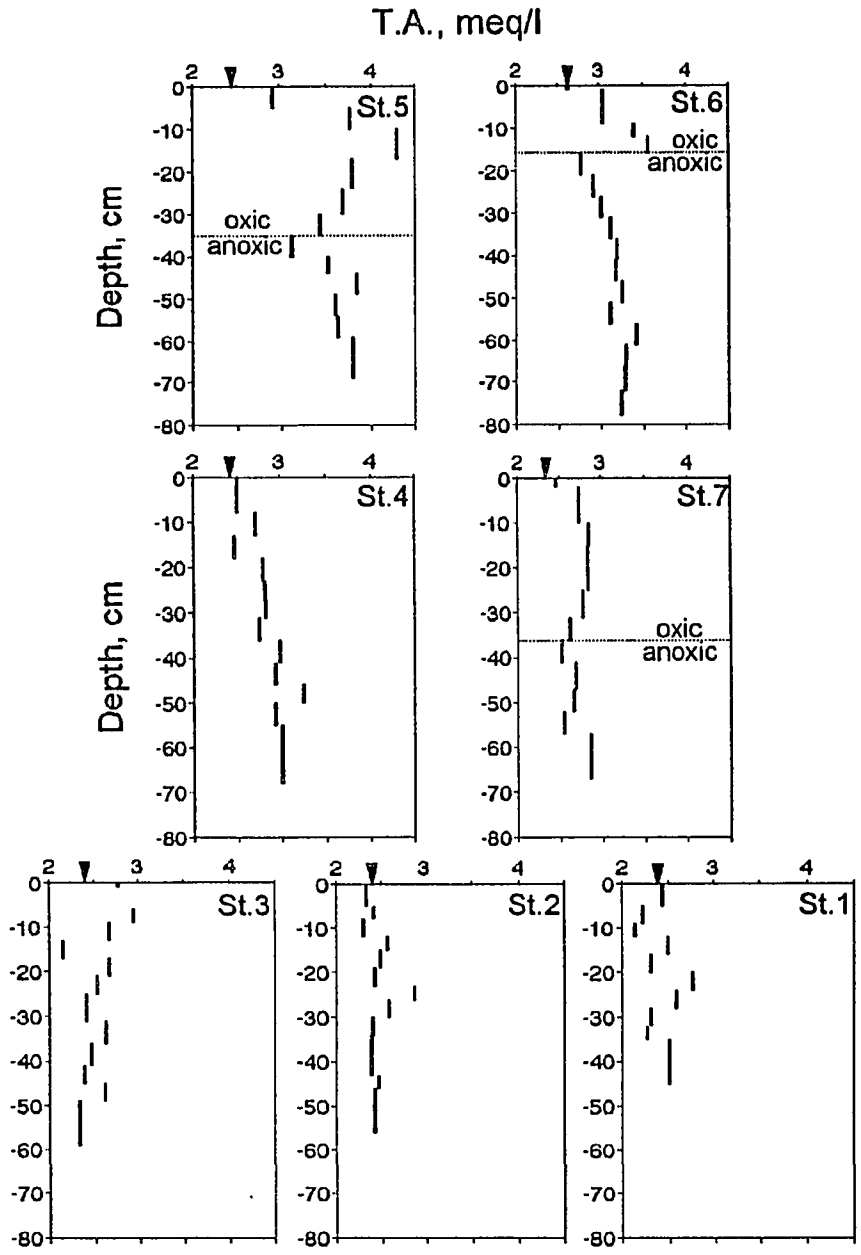

Figure 4.4. Total alkalinity profiles of seven sediment cores from the upper Gulf of Thailand. Bottom water TA values are marked by triangles. Arbitrary oxic/anoxic boundaries are shown for Core# 5, 6 and 7, where flux chamber data suggested the presence of SO_4^{2-} reduction.

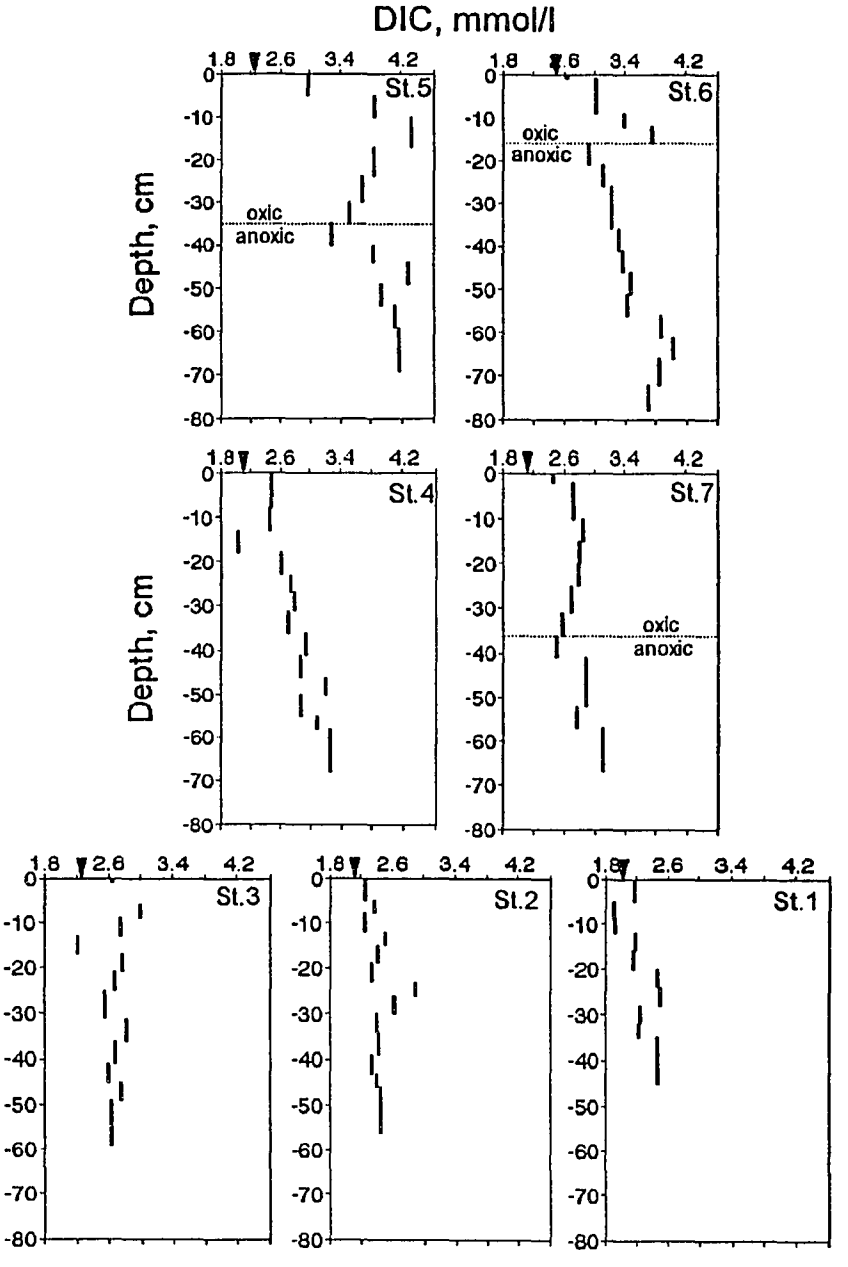

Figure 4.5. DIC concentration profiles of seven sediment cores from the upper Gulf of Thailand. All other details are the same as in Fig. 4.4.

(those included in the core) and the basal sediments (those deeper than the core) was small and will be neglected in all subsequent models. This condition allows direct comparison between the net change in porewater chemistry of the core with flux data in Chapter 3.

From the flux chamber data analysis in Chapter 3, these surface sediment cores may be divided into two groups according to the absence or presence of SO_4^{2-} reduction. Respiration in sediments at Stations 1, 2, 3 and 4 was almost entirely via O_2 reduction (Fig. 3.3), while O_2 and SO_4^{2-} reduction were significant processes in sediments at Stations 5, 6 and 7 (Fig. 3.5). Apparently, the porewater TA-DIC relationship in Core# 5, 6 and 7 may also be differentiated into two distinct zones. In sediments covered by this study, other oxidants besides O_2 and SO_4^{2-} reduction were not important in terms of organic-C oxidation.

Sediments Without SO_4^{2-} Reduction: Stations 1, 2, 3, and 4

Porewater in the uppermost sections of these cores, except for Core# 1, shows significant decreases in $CaCO_3$ saturation state compared with overlying seawater (Fig. 4.6). After the sharp decreases near the surface, the net changes of the degree of saturation over the rest of the core were relatively small. In general, most porewater in Core# 2 and 4 appeared to be saturated with respect to low (<10 mol%) Mg calcite. Porewater between 0 and 24 cm in Core# 1 seemed to be saturated with respect to high (>10 mol%) Mg calcite, but the saturated mineral phases decreased to low Mg calcite in the lower portion of the core. However, I believe that this might be an artifact, because the top layers of sediment in Core# 1 were loosely packed sands

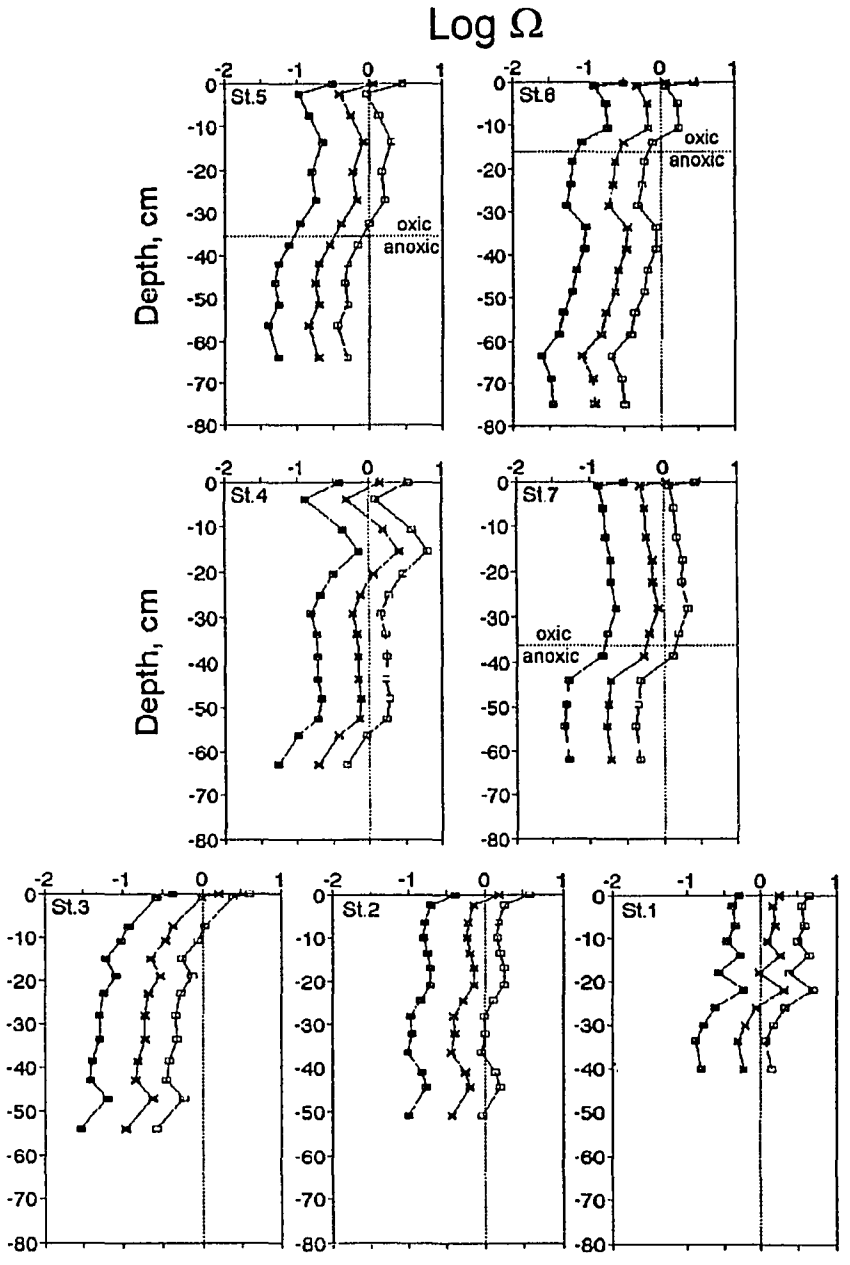

Figure 4.6. Degree of saturation of porewater with respect to 0, 10 and 20 mol% Mg calcite (open square, X and closed square, respectively).

(possibly because of turbulence created around the nearby islands) that could be easily disturbed when the core was carried by divers from the sea bed to the boat as well as when the contents of the core were pushed out. Sediments in all other cores were much more consistent in texture than Core# 1, so this problem was less significant. Most porewater in Core# 3 was highly undersaturated with respected to all Mg calcite phases, suggesting less extensive $CaCO_3$ dissolution relative to respiration. The lack of a significant TA gradient in Core# 3 is consistent with the idea of less extensive $CaCO_3$ dissolution (Fig. 4.4).

Sediments With SO_4^{2-} Reduction: Stations 5, 6, and 7

The DIC profiles for Core# 5, 6 and 7 sediments exhibited TA and DIC maxima about 10-20 cm below the sediment-water interface (Figs. 4.4 and 4.5). Below these mid-depth maxima, TA and DIC concentrations sharply decreased and then gradually increased again with depth. The concentration maximum in each core could create a large downward flux into the sediment layer where concentration was lower. If these maxima were permanent features in these cores, TA and DIC had to be taken up by some internal mechanisms in the sediment horizon below the peaks. The magnitude of these mechanisms would have to be of the order of 10 mmol m^{-2} d^{-1} of TA and DIC. This possibility seems quite unlikely, because there are no known mechanisms in sediments that can take up TA and DIC at this rate.

An alternative explanation for these TA and DIC maxima in surface sediments of Core# 5, 6 and 7 is that the maxima might be due to fluctuations in benthic respiration of sediment organic matter. The sediment organic content near river

mouths varies seasonally and is strongly correlated with river discharge. The pattern in the four years of monthly data taken at a fixed station at the Chao Phraya river mouth (Silpipat et al., 1984) clearly shows that the highest sediment organic content occurs during peak discharge (Figs. 1.2 and 4.7). However, it is not known whether the observed organic matter in sediments is of riverine/terrestrial origin or of marine origin associated with plankton blooms induced by riverine nutrient input. In any case, it is possible that benthic respiration is episodic. The DIC peaks in sediments near river mouths could be related to the high runoff. This temporarily high DIC concentration decreases $CaCO_3$ saturation and accelerates dissolution. Thus high TA is also observed. When riverine runoff slows, benthic respiration rates decrease, and the TA and DIC maxima in surface sediments dissipates relatively rapidly.

There are at least three lines of evidence to suggest that respiration in surface sediments, that is the layer with TA and DIC peaks, at Stations 5 to 7 was oxic rather than suboxic. First, benthic macrofauna were abundant in the top 20 cm of all sediment cores, indicating the presence of dissolved O_2 in porewater. Second, the TA and DIC maxima below the sediment-water interface could be a result of rapid surface mixing relative to respiration rate. Third, the low and relatively constant DIP:DIC ratio of surface porewater of Core# 5 to 7 (Fig. 4.8) might be a result of two causes: a) dilution of porewater by seawater which has a very low DIP:DIC ratio ($\approx$0.02:106); or b) adsorption of DIP by oxidized iron minerals. Either of these explanations for the low DIP:DIC implies oxic rather than anoxic surface sediments.

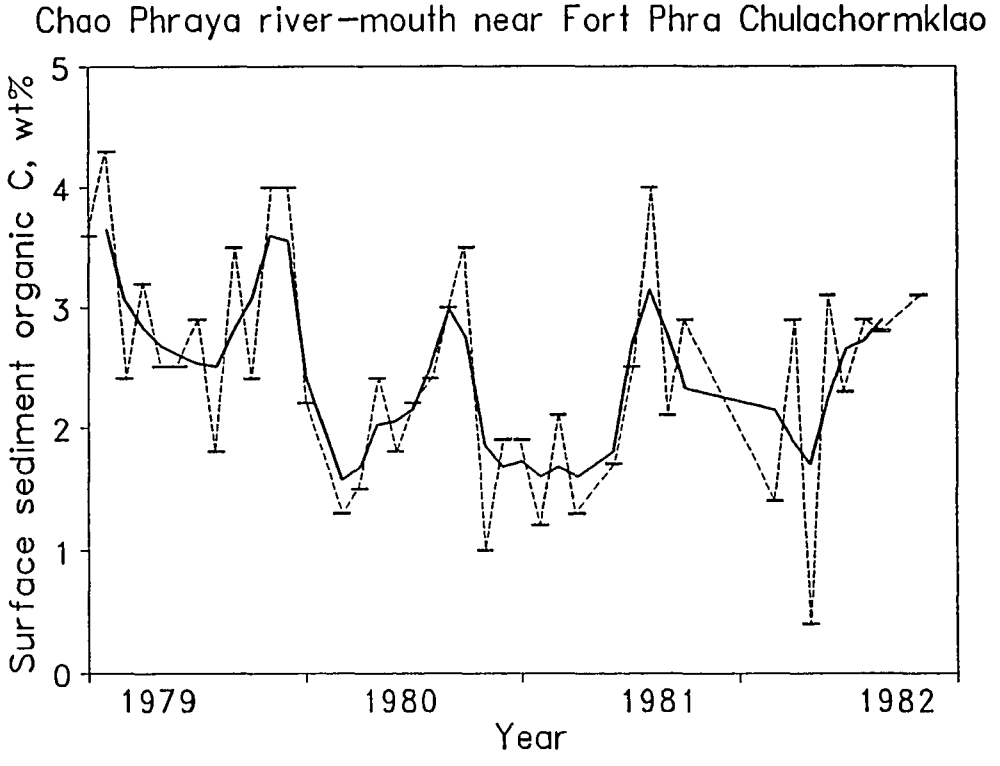

Figure 4.7. Monthly data of weight percentage of oxidizable organic matter content ($K_2Cr_2O_7$ oxidation) in surface sediments (grab sample) at a permanent sampling station at Chao Phraya river mouth near Fort Phra Chulachomklao (from Silpipat et al., 1984). The smoothed curve (solid line) connects the averages of three sequential data points.

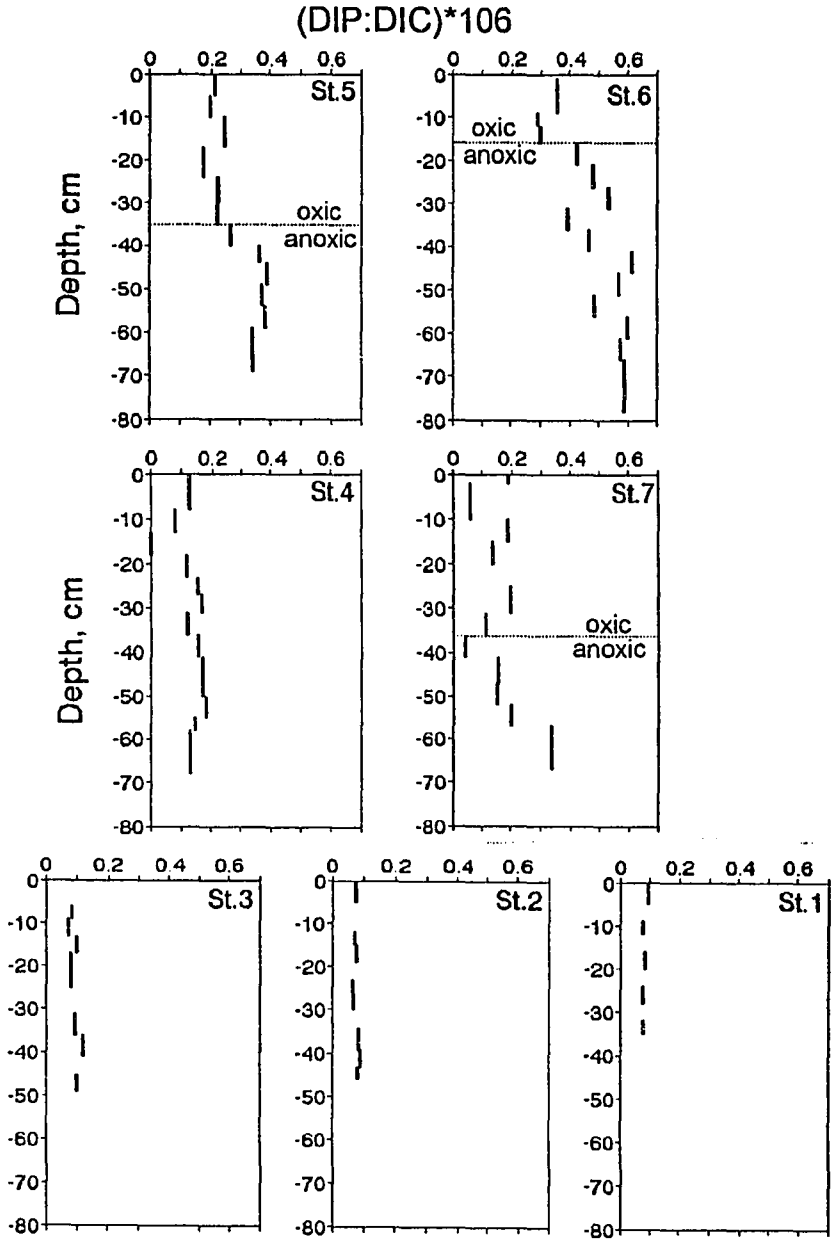

Figure 4.8. DIP:DIC molar ratio of sediment porewater from seven cores in this study.

Porewater DIP could be partially controlled by phosphate minerals, largely carbonate fluorapatite or francolite (Jahnke et al., 1983; Van Cappellen and Berner, 1988). However, the sharp increase in the DIP:DIC ratio near the assumed oxic/anoxic boundaries in Core# 5, 6 and 7 (Fig. 4.8) suggests that authigenic uptake within the deep sediment zone is probably smaller than desorption. The net DIP uptake by authigenic francolite formation in near surface oxic sediments could be slower than that in deep sediments, because the concentrations of both DIP and CO_3^{2-} in shallow porewater are much less than those in deep porewater.

I believe that the increasing trend of the porewater DIP:DIC ratio with depth in Core# 5, 6 and 7 could be a combined result of DIP accumulation due to the lack of bioturbation and of phosphate desorption as Fe(III) minerals were reduced to Fe^{2+} (e.g., Caraco et al., 1990; Sunby et al., 1992). High DIP concentrations in porewater could decrease the $CaCO_3$ dissolution rate (Berner and Morse, 1974; Walter and Burton, 1986). It is unfortunate that the sampling method used in this study, which allows sediments to be exposed to atmospheric O_2 for up to several hours before porewaters were extracted, may cause re-adsorption of phosphate and thus lessen the DIP concentration (Brey et al., 1973). This possibility prohibits further modeling of P in the sediments.

$CaCO_3$ Dissolution Models

Interaction Between Oxic/Suboxic Respiration and $CaCO_3$ Reaction

Model Synthesis

The partitioning of respiratory CO_2 in $CaCO_3$ dissolution is an important factor in sedimentary carbon cycle modeling. This information cannot be derived from thermodynamic analysis alone. Hence, in this section a CO_2 partitioning model will be derived based on the fact that these three important reactions in surface sediments--a) oxic respiration, b) SO_4^{2-} reduction, and c) $CaCO_3$ dissolution--produce different TA:DIC ratios. Moreover, oxic respiration is assumed not to coexist in the same sediment horizon with SO_4^{2-} reduction (i.e., the calculations ignore any sediment microzones). With these two conditions, the relative rates among these three reactions can be determined from the net TA and DIC production data.

Complete oxic respiration of organic matter (i.e., all organic C is oxidized into CO_2, and all N is oxidized into NO_3^-) with a C:N ratio of 6.6:1 may be written by the reaction modified from Richards (1965) as:

$$(CH_2O)_{6.6}(NH_3) + 8.6O_2 \rightleftharpoons 6.6CO_2 + HNO_3 + 7.6H_2O \qquad \text{(I)}.$$

According to this reaction, the relative TA:DIC production ratio is -1/6.6 = -0.15. If a fraction f of CO_2 produced by oxic respiration is used to dissolve $CaCO_3$ according to:

$$CaCO_3 + CO_2 + H_2O \rightleftharpoons Ca^{2+} + 2HCO_3^- \qquad \text{(II)}$$

(e.g., Garrels and Mackenzie, 1980), then the net production ratio between TA and DIC (R_{TA}/R_{DIC}) will be:

$$\frac{R_{TA}}{R_{DIC}} = \frac{2f - 0.15}{f + 1} \qquad (4.3)$$

for oxic respiration.

One way to describe SO_4^{2-} reduction of organic matter is:

$$CH_2O + 0.5SO_4^{2-} \rightleftharpoons HCO_3^- + 0.5HS^- + 5H_2O \qquad \text{(III)}.$$

If f moles of CO_2 produced by SO_4^{2-} reduction (reaction III) are consumed by $CaCO_3$ dissolution, then the relative TA and DIC production is:

$$\frac{R_{TA}}{R_{DIC}} = \frac{2f + 1}{f + 1} \qquad (4.4)$$

In addition, the reaction:

$$CH_2O + 0.5SO_4^{2-} + 0.5Fe^{2+} + H^+ \rightleftharpoons HCO_3^- + 0.5FeS + H_2O \qquad \text{(IV)}$$

may be a more important SO_4^{2-} reduction mode as far as $CaCO_3$ dissolution is concerned (e.g., Goldhaber and Kaplan, 1974; Berner, 1984; Sansone et al., 1990; Morse et al., 1992). For reaction IV, R_{TA}/R_{DIC} is:

$$\frac{R_{TA}}{R_{DIC}} = \frac{2f}{f + 1} \qquad (4.5)$$

R_{TA} and R_{DIC} in sediments can be estimated from the steady state one dimensional mass balance equations (e.g., Berner, 1980):

$$\frac{dDIC}{dt} = \phi K_{DIC}\frac{d^2DIC}{dz^2} - \phi w\frac{dDIC}{dz} + R_{DIC} = 0 \qquad (4.6)$$

for DIC, and:

$$\frac{dTA}{dt} = \phi K_{TA}\frac{d^2TA}{dz^2} - \phi w\frac{dTA}{dz} + R_{TA} = 0 \qquad (4.7)$$

for TA. Where: ϕ = porosity, K_{DIC} and K_{TA} = effective diffusion coefficients (molecular diffusion plus "biodiffusion") for DIC and TA, respectively, z = depth in sediments, and w = sedimentation rate.

In this study, concentration profiles in each core are broken down into zones where the concentration gradient can be approximated by straight lines. Within each of these sediment zones, the 2nd derivative terms in equations (4.6) and (4.7) are zero. By combining equations (4.6) and (4.7), the relative reaction rate between TA and DIC in each sediment zone is:

$$\frac{R_{TA}}{R_{DIC}} = \frac{dTA}{dDIC} \qquad (4.8)$$

By applying equation (4.8) and one of the equations (4.3), (4.4) or (4.5) as appropriate to the observed dTA/dDIC data, the CO_2 partitioning coefficient f for each sediment zone can be estimated.

Application of the Model to Observed Data

The slopes between TA and DIC concentrations in porewater in the oxic Cores# 1, 2 and 3 (Table 4.2) are not significantly different from the value of 0.925 predicted by equation 4.3 for f=1. Even though the slope for Core# 4 is less than 0.925, when the section from 13-18 cm of this core, where pH is anomalously high (8.38), is excluded, the new adjusted slope of 0.738 is not significantly different

Table 4.2. Relative changes in TA and DIC concentration gradients under three respiration scenarios. 95% confidence intervals are given in parentheses. Theoretical slopes are -0.15 for complete oxic respiration (reaction I), 2 for $CaCO_3$ dissolution (reaction II), 1 for SO_4^{2-} reduction that produces H_2S (reaction III), and 0 for SO_4^{2-} reduction that produces FeS (reaction IV).

Stations:	1	2	3	4	5	6	7
Oxic respiration (reaction I)							
Depth range, cm	0-45	0-30*	0-59	0-68	0-35	0-16	0-41
dTA	0.942	0.853	1.187	0.646	0.962	0.858	1.079
dDIC	(0.421)	(0.119)	(0.429)	(0.166)	(0.087)	(0.457)	(0.200)
f	1.032	0.875	1.646	0.587**	1.072	0.883	1.334
SO_4^{2-} reduction							
with H_2S formation (reaction III)							
dTA	---------- not applicable ----------				0.760	0.607	0.758
dDIC					(0.203)	(0.209)	(0.520)
f					-0.194	-0.282	-0.195
with FeS formation (reaction IV)							
dTA	---------- not applicable ----------				0.707	0.538	0.621
dDIC					(0.175)	(0.170)	(0.427)
f					0.547	0.368	0.450

* Samples below 30 cm are excluded because TA are low and nearly constant with depth, indicating insignificant $CaCO_3$ dissolution.

** When the data from 13-18 cm are excluded, the adjusted *f* value is 0.704.

from 0.925 ($p<0.05$). These results suggest that tight (1:1) coupling between $CaCO_3$ dissolution and oxic respiration was common in oxic sediments at Stations 1 to 4.

The degree of calcite saturation of the uppermost porewater of Core# 5, 6 and 7 is much lower than that of the overlying seawater (Fig. 4.6). Below the sediment-water interface, the $CaCO_3$ saturation state increased slightly but eventually dropped again near the assumed oxic/anoxic boundary. The ratio of TA and DIC concentrations in porewaters of these presumably oxidized sediment zones was close to the ratio of 0.925:1, as predicted by equation (4.3) for $f=1$ (Table 4.2). Accordingly, the coupling between $CaCO_3$ dissolution and oxic respiration in the surface sediments of these cores was very tight.

Porewaters below the oxidized zone of Core# 5 to 7, in the SO_4^{2-} reduction zone, were undersaturated with respect to all calcite phases (Fig. 4.6). However, all dTA/dDIC relationships were less than 1 for these porewaters (Table 4.2). All CO_2 partitioning coefficients were negative when reduced S was assumed to be dissolved in porewaters (reaction III), therefore this SO_4^{2-} reduction pathway is unlikely. This conclusion is substantiated by field observations in which no H_2S smell (rotten eggs) was detected in these cores. With the formation of FeS (reaction IV), f values calculated for these cores were about 0.5 (Table 4.2). This value suggests that the coupling between $CaCO_3$ dissolution with SO_4^{2-} reduction was less tight than that with oxic respiration.

Kinetic Analysis of *In Situ* $CaCO_3$ Dissolution

Model Synthesis

Several laboratory studies have found that the specific $CaCO_3$ dissolution rate (rate/mass) obeys the rate law:

$$CD\%_x = CD\%_x^o \left(1 - \frac{IAP_x}{K_x}\right)^n \qquad (4.9)$$

where $CD\%_x$ = specific dissolution rate of x mol% Mg calcite (in % d^{-1}), $CD\%_x^o$ = infinite dissolution rate when $\Omega_x = 0$, and n = the reaction order which usually varies between 3 and 5 (Morse, 1978; Keir, 1980; Walter, 1986).

In this study, porewater in the oxic zone that is undersaturated with respect to some Mg calcite phases will be used to estimate the *in situ* $CaCO_3$ dissolution rate according to equation (4.9). To simplify the diagenetic model, all O_2 uptake across the sediment-water interface is assumed to be used in oxic respiration (reaction I). Thus, the average dissolution rate--$<CD\%_x>$--can be calculated by:

$$<CD\%_x> = \frac{f\,F_{O2}}{g_x <M_{CaCO3}> z_{oxic}} \qquad (4.10)$$

where: f = CO_2 partitioning coefficient, F_{O2} = O_2 uptake across sediment-water interface (from flux chamber data in Chapter 3), g_x = relative abundance of x mol% Mg calcite, $<M_{CaCO3}>$ = average bulk $CaCO_3$ content in the oxic layer (Fig. 4.2), and z_{oxic} = thickness of oxic layer.

By taking the average of both sides of equation (4.9) and substituting equation (4.10) for $<CD\%_x>$, the equation

$$\left(\frac{f\,F_{O2}}{\langle M_{CaCO3}\rangle z_{oxic}}\right)^{1/n} = (g_xCD\%_x^o)^{1/n} - \left[\frac{(g_xCD\%_x^o)^{1/n}}{K_x}\right]\langle IAP_x\rangle \qquad (4.11)$$

is obtained. For $g_xCD\%_x^o$ that is less than 10 and n that is relatively large (e.g. $\approx$4), the term $g_xCD\%_x^o$ can be assumed to be constant with only small effects on the general shape of the line defined by equation (4.11). Thus, K_x and $g_xCD\%_x^o$ for different combinations of n and x can be estimated by fitting equation (4.11) to the observed data. In this study I chose n values between 3 and 5 (which covers most of the range of dissolution order reported in the literature; Morse, 1978; Keir, 1980; Walter, 1986) and x values between 0 and 25 mol% Mg (which covers most biogenic Mg calcite; Mackenzie et al., 1983).

Application of the Model to Observed Data

Porewater chemistry of the oxic layer of Core# 5, 6 and 7 as well as that of oxic Core# 2 and 3 was used to test the *in situ* dissolution kinetic model (equation 4.11). Core# 1 is rejected, because of the possibility that the upper portion might be disturbed and mixed with seawater. Core# 3 is excluded, because its porewaters were highly undersaturated (Fig. 4.6), suggesting that $CaCO_3$ dissolution in this core might not be a function of degree of saturation alone.

The specific $CaCO_3$ dissolution rates calculated by using equation (4.10) are shown in Table 4.3. When these rate data are plotted according to equation (4.11) for different combinations of n and x, all results show strong linear trends with r^2 greater than 0.7. An example of such a plot for n=4 and x=10 mol% is shown in Fig. 4.9. The data are repeatedly analyzed by varying n and x so the best-fit log K_x

Table 4.3. Specific $CaCO_3$ dissolution rates relative to total $CaCO_3$ mass in oxic sediment layer of 5 cores from the upper Gulf of Thailand.

Core#	Calculated Dissolution Rate (% d^{-1})
2	0.0026
4	0.0048
5	0.0131
6	0.0588
7	0.0087

values for x between 0 and 25 mol% Mg (Fig. 4.10) are obtained. Although the uncertainty range shown in Fig. 4.10 (± 1 SE) seems to be large, when this data set is superimposed on top of the log K_x data compiled by Morse and Mackenzie (1990), the uncertainty obtained for any particular mol% Mg calcite in this study is comparable with the natural variation of log K_x for each Mg calcite phase (Fig. 4.11).

Discussion

Analysis of $CaCO_3$ dissolution in a real sedimentary environment based on thermodynamic data can be subject to considerable error because of uncertainty associated with the estimation of stability constants (Morse et al., 1985; Bischoff et al., 1987; Morse and Mackenzie, 1990). To overcome the problem, several

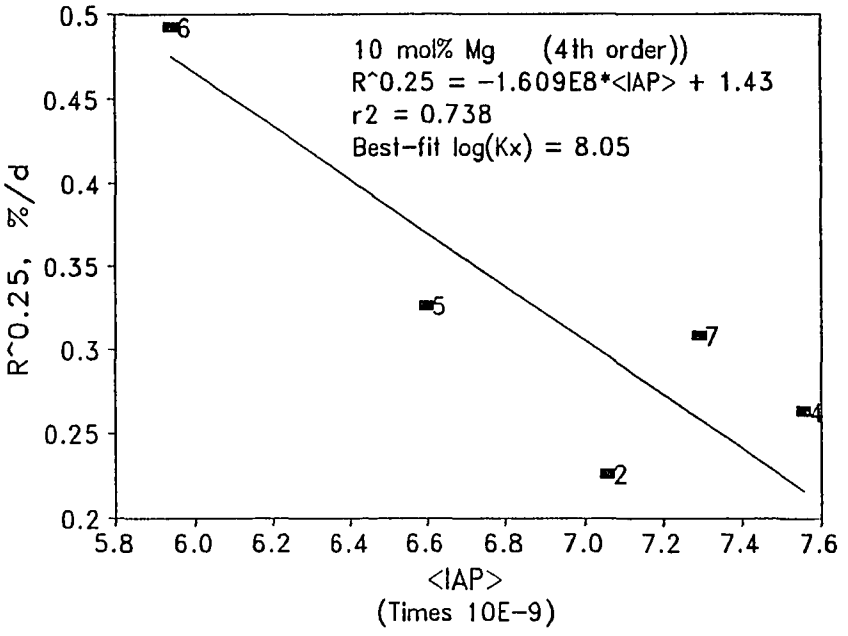

Figure 4.9. An example of the plot according to equation (4.11) for n=4 and x=10 mol% Mg. Core numbers are shown near data points.

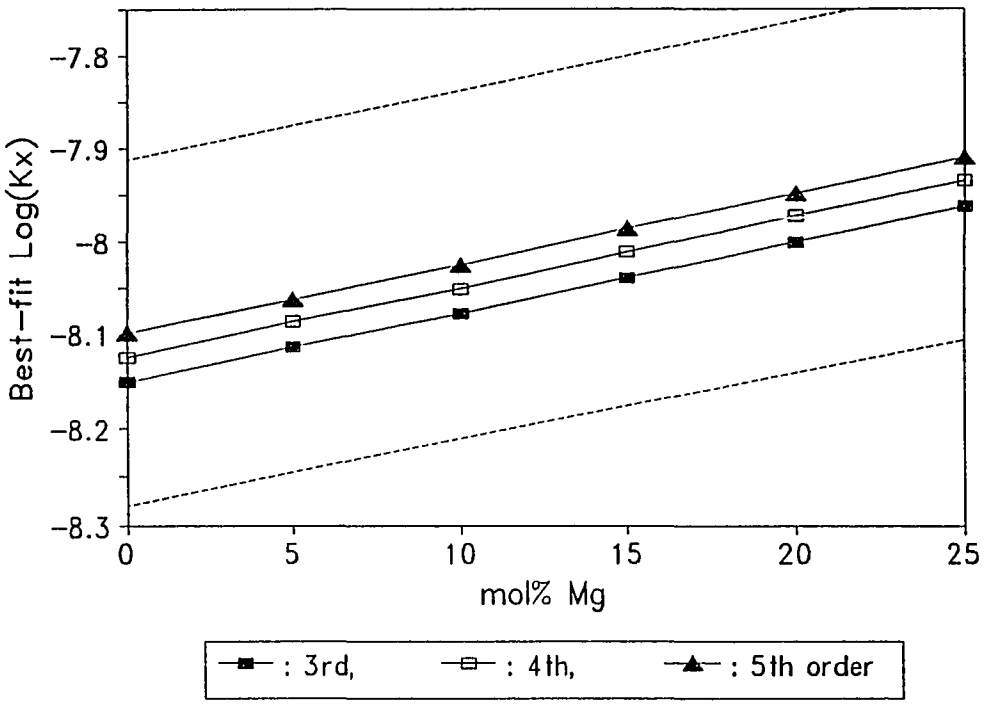

Figure 4.10. The best-fit solubilities at saturation as a logarithmic linear function of the mol% Mg content in calcite. Dashed lines represent the approximate ± 1 standard error.

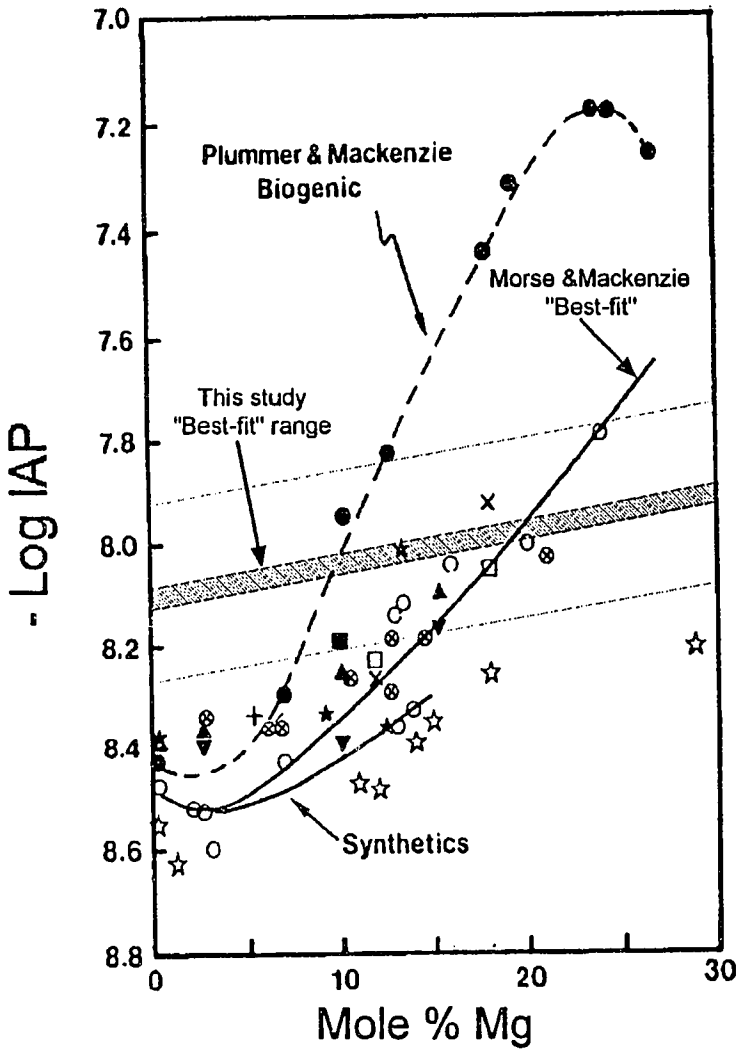

Figure 4.11. The range of best-fit solubilities at saturation obtained by this study (shaded area) with ± 1 standard error (dotted lines) compared with data compiled by Morse and Mackenzie (1990). See this reference for details about data sources.

incubation techniques have been developed. Unfortunately most of the techniques, for one reason or another, manipulate the environment, such as by introducing "foreign" materials into the sediments, or by experimenting with synthetic $CaCO_3$ under laboratory conditions. Although such studies yield valuable background information on the dissolution mechanism, their application to actual dissolution rates in natural sediments is equivocal.

In this study, I have attempted to study $CaCO_3$ dissolution in a tropical sedimentary environment without manipulating the natural environment. The results indicate that $CaCO_3$ dissolution due to aerobic respiration in this study was not sensitive to the reaction order (Fig. 4.10). Any order between 3 and 5 could describe the reaction kinetics reasonably well. However, $CaCO_3$ dissolution in sediments was apparently sensitive to the mol% $MgCO_3$ in the "reactive" calcite pool and to the choice of solubility constants of those Mg-calcite phases. The range of values for these two factors in the Gulf of Thailand sediments was established (Fig. 4.10). To show on the plot in Fig. 4.10, the actual mol% $MgCO_3$ and log K_x of calcite that underwent dissolution, one of these factors must be fixed or assumed. For example, if the biogenic K_x data of Plummer and Mackenzie (1974) was chosen as a reference, the intercept point in Fig. 4.11 suggests that the "reactive" calcite contained about 10 mol% Mg. If the biogenic "best-fit" dataset of Morse and Mackenzie (1990) was used, the "reactive" calcite contained about 20 mol% Mg (Fig. 4.11).

The problem of which composition of Mg calcite was actually the "reactive" phase remains unsolved. I feel that the 20 mol% Mg calcite may be the less likely

possibility, because these very high Mg calcites come primarily from calcareous algae skeletons (Mackenzie et al., 1983). Such algal remains are very rare or absent in sediment samples from the Gulf of Thailand. In contrast, echinoderm (mainly sea urchin) skeletons were present in almost every sample. These organisms are known to secrete calcite that contains 9-16 mol% Mg (Mackenzie et al., 1983). By implication from this indirect information, porewater in the surface sediments in the upper Gulf of Thailand might be at saturation with respect to 10 mol% Mg calcite, and the saturation state would be best described by the solubility constants of Plummer and Mackenzie (1974).

The relative abundance in sediments of the x mol% Mg calcite (g_x) that is at saturation with the porewater carbonate chemistry can be estimated from the constant term of equation (4.11). The best-fits $g_x CD\%_x^o$ for n between 3 and 5 and x between 0 and 25 mol% are shown in Table 4.4. The infinite dissolution rates ($CD\%_x^o$) of cleaned biogenic Mg calcite under laboratory conditions are on the order of 10^2 to 10^4 % d^{-1} (Morse, 1978; Keir, 1980; Walter, 1986). Because these published rates may be higher than those for natural materials in the environment (Walter and Morse, 1984; Bischoff et al., 1987), the literature values may be considered only as the upper limit for field $CD\%_x^o$. By taking the $CD\%_x^o$ of 10^2 % d^{-1} and dividing that into the $g_x CD\%_x^o$ values in Table 4.4, most of the g_x values obtained are on the order of 10^{-2}. In other words, the relative abundance of "reactive" x mol% Mg calcite in the upper Gulf of Thailand sediments is apparently less than 10% of the bulk $CaCO_3$. This magnitude seems to agree with the conclusion of previous investigators that Mg

Table 4.4. The best-fit $g_x CD\%_x^o$ for dissolution order (n) between 3 and 5 and mol% $MgCO_3$ in calcite (x) between 0 and 25 (see text).

Reaction order:	3	4	5
Mol% $MgCO_3$			
0	2.36	4.86	8.77
5	2.31	4.75	8.54
10	2.10	4.19	7.38
15	2.22	4.52	8.04
20	2.18	4.17	7.80
25	2.12	4.26	7.51

calcite, despite its lower abundance, controls the carbonate chemistry of sediment porewater (e.g., Berner, 1966; Schmalz, 1967; Morse et al., 1985). In addition, because $CaCO_3$ dissolution in the upper Gulf of Thailand surface sediments was coupled tightly (near 1:1; Table 4.2) with oxic respiration, it implies that the dissolution process was operating at its highest possible efficiency. Organic matter respiration is more likely to be the rate limiting step than is $CaCO_3$ dissolution.

Another $CaCO_3$ phase that deserves mention here because of its possible role in porewater carbonate chemistry is aragonite. Coral fragments, from colonial as well as solitary forms, were found in several sediment samples from the Gulf of Thailand.

These animals are known to precipitate aragonitic skeletons (Morse and Mackenzie, 1990). Aragonite has a log *IAP* at saturation at 25°C of about -8.3 (Morse and Mackenzie, 1990). This value is slightly lower than the range of best-fit log K_x of -8.1 for a pure $CaCO_3$ phase suggested by this study (Fig. 4.10). However, as it was in the case of calcites, the saturated *IAP* found for aragonite in laboratory conditions may be lower than that in the natural environment because of the lattice disordering common in biogenic aragonite (Urmos et al., 1986). It is also quite possible that the log saturated *IAP* of aragonite in marine sediments may be nearer to -8.1.

The continuous undersaturation with respect to all calcite phases in the suboxic zone of Cores# 5 to 7 (Fig. 4.6) must be maintained by a slow $CaCO_3$ dissolution relative to the SO_4^{2-} reduction rate. If reaction IV (FeS formation) is assumed, the specific calcite dissolution rate can be estimated from f's (Table 4.2), SO_4^{2-} reduction rate (Chapter 3), and the "reactive" calcite pool by a relationship analogous to equation (4.10). Because the net transport at the base of all cores was insignificant (Table 4.1), all SO_4^{2-} reduction detectable at the sediment-water interface (see Chapter 3) is assumed to be taking place in the sediment layers reached by core sampling. With this assumption, the specific dissolution rate relative to the total $CaCO_3$ pool can be calculated for each core. From the calculated dissolution rates obtained, even when all $CaCO_3$ is assumed to be pure calcite (i.e., minimizing Ω), the rates were still 100-1000 times less than the rates in the oxic zone at the same degree of undersaturation (Fig. 4.12).

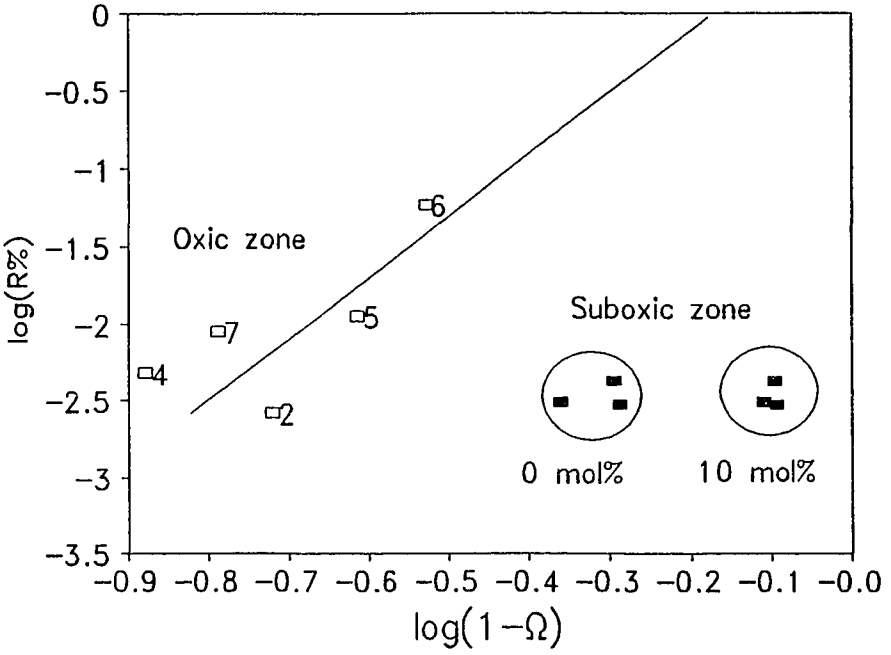

Figure 4.12. Specific $CaCO_3$ dissolution rate as a function of degree of saturation. Data points for the oxic zone are for $n=4$ and $x=10$ mol% Mg (i.e. same data as in Fig. 4.8). Oxic Ω's are calculated using solubility constants estimated in Fig. 4.9. Specific dissolution rates in anoxic sediments are calculated from SO_4^{2-} reduction rate (Chapter 3) and f values in Table 4.2.

There are several possible explanations for the slower dissolution rate in the SO_4^{2-} reduction zone than in the aerobic zone. First, the slow rate in a more reduced environment might be due to the inhibitory effect of phosphate desorped from iron minerals as Fe(III) is reduced to Fe(II). However, a laboratory study by Walter and Burton (1986) found that when phosphate concentration was raised from <1 μM to 50 μM, dissolution rate was decreased by only one half of an order of magnitude (about 3 times). The DIP concentrations in porewaters in this study are well below 50 μM. Thus, phosphate alone could not be a sufficient explanation, although it might explain part of the problem.

Second, most of the fine-grained $CaCO_3$ was dissolved in shallow aerobic sediments, leaving behind large particles with a low surface area:mass ratio. This ratio is known to be an important factor controlling $CaCO_3$ reactivity in sediments (e.g., Chave and Schmalz, 1966; Keir, 1980). The contribution of surface area:mass ratio to $CaCO_3$ dissolution in the present study is not known.

Third, the use of bulk $CaCO_3$ in sediment as the reference to calculate specific dissolution rate may not be a correct assumption for the suboxic horizon even though the assumption seems to work well in the oxic zone. A large fraction of $CaCO_3$ mass might not be "reactive" but may be "isolated" from solution by some mechanism. In order for the specific dissolution rates for suboxic sediments to be comparable with those for oxic sediments with the same degree of $CaCO_3$ saturation (i.e., a 100% increase), "reactive" calcite must be only 1% of the bulk $CaCO_3$ in anoxic sediments. The inhibitory mechanisms are not known, but an example might be the coatings of

organic material coating (e.g., Suess, 1970). Yet, Morse (1974) reported that dissolved organic matter of up to the concentration found in deep-sea sediments had only small effects on $CaCO_3$ dissolution rates. The effects of dissolved organic matter on *in situ* $CaCO_3$ dissolution in coastal sediments certainly needs more study.

The CO_2 partitioning in the SO_4^{2-} reduction zone found in this study (0.37-0.55; Table 4.2) is comparable to 0.25 reported for a SO_4^{2-} reducing coral-reef framework (Tribble et al., 1990). Clearly, SO_4^{2-} reduction at these locations generates CO_2 in excess of that consumed by *in situ* $CaCO_3$ dissolution. Thus, the latter step appears to be the rate limiting step for $CaCO_3$ dissolution in SO_4^{2-} reduction zones. In contrast, $CaCO_3$ dissolution in the oxic zone of the sediments appears to be limited by the CO_2 generating step. The results of this study and that of Moulin et al. (1985) indicate a tight coupling between oxic respiration and $CaCO_3$ dissolution, i.e. no or little DIC loss from sediments as CO_2.

Conclusion

1. In oxic sediments, the expected 1:1 coupling between organic respiration and $CaCO_3$ dissolution was observed. This implies that CO_2 production can be the rate limiting step of the overall net reaction. $CaCO_3$ dissolution in oxic sediments could be described by a rate law analogous to that found in laboratory experiments.
2. Sulfate reduction in sediment horizons immediately below the oxic zone is coupled with sulfide mineral, generalized as FeS, formation. In these SO_4^{2-} reducing sediments, even when porewaters were undersaturated with respect to all Mg calcite phases, only about one half of the CO_2 produced was used to dissolve $CaCO_3$.

Apparently, solid phase reaction was the rate limiting step of the overall net reaction. The degree of saturation alone was probably not the only factor that controlled $CaCO_3$ reaction rate. Dissolution rates of $CaCO_3$ in the SO_4^{2-} reduction environment are slow, at least 100 times less than the rate in oxic sediments with the same degree of undersaturation.

References

Aller, R. C. 1982. Carbonate dissolution in nearshore terrigenous muds: the role of physical and biological reworking. J. Geol. 90: 79-95.

Ben-Yaakov, S. 1973. pH buffering of pore water of recent anoxic marine sediments. Limnol. Oceanogr. 18: 86-94.

Berner, R. A. 1966. Chemical diagenesis of some modern carbonate sediments. Am. J. Sci. 264: 1-36.

Berner, R. A. 1980. Early Diagenesis: A Theoretical Approach. Princeton: Princeton University Press, 241 pp.

Berner, R. A. 1984. Sedimentary pyrite formation: an update. Geochim. Cosmochim. Acta 48: 605-615.

Berner, R. A. and Morse, J. W. 1974. Dissolution kinetics of calcium carbonate in seawater: IV. Theory of calcite dissolution. Am. J. Sci. 274: 108-134.

Bischoff, W. D., Mackenzie, F. T. and Bishop, F. C. 1987. Stabilities of synthetic magnesian calcites in aqueous solution: Comparison with biogenic materials. Geochim. Cosmochim. Acta 51: 1413-1423.

Brey, J. T., Bricker, O. P. and Troup, B. N. 1973. Phosphate in interstitial waters of anoxic sediments: Oxidation effects during sampling procedure. Science 180: 1362-1364.

Broecker, W. S., Takahashi, T., Simpson, H. J. and Peng, T.-H. 1979. Fate of fossil fuel carbon dioxide and the global carbon budget. Science 206: 409-418.

Caraco, N., Cole, J. and Likens, G. E. 1990. A comparison of phosphorus immobilization in sediments of freshwater and coastal marine systems. Biogeochemistry 9: 277-290.

Chave, K. E. and Schmalz, R. F. 1966. Carbonate-seawater interactions. Geochim. Cosmochim. Acta 30: 1037-1048.

Edmond, J. M. 1970. High precision determination of titration alkalinity and total carbon dioxide content of sea water by potentiometric titration. Deep-Sea Res. 17: 737-750.

Garrels, R. M. and Mackenzie, F. T. 1980. Some Aspects of the Role of the Shallow Ocean in Global Carbon Dioxide Uptake. U.S. Dept. of Energy, CONF-8003115, 19 pp. + appendices.

Goldhaber, M. B. and Kaplan, I. R. 1974. The sulfur cycle. In: Goldberg, E. D. (ed.) The Sea, Volume 5. New York: Wiley, pp. 568-655.

Goldhaber, M. B. and Kaplan, I. R. 1975. Apparent dissociation constants of hydrogen sulfide in chloride solution. Mar. Chem. 3: 83-104.

Jahnke, R. A., Emerson, S. R., Roe, K. K. and Burnett, W. C. 1983. The present day formation of apatite in Mexican continental margin sediments. Geochim. Cosmochim. Acta 47: 259-266.

Johansson, O. and Wedborg, M. 1980. The ammonia-ammonium equilibrium in seawater at temperature between 5 and 25°C. J. Solut. Chem. 9: 37-44.

Keir, R. S. 1980. The dissolution kinetics of biogenic calcium carbonates in seawater. Geochim. Cosmochim. Acta 44: 241-252.

Li, Y.-H., Takahashi, T. and Broecker, W. S. 1969. Degree of saturation of $CaCO_3$ in the ocean. J. Geophys. Res. 74: 5507-5525.

Mackenzie, F. T., Bischoff, W. D., Bishop, F. C., Loijens, M., Schoonmaker, J. and Wollast, R. 1983. Magnesian calcites: Low-temperature occurrence, solubility and solid-solution behavior. In: Reeder, R. J. (ed.) Carbonates: Mineralogy and Chemistry, Mineral. Soc. Am. Rev. Mineral. 11: 97-144.

Morse, J. W. 1974. Dissolution kinetics of calcium carbonate in sea water: V. Effects of natural inhibitors and position of the chemical lysocline. Am. J. Sci. 274: 638-647.

Morse, J. W. 1978. Dissolution kinetics of calcium carbonate in sea water: VI. The near-equilibrium dissolution kinetics of calcium carbonate-rich deep sea sediments. Am. J. Sci. 278: 344-353.

Morse, J. W., Zullig, J. J., Bernstein, L. D., Millero, F. J., Milne, P., Mucci, A. and Choppin, G. R. 1985. Chemistry of calcium carbonate-rich shallow water sediments in the Bahamas. Am. J. Sci. 285: 147-185.

Morse, J. W. and Mackenzie, F. T. 1990. Geochemistry of Sedimentary Carbonates. Amsterdam: Elsevier, 707 pp.

Morse, J. W., Cornwell, J. C., Arakaki, T., Lin, S. and Huerta-Diaz, M. 1992. Iron sulfide and carbonate mineral diagenesis in Baffin Bay, Texas. J. Sed. Petrol. 62: 671-680.

Moulin, E., Jordens, A. and Wollast, R. 1985. Influence of the aerobic bacterial respiration on the early dissolution of carbonates in coastal sediments. In: Van Grieken, R. and Wollast, R. (eds.) Proceeding Progress in Belgian Oceanographic Research. Brussels, pp. 196-208.

Parsons, T. R., Maita, Y. and Lalli, C. M. 1984. A Manual of Chemical and Biological Methods for Seawater Analysis. Oxford: Pergamon Press, 173 pp.

Plummer, L. N. and Mackenzie, F. T. 1974. Predicting mineral solubility from rate data: application to the dissolution of magnesian calcites. Am. J. Sci. 274: 61-83.

Reaves, C. M. 1986. Organic matter metabolizability and calcium carbonate dissolution in nearshore marine muds. J. Sediment. Petrol. 56: 486-494.

Richards, F. A. 1965. Anoxic basins and fjords. In: Riley, J. P. and Skirrow, G. (eds.) Chemical Oceanography, Volume 1. New York: Academic Press, pp. 415-419.

Sansone, F. J., Tribble, G. W., Andrews, C. C. and Chanton, J. P. 1990. Anaerobic diagenesis within Recent, Pleistocene, and Eocene marine carbonate frameworks. Sedimentology 37: 997-1009.

Schmalz, R. F. 1967. Kinetics and diagenesis of carbonate sediments. J. Sed. Petrol. 37: 60-67.

Silpipat, S., Kaewsriprakai, L., Chantarasakul, W., Viseshom, S. and Sinthupinyo, Y. 1984. Observation of eutrophication and nutrient cycles in the upper Gulf of Thailand during the period of 1981 through 1983. In: Tamiyavanich, S. (ed.) Proceeding of the Third Seminar on the Water Quality and the Quality of Living Resources in Thai Waters. Bangkok: National Research Council of Thailand, pp. 335-351.

Skirrow, G. 1975. The dissolved gas--carbon dioxide. In: Riley, J. P. and Skirrow, G. (eds.) Chemical Oceanography, Second Edition, Volume 2, London: Academic Press, pp. 1-92.

Smith, S. V. and Kinsey, D. W. 1978. Calcification and organic carbon metabolism as indicated by carbon dioxide. In: Stoddart, D. R. and Johannes, R. E. (eds.) Coral Reefs; Research Methods. Paris: Unesco, pp. 469-484.

Snedecor, G. W. and Cochran, W. G. 1980. Statistical Methods, Seventh Edition. Ames: The Iowa State University Press, 507 pp.

Snidvongs, A. in press. Sedimentary calcium carbonate dissolution in the Gulf of Thailand and its role as a minor carbon dioxide sink. Chemosphere 27: 1083-1095.

Suess, E. 1970. Interaction of organic compounds with calcium carbonate--I. Association phenomena and geochemical implications. Geochim. Cosmochim. Acta 34: 157-168.

Sunby, B., Gobeil, C., Silverberg, N. and Mucci, A. 1992. The phosphorus cycle in coastal marine sediments. Limnol. Oceanogr. 37: 1129-1145.

Thorstenson, D. C. and Mackenzie, F. T. 1974. Time variability of pore water chemistry in recent carbonate sediments, Devil's Hole, Harrington Sound, Bermuda. Geochim. Cosmochim. Acta 38: 1-19.

Thorstenson, D. C. and Plummer, L. N. 1977. Equilibrium criteria for two-component solids reacting with fixed composition in an aqueous phase--example: the magnesian calcites. Am. J. Sci. 277: 1203-1223.

Tribble, G. W. 1993. Organic matter oxidation and aragonite diagenesis in a coral reef. J. Sed. Petrol. 63: 523-527.

Tribble, G. W., Sansone, F. J. and Smith, S. V. 1990. Stoichiometric modeling of carbon diagenesis within a coral reef framework. Geochim. Cosmochim. Acta 54: 2439-2449.

Urmos, J., Sharma, S. K. and Mackenzie, F. T. 1986. Characterization of biominerals with Raman spectroscopy. Eos 67: 1271.

Van Cappellen, P. and Berner, R. A. 1988. A mathematical model for the early diagenesis of phosphorus and fluorine in marine sediments: apatite precipitation. Am. J. Sci. 288: 289-333.

Walter, L. M. 1986. Relative efficiency of carbonate dissolution and precipitation during diagenesis: A progress report on the role of solution chemistry. In: Guatier, D. L. (ed.) Roles of Organic Matter in Sediment Diagenesis. Tulsa, Oklahoma: Soc. Econ. Paleontol. Mineral. Spec. Publ. 38, pp. 1-11.

Walter, L. M. and Burton, E. A. 1986. The effect of orthophosphate on carbonate mineral dissolution rates in seawater. Chem. Geol. 56: 313-323.

Walter, L. M. and Burton, E. A. 1990. Dissolution of recent platform carbonate sediments in marine pore fluids. Am. J. Sci. 290: 601-643.

Walter, L. M. and Morse, J. W. 1984. Magnesian calcite stabilities: A reevaluation. Geochim. Cosmochim. Acta 48: 1059-1069.

CHAPTER 5

GENERAL CONCLUSION

Mass balance models for P, N, and C in the water column of the upper Gulf of Thailand indicate that nutrient inputs from both up-river and lower gulf sources are much too small to account for the net ecosystem production of the bay. The additional P requirement of 0.6 Mmol d^{-1} could be met by anthropogenic sources in estuaries and along the northern boundary of the bay. However, all the above mentioned sources are still not enough to explain the N discrepancy. Because *Trichodesmium* and many other planktonic cyanobacteria are highly abundant near the bay head, it is suggested that planktonic N_2 fixation may be significant and may generate up to 18 Mmol N d^{-1}.

Nearly all of the N loading into the head of the upper Gulf of Thailand is lost via denitrification in the main body of the bay. Most denitrification occurs in sediments by utilizing NO_3^- derived from organic N via nitrification. Availability of suitable organic substrates and the supply of O_2 to sediments are two important controlling factors for the net denitrification.

Respiratory CO_2 reacts with $CaCO_3$ in sediments. An indirect modeling result suggests that carbonate chemistry of porewater reflects a saturation state with respect to about 10 mol% Mg calcite (but could also be in equilibrium with aragonite as well). The $CaCO_3$ dissolution rate in SO_4^{2-} reducing sediments is much slower than that in oxic sediments with the same degree of saturation. In oxic sediments, the coupling between organic respiration and dissolution of undersaturated $CaCO_3$ is tight,

mostly near 1:1. The coupling between SO_4^{2-} reduction and $CaCO_3$ is less tight, all of the suboxic coupling are about 0.5:1 or less.

APPENDIX A

WATER SAMPLING STATIONS IN THE UPPER GULF OF THAILAND

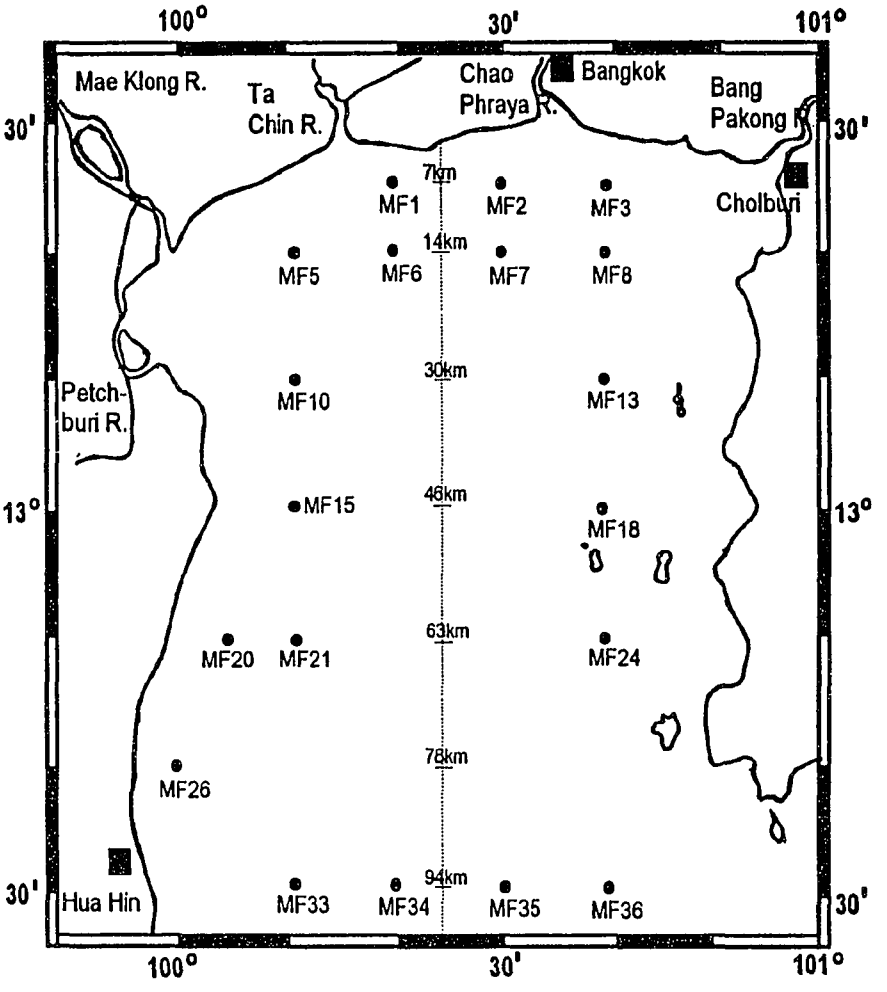

Figure A.1. Water sampling stations in the upper Gulf of Thailand. Modified from Marine Fishery Division (unpublished).

APPENDIX B

WATER CHEMISTRY DATA OF THE UPPER GULF OF THAILAND

Stations	z m	S‰	DIP μM	$NO_3^-+NO_2^-$ μM	NH_4^+ μM	DIN μM	TA meq l^{-1}	DIC mM
RIVER WATER SAMPLES								
Mae Klong at Ratchburi	0	0.008	1.04	13.28	16.41	29.69	2.307	2.160
Ta Chin at Nakornchaisri	0	0.007	3.46	19.54	17.63	37.17	1.927	1.817
Chao Phraya at Nonthaburi	0	0.010	1.18	39.45	3.92	43.37	1.594	1.483
Chao Phraya at Fort Phra Chulachomklao	0	0.037	0.69	4.42	18.51	22.93	1.456	1.356
Bangpakong at Chachoengsao	0	0.006	1.03	12.27	4.88	17.15	0.394	0.353
Bangpakong at Thep-hasdin Bridge	0	0.027	1.39	25.27	2.04	27.31	0.656	0.595

APPENDIX B (Continued)

Stations	z m	S‰	DIP μM	$NO_3^-+NO_2^-$ μM	NH_4^+ μM	DIN μM	TA meq l^{-1}	DIC mM
WEST TRANSECT								
MF1	0	28.196	0.19	0.08	0.44	0.52	2.394	2.104
MF1	3.5	29.364	0.19	0.06	0.49	0.55	2.423	2.127
MF5	0	30.727	0.13	0.03	0.09	0.12	2.403	2.132
MF5	4	30.868	0.14	0.03	0.17	0.20	2.316	2.057
MF5	7	30.783	0.15	0.03	0.17	0.20	2.321	2.063
MF6	0	30.412	0.16	0.05	0.15	0.20	2.307	2.010
MF6	4	30.428	0.16	0.03	0.20	0.23	2.333	2.033
MF6	8	30.642	0.16	0.04	0.20	0.24	2.303	2.015
MF10	0	31.432	0.13	0.14	0.24	0.38	2.265	2.024
MF10	9	31.467	0.69	0.06	0.26	0.32	2.169	1.933
MF10	15	31.517	0.12	0.07	0.29	0.36	2.260	2.020
MF15	0	31.915	0.13	0.03	0.16	0.19	2.198	1.994
MF15	9	31.983	0.13	0.02	0.14	0.16	2.170	1.970
MF15	15	31.997	0.10	0.03	0.18	0.21	2.179	1.977
MF20	0	32.159	0.23	0.10	0.46	0.56	2.267	2.006
MF20	7	32.095	0.18	0.15	0.29	0.44	2.263	2.005
MF20	11	32.145	0.12	0.08	0.20	0.28	2.274	2.018
MF21	0	32.279	0.11	0.04	0.18	0.22	2.160	1.971
MF21	6	32.229	0.09	0.02	0.13	0.15	2.187	1.995
MF21	15	32.322	0.10	0.03	0.11	0.14	2.178	1.988
MF26	0	32.070	0.25	0.19	0.38	0.57	2.284	2.028
MF26	5	32.515	0.26	0.15	0.24	0.39	2.376	2.108
MF26	9	32.430	0.26	0.10	0.20	0.30	2.311	2.051
MF33	0	33.139	0.13	0.11	0.19	0.30	2.196	2.025
MF33	10	33.077	0.10	0.05	0.10	0.15	2.107	1.941
MF33	22	33.155		0.07	0.15	0.22	2.222	2.050
MF34	0	33.197	0.10	0.03	0.14	0.17	2.152	1.969
MF34	10	33.173	0.07	0.02	0.18	0.20	2.154	1.969
MF34	23	33.281	0.08	0.03	0.14	0.17	2.143	1.960

APPENDIX B (Continued)

Stations	z m	S‰	DIP μM	$NO_3^-+NO_2^-$ μM	NH_4^+ μM	DIN μM	TA meq l^{-1}	DIC mM
EAST TRANSECT								
MF2	0	25.581	0.33	0.38	0.49	0.87	2.429	2.161
MF2	3	27.574	0.37	0.31	0.91	1.22	2.417	2.152
MF2	7	27.636	0.34	0.73	0.88	1.61	2.400	2.140
MF3	0	22.091	1.40	5.13	11.10	16.23	2.302	1.986
MF3	6	25.361	1.03	1.18	3.37	4.55	2.397	2.019
MF7	0	28.867	0.16	0.29	0.14	0.43	2.311	2.054
MF7	6	29.789	0.15	0.01	0.12	0.13	2.279	2.029
MF7	9	29.970	0.18	0.84	0.15	0.99	2.309	2.078
MF8	0	28.711	0.15	0.83	0.67	1.50	2.243	1.708
MF8	10	29.360	0.21	0.08	0.68	0.76		
MF8	14	29.804	0.23	1.12	0.18	1.30	2.309	2.027
MF13	0	31.409	0.23	0.02	0.33	0.35	2.253	1.997
MF13	10	31.516	0.29	0.41	0.34	0.75	2.232	2.004
MF13	19	32.015	0.28	0.62	0.58	1.20	2.238	2.014
MF18	0	32.194	0.21	0.03	0.28	0.31	2.213	1.978
MF18	6	32.221	0.21	0.02	0.70	0.72	2.250	2.014
MF18	13	32.267					2.211	1.979
MF24	0	32.505	0.12	0.04	0.38	0.42	2.206	1.992
MF24	10	32.533	0.14	0.02	0.14	0.16	2.224	2.009
MF24	29	32.573	0.14	0.04	0.14	0.18	2.199	1.987
MF35	0	33.006	0.12	0.11	0.04	0.15	2.239	2.045
MF35	12	33.055	0.15	0.06	0.12	0.18	2.222	2.023
MF35	22	33.089	0.13	0.06	0.12	0.18	2.210	2.013
MF36	0	32.689	0.11	0.03	0.19	0.22	2.148	1.952
MF36	10	32.702	0.11	0.03	0.15	0.18	2.221	2.022
MF36	33	32.726	0.10	0.06	0.31	0.37	2.214	2.016

APPENDIX B (Continued)

Stations	z m	DOP μM	DON μM	DOC μM	POP μM	PON μM	POC μM	SS mg l^{-1}
RIVER WATER SAMPLES								
Mae Klong at Ratchburi	0	0.61	25.49	395.55	6.48	73.52	815.83	49.32
Ta Chin at Nakornchaisri	0	0.26	21.54	384.58	5.70	48.33	475.61	35.21
Chao Phraya at Nontheburi	0	0.17	15.27	506.10	6.11	55.50	748.41	105.8
Chao Phraya at Fort Phra Chulachomklao	0	0.23	27.81	794.58	8.68	66.05	678.17	70.12
Bang Pakong at Chachoengsao	0	0.25	18.16	401.53	4.14	43.76	576.45	74.85
Bang Pakong at Thep-hasdin Bridge	0	-0.06	23.75	544.18	15.80	147.6	2140.0	353.4

APPENDIX B (Continued)

Stations	z m	DOP μM	DON μM	DOC μM	POP μM	PON μM	POC μM	SS mg l^{-1}
WEST TRANSECT								
MF1	0	0.45	14.81	73.27	1.51	23.37	223.96	16.35
MF1	3.5	0.35	13.62	73.84	1.03	14.73	139.74	21.07
MF5	0	0.35	7.68	65.88	0.93	18.38	145.72	18.50
MF5	4	0.34	9.99	63.04	0.85	17.06	138.81	19.31
MF5	7	0.34	7.94	61.43	0.96	19.21	154.78	19.19
MF6	0	0.33	9.20	67.74	0.97	26.21	212.87	21.44
MF6	4	0.33	7.87	62.72	0.95	26.12	221.30	23.75
MF6	8	0.35	10.17	64.99	1.02	23.89	226.68	20.87
MF10	0	0.47	9.90	77.46	0.39	8.95	71.37	9.68
MF10	9	0.55	6.81	65.78	0.43	8.10	53.37	9.34
MF10	15	0.39	6.53	65.28	0.41	8.45	60.51	9.13
MF15	0	0.31	7.70	74.08	0.30	6.18	37.37	5.88
MF15	9	0.31	7.10	63.81	0.41	5.68	32.45	5.85
MF15	15	0.26	5.03	64.96	0.28	5.45	33.29	5.68
MF20	0	0.35	20.27	76.47				
MF20	7	0.27	10.88	62.99				
MF20	11	0.32	12.94	66.92				
MF21	0	0.20	5.60	65.12	0.33	5.59	39.51	5.81
MF21	6	0.22	4.93	61.52	0.27	4.33	31.76	5.67
MF21	15	0.26	6.65	67.33	0.30	5.37	33.76	5.62
MF26	0	0.26	10.28	60.29				
MF26	5	0.29	10.40	65.28				
MF26	9	0.33	13.41	67.09				
MF33	0	0.16	6.15	69.30				
MF33	10	0.13	4.54	56.29				
MF33	22	0.14	4.94	62.58				
MF34	0	0.17	5.66	67.25	0.18	2.35	24.34	4.58
MF34	10	0.16	4.75	55.94	0.22	3.49	29.09	4.51
MF34	23	0.18	6.35	56.54	0.18	3.40	29.08	4.00

APPENDIX B (Continued)

Stations	z m	DOP μM	DON μM	DOC μM	POP μM	PON μM	POC μM	SS mg l^{-1}
EAST TRANSECT								
MF2	0	0.39	15.72	89.65	1.70	20.78	193.72	28.74
MF2	3	0.39	18.39	94.68	1.32	17.41	166.78	27.62
MF2	7	0.40	15.91	90.72	1.11	18.99	195.07	29.51
MF3	0	0.57	23.55	136.13	6.83	70.28	480.57	70.70
MF3	6	0.79	21.60	120.50	5.20	63.59	519.74	79.13
MF7	0	0.14	9.41	81.68	1.33	21.30	260.29	23.88
MF7	6	0.13	6.98	69.37	1.05	47.54	220.99	22.34
MF7	9	0.13	7.18	69.20	1.21	33.63	221.40	30.42
MF8	0	0.27	8.98	124.46	1.95	44.95	396.57	71.12
MF8	10	0.32	14.99	116.05	0.97	46.57	350.07	26.60
MF8	14	0.19	11.59	98.31	1.04	35.46	208.29	26.60
MF13	0	0.24	6.61	72.92	0.42	9.65	70.00	8.10
MF13	10	0.21	7.27	70.78	0.42	9.01	73.08	12.02
MF13	19	0.22	6.60	64.71	0.44	12.00	86.33	13.03
MF18	0			73.17	0.33	7.44	63.63	9.26
MF18	6	0.20	5.39	78.53	0.27	5.86	46.14	7.56
MF18	13			58.17	0.33	5.00	42.97	7.82
MF24	0			66.19	0.31	5.71	67.36	7.61
MF24	10	0.15	3.47	53.12	0.34	5.06	53.07	8.16
MF24	29	0.13	6.80	67.50	0.41	4.19	54.72	7.91
MF35	0	0.12	3.42	56.78				
MF35	12	0.14	7.67	68.73				
MF35	22	0.11	3.92	56.86				
MF36	0	0.11	3.76	51.90	0.23	3.50	37.54	4.48
MF36	10	0.10	3.87	51.66	0.22	2.75	24.36	4.45
MF36	33	0.14	5.51	60.37	0.18	2.72	29.05	4.75

APPENDIX C

GEOMETRIC MEAN LINEAR REGRESSION AND STATISTICAL TESTING FOR OUTLIERS

Program Outline Description

The program written in BASIC reads sequential X, Y data from an ASCII file "data1.prn". The geometric mean between X on Y and Y on X regression slopes is calculated according to Ricker (1973). The regression constant (i.e., Y intercept) is calculated assuming the regression line passes through means of X and of Y. The resulting linear regression equation is used to calculated predicted Y for each observed X. The data point with largest deviation is tested for an outlier by omitting it from the data set and recomputing the regression. If the deviation of the suspected point from the new regression line (calculated without it) is greater than sampling error, that data point will be considered an outlier (Snedecor and Cochran, 1980). The significance probability of t (2 tails) at different degrees of freedom are interpolated from values in t table in Edwards (1979).

The Program

```
10 CLEAR:CLS
20 DIM X(1000),Y(1000),ID(1000),OUTLY(1000)
30 OPEN "data1.prn" FOR INPUT AS #1
40 OPEN "outlier.prn" FOR OUTPUT AS #2
50 N=N+1
60 INPUT #1,X(N),Y(N)
70 ID(N)=N
80 SUMX=SUMX+X(N):SUMY=SUMY+Y(N)
90 SUMX2=SUMX2+X(N)^2:SUMY2=SUMY2+Y(N)^2
   :SUMXY=SUMXY+X(N)*Y(N)
100 IF EOF(1) THEN 110 ELSE 50
110 PRINT:PRINT "N =";N
```

```
120 GOSUB 1010
130 GOSUB 1510
140 PRINT:PRINT "slope =";SLOPE;"   +/- ";C95;"   (95% CI)"
150 PRINT "                 +/- ";C99;"   (99% CI)"
160 PRINT "                 +/- ";C999;"  (99.9% CI)"
170 PRINT "Y-int =";Y.INT;"     r^2 =";R2
180 PRINT:PRINT "Outliers are:";
190 FOR I=1 TO O
200 PRINT OUTLY(I);
210 PRINT #2, OUTLY(I)
220 NEXT I
225 PRINT:PRINT "slope+ =";SLOPE+C95
230 END
1000 '
1010 '******************** outlier omission **********************
1020 '
1030 AVGX=SUMX/N:AVGY=SUMY/N
1040 B=SUMXY/SUMX2                          'model I slope
1050 IF B<0 THEN SLOPE=-(SUMY2/SUMX2)^.5:GOTO 1070
1060 SLOPE=(SUMY2/SUMX2)^.5                 'Ricker eq. 11
1070 Y.INT=AVGY-SLOPE*AVGX
1080 SUMD2=SUMY2-SUMXY^2/SUMX2
1090 FOR I=1 TO N
1100 DEV=ABS(Y(I)-AVGY-SLOPE*(X(I)-AVGX))   'eq. 9.2.4 & 9.11.2
1110 IF DEV<=DEVMAX THEN 1130
1120 DEVMAX=DEV:SP=I
1130 NEXT I
1140 SUSPECT=DEVMAX^2/(1-1/N-X(SP)^2/SUMX2)     'eq. 9.11.2
1150 S=((SUMD2-SUSPECT)/(N-3))^.5           'eq. 9.11.3
1160 T=DEVMAX/(S*(1-1/N-X(SP)^2/SUMX2)^.5)
1170 IF N-3<=0 THEN PRINT "No solution":GOTO 1280
1180 TCR=1/(-1.05948/(N-3)+.2248) 'interpolate from Edwards(1980)
1190 IF T<=TCR THEN 1280
1200 O=O+1
1210 OUTLY(O)=ID(SP)
1220 SUMX=SUMX-X(SP):SUMY=SUMY-Y(SP)
1230 SUMX2=SUMX2-X(SP)^2:SUMY2=SUMY2-Y(SP)^2
       :SUMXY=SUMXY-X(SP)*Y(SP)
1240 FOR J=SP TO N
1250 X(J)=X(J+1):Y(J)=Y(J+1):ID(J)=ID(J+1)
1260 NEXT J
1270 N=N-1:DEVMAX=0:GOTO 1030
1280 RETURN
1500 '
```

```
1510 '****** Calculate 95%, 99% and 99.9% CI for slope *******
1520 '
1530 R2=SUMXY^2/SUMX2/SUMY2
1540 IF N-2<=0 THEN PRINT "No solution":GOTO 1630
1550 TCR=1/(-.61499/(N-2)+.5102001)  'interpolation for t.05
1560 C95=TCR*(SLOPE^2*(1-R2)/(N-2))^.5      'Ricker p. 413
1570 IF N-2<=0 THEN PRINT "No solution":GOTO 1630
1580 TCR=1/(-.72929/(N-2)+.388)      'interpolation for t.01
1590 C99=TCR*(SLOPE^2*(1-R2)/(N-2))^.5
1600 IF N-2<=0 THEN PRINT "No solution":GOTO 1630
1610 TCR=1/(-.86591/(N-2)+.3034)  'interpolation for t.001
1620 C999=TCR*(SLOPE^2*(1-R2)/(N-2))^.5
1630 RETURN
```

References

Edwards, A. L. 1979. Multiple Regression and the Analysis of Variance and Covariance. San Francisco: W. H. Freeman, 212 pp.

Ricker, W. E. 1973. Linear regression in fishery research. J. Fish. Res. Bd. Can. 30: 409-434.

Snedecor, G. W. and Cochran, W. G. 1980. Statistical Methods Seventh Edition. Ames: The Iowa State University Press, 507 pp.